Response surface analysis of rat bone composition changes

by dietary calcium and silicon.

by

Shelly McCrady

A Research Paper

Submitted in Partial Fulfillment of the

Requirements for the

Master of Science Degree

in

Food and Nutritional Sciences

Approved: 6 Semester Credits

_____

Research Advisor

Thesis Committee Members

_____

_____

The Graduate School
University of Wisconsin-Stout
December, 2003
The Graduate School

University of Wisconsin Stout
Menomonie, WI 54751

ABSTRACT

McCrady Shelly K
(Last Name) (First Name) (Initial)

Response surface analysis of rat bone composition changes by dietary calcium and silicon
(Title)

Food and Nutritional Sciences Dr. Carol Seaborn December 2003 124
(Graduate Major) (Research Advisor) (Month / Year) (# of Pages)

Turabian, Kate. A Manual for Writers of Term Papers, Theses, and Dissertations. 1987
(Name of Style Manual Used in the Study)

Silicon (Si) apparently is involved in bone calcification; however, its affect appears to be related to dietary calcium. The objective of this experiment was to determine the effects of varying concentrations of dietary silicon on bone mineralization when there were incremental increases in dietary calcium. A second objective was to determine if pharmacological effects on bone would be evident at very high levels of dietary silicon (350 to 870 μg Si/g diet). Sixty weanling male Sprague-Dawley rats were randomly assigned to one of nine treatment groups in a two factor, central composite, response surface design. Silicon as sodium meta-silicate and calcium as calcium carbonate were added to a casein-based diet (containing 0.6 μg Si/g diet) at concentrations between 0 and 870 μg Si/g diet and between 0.15% and 0.85% Ca. The rats were fed their respective diets for nine weeks. DNA and hydroxyproline from the humerus bone and alkaline phosphatase from the plasma were determined by colorimetric methods. The femur, L4 vertebra, skull and one incisor tooth were ashed using the lithium-boron fusion technique and their mineral concentrations were determined by inductively coupled argon plasma atomic

emission spectrometry. Response surface and regression analyses were utilized to analyze the data. There were no differences in mean body weight between the groups. Increasing dietary silicon increased calcium, phosphorus and magnesium concentrations in the vertebra and skull. The highest skull concentration of calcium, phosphorus and magnesium occurred at the predicted values of 36, 45, 39 μg Si/g diet, respectively. Silicon impacted the copper concentration in the vertebra and femur, with the minimum copper content occurring at the predicted values of 25 and 28 μg Si/g diet, respectively; with increases in copper occurring with both silicon deficiency and silicon excess. Changes in copper were opposite those of the hydroxyproline concentrations of the humeri, where both low and high dietary silicon decreased the hydroxyproline or collagen content, with the maximum collagen production in humeri bones occurring at the predicted value of 59 μg Si/g diet. Dietary silicon impacts bone mineralization in ways that can be generally regarded as positive, because it increases calcium, phosphorus, and magnesium concentrations. These effects may be the result of alterations in the organic matrix, reflected by the changes in copper and hydroxyproline concentrations. Regardless of the mechanism, silicon has such a strong impact on bone maturation and mineralization that is should be considered a mineral of concern in human nutrition.

Research was conducted and funded by the USDA, ARS, Grand Forks Human Nutrition Research Center, Grand Forks, North Dakota. Interpretation of the response surface analysis data was conducted at the University of Wisconsin-Stout.

ACKNOWLEDGEMENTS

It gives me great pleasure to acknowledge the following people who have made the completion of this thesis possible. Dr. Carol Seaborn, my thesis advisor, words cannot express what your assistance over the past three years has meant to me. You have continued to believe in my ability to complete this thesis even when I did not. Thank you for your continuing words of encouragement, your understanding, your dedication, your nonjudgmental character and your ability to always speak the truth. You are a great professor and friend; I am honored to have spent the past five years under your guidance. I would also like to sincerely thank my thesis committee members; Dr. Janice Coker and Dr. Ann Parsons, thank you both for your patience and for the expertise you have brought to this thesis; all of your contributions have been greatly appreciated. Dr. Gour Choudhury, I would also like to thank you for all the help you provided me when interpreting the response surface analysis results, I appreciate the literature you provided me on this complex analysis and for the time you made to read my results.

Sincere thanks are also directed to the individuals at the Grand Forks Human Nutrition Research Center in Grand Forks, North Dakota; where this great research study was conducted. Thank you to all those involved in preparing the animal diets, caring for the animals, conducting the study and analyzing the samples. Special thanks are also intended for Dr. Forrest Neilsen and LuAnn Johnson. Dr. Neilsen, thank you for the grand tour of the Human Nutrition Research Center in Grand Forks, for the great articles you provided me for my literature review and for your continued guidance and assistance in the writing process of this thesis, it has been an honor for me to meet and interact with such a renowned researcher in the world of trace minerals. LuAnn Johnson thank you, for conducting the response surface analysis of the data, your assistance in understanding the data is greatly appreciated, I could not have completed this thesis without you.

TABLE OF CONTENTS

Page

LIST OF TABLES

LIST OF FIGURES

Figures Page

CHAPTER ONE

INTRODUCTION

Introduction

The essentiality of silicon was first suggested over thirty years ago due to the bone and collagen abnormalities produced in experimental animals following silicon deprivation (Carlisle 1974). When chicks were fed silicon deficient diets, abnormalities in skeletal growth were noticeable after 1-2 weeks, with chicks retarded in size, bone circumferences reduced, bone cortexes thinned and skull sizes decreased (Carlisle, 1972). Schwartz and Milne (1972) reproduced a similar effect in rats, reporting rats fed a silicon deficient diet have significant growth retardation and skull and bone architecture disturbances, when compared to rats consuming silicon supplemented diets. Collagen development abnormalities were also visible after 1-2 weeks in chicks fed a silicon deficient diet, with legs appearing thinner and combs appearing smaller (Carlisle, 1976). The long-bone tibial joints were also decreased in size, with less articular cartilage when compared to the joints of silicon supplemented chicks. Hexosamine content (used to assess cartilage and glycosaminoglycan content) in the articular cartilage and in the comb were also decreased in the silicon deficient chicks. Other reports supporting the nutritional essentiality of silicon for bone and collagen include its presence in the active growth areas of mice and rat bone, its structural role in several glycosaminoglycans and polyuronides and its ability to stimulate prolylhydroxylase in bone tissue culture (Carlisle, 1970; Schwartz 1973; Carlisle, 1997).

Carlisle (1986) investigated the effect of different levels of silicon (10, 25, and 250 ppm) and calcium (0.08, 0.40, and 1.20%) intake on rat tibia mineralization. Increases of silicon in the low-calcium (0.08%) diet resulted in a highly significant increase in percentage ash content and calcium concentration during the first three weeks. Similarly, Brossart, Shuler and Nielsen (1990) found that feeding 50 μg silicon as sodium metasilicate enhanced the incorporation of mineral

elements into tibias of six-week old rats maintained on a low calcium diet (2.5 g/kg). Thus, the effect of silicon on bone mineralization appears to be related to the amount of dietary calcium.

Statement of the Problem

Although several researchers have proposed the essentiality of silicon, an adequate intake level has not been recommended by the Food and Nutrition Board (Institute of Medicine, 1998). The National Research Council (1978) has also not recommended an adequate silicon intake for rats even though several animal studies provide evidence for the addition of silicon to the list of essential elements for laboratory animals. The interaction of silicon with varying levels of calcium upon bone mineralization has not been determined.

Reported concentrations of silicon added to experimental animal diets have ranged from 10-540 μg/g diet (Seaborn, Nielsen, 2002a; Stewart, Emerick, Kayongo-Male, 2003). In humans, the estimated dietary intake of silicon in the United States ranges from 21 to 46 mg/day, whether silicon additions in excess of those amounts found in the typical American diet are beneficial or are exerting a pharmacological effect have not been evaluated (Nielsen, 1999).

Purpose of the Study

The objective of this experiment was to determine the effects of varying concentrations of dietary silicon on bone mineralization when there were incremental increases in dietary calcium. A second objective was to determine if pharmacological effects on bone would be evident at very high levels of dietary silicon (350 to 870 μg Si/g diet).

Assumptions of the Study

An advantage of the response surface experimental design is the ability to predict the dietary intake of silicon or calcium necessary to see minimum or maximum mineralization responses. When using response surface analysis, the researcher is required to assume the normal level for each of the two variables (in this study the estimated requirement for silicon and calcium, 35 µg/g Si and 0.50% Ca, respectively).

Definition of Terms

Cuneiform: wedge shaped.

Resorb: to break down and integrate into oneself.

Mesenchymal: being of loosely arranged cells, that become connective tissue, blood lymphatics, cartilage and/or bone.

CHAPTER TWO

REVIEW OF LITERATURE

Introduction

This chapter covers the biology of bone, collagen, and teeth: identifying their structure, properties, and physiological roles. Calcium and silicon are also discussed in detail in this section; addressing their metabolism, biochemical functions, deficiency and toxicity symptoms, nutrient interactions, and current dietary recommendations.

Bone Biology

This brief overview of bone biology will focus primarily on the anatomy of bone, its tissues, cells, and matrix. With this focus, bone formation and mineralization will also be addressed. This section will conclude with a look at potential serum and urine markers of bone turnover.

Anatomy

Bones are classified into three primary groups based on their general shape: short, flat, or long bones. Short bones are approximately the same in measurement in all directions and possess a trapezoidal, cuboidal, cuneiform, or irregular shape. These bones have a relatively thin cortical layer. Tarsals, carpals, and vertebral bodies are examples of short bones. Flat bones have one dimension that differs in length from the other two. The bones of the skull, scapula, mandible, and ilium are examples of flat bones. Long bones, such as tibia, femur, and humerus, consist of three anatomical divisions: the epiphyses, the metaphyses, and the diaphysis (Figure 2.1). The epiphysis is the term used for the ends of the bone and consists of a thin cortical layer of bone

surrounding trabecular bone. The metaphysis is the region of the bone between the epiphysis and diaphysis, containing both trabecular and cortical bone. A plate of cartilage separates the epiphysis from the metaphysis and is known as the epiphyseal growth plate; this plate is the site at which elongation of long bones can occur. The diaphysis, or shaft of the bone, is a hollow cylinder in shape, surrounded by a layer of cortical bone. The outer surface of the bone is known as the periosteum and the inner surface is known as the endosteum (Garner, Anderson, Ambrose, 1996; Buckwalter, Glimcher, Cooper, Recker, 1996).

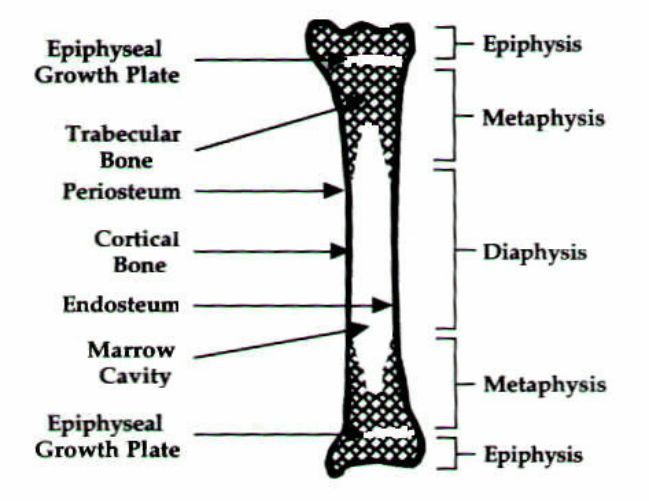

Figure 2.1. The anatomy of long bones. Garner, S.C., Anderson, J.J.B., Ambrose, W.W. (1996) Skeletal tissues and mineralization. In: *Calcium and Phosphorus in Health and Disease*. (Anderson, J.J.B., Garner, S.C., eds.), pp. 100, CRC Press Inc, Boca Raton, Florida.

Bone Tissue

Bone is composed of two forms of bone tissues: cortical (compact) bone and cancellous (trabecular or spongy) bone. Although cortical and cancellous bones possess the same matrix composition and structure, the matrix of cortical bone is 80 – 90% calcified while only 15 – 25% of cancellous bone is calcified (Garner, Anderson, Ambrose, 1996). Thus, cortical bone is denser or less porous than cancellous bone. Cortical bone provides a mechanical and protective role for bone, forming the shafts of long bones and covering nearly all other bones in the body. Cancellous

bone, however, fills the ends of long bones and comprises most of the structure of vertebrae bones (Buckwalter, Glimcher, Cooper, Recker, 1996).

On even a finer scale it has been shown that cortical and cancellous bone may consist of two other forms of bone tissues: woven (fiber or primary) bone or lamellar (secondary) bone. Woven bone is a rapidly formed, poorly organized tissue consisting of collagen fibers and mineral crystals randomly arranged. In contrast, lamellar bone is a slowly formed, well-organized tissue consisting of parallel layers of matrix crystals and collagen fibers (Martin, Burr, Sharkey, 1998). Woven bone is present when bone is first formed, such as in the embryonic skeleton, or during fracture repair. Lamellar bone, however, is present after bone is remodeled during growth or during normal bone turnover; thus lamellar bone is present in mature bone (Garner, Anderson, Ambrose, 1996).

Bone Cells

Bone is composed of several cell types that execute the functions required to form and maintain bone structure. These cells also perform the homeostatic roles of bone. Osteoblasts, osteocytes, bone lining cells, and osteoclasts are the four cell types of which bone is composed. These cells can be divided into two functional categories: those that form bone or those that resorb bone (Garner, Anderson, Ambrose, 1996; Martin, Burr, Sharkey, 1998).

Osteoblasts are bone-forming cells; these cells are derived from mesenchymal cells and are associated with fibroblasts and the cells that form blood vessel walls. Osteoblasts perform several functions that result in the formation of bone, they secrete type I collagen to form the osteoid (unmineralized bone matrix) and regulate the procedures that initiate mineralization. Osteoblasts are capable of forming osteoid at a rate of approximately one micrometer per day. These bone-forming cells also express the membrane protein alkaline phosphatase, an enzyme that is believed to be a regulator of mineralization. Osteoblasts also assist in the homeostasis of calcium by

possessing receptors for the two primary calcium and bone regulating hormones, parathyroid hormone and 1,25-dihydroxyvitamin D. Active osteoblasts may follow one of three courses once bone has been formed: 1) enclose themselves in bone, forming osteocytes, 2) remain on the bone surface, forming bone-lining cells, or 3) disappear from the site of bone formation by undergoing apoptosis (Garner, Anderson, Ambrose, 1996; Martin, Burr, Sharkey, 1998; Marks, Hermey, 1996).

Osteocytes are bone cells lying within small cavities known as lacunae that are completely immersed in bone. These former osteoblasts comprise more than 90% of the bone cells in mature bone (Buckwalter, Glimcher, Cooper, Recker, 1996). Osteocytes remain associated with each other and cells on the bone surface by communicating via small tubular channels known as canaliculi. These tunnels provide a means for the diffusion of nutrients from extracellular fluid to these cells (Garner, Anderson, Ambrose, 1996; Martin, Burr, Sharkey, 1998).

Bone-lining cells are osteoblasts that are no longer actively materializing bone, these cells lie directly on the bone matrix with cytoplasmic extensions that infiltrate the bone matrix and contact the cytoplasmic extensions of osteocytes. These bone-lining cells are believed to be central in the maintenance of blood calcium levels, although the manner in which this occurs remains speculative (Garner, Anderson, Ambrose, 1996). Bone-lining cells appear to retain their receptors for parathyroid hormone, contracting and secreting enzymes that remove the thin layer of osteoid covering the mineralized matrix when exposed to this hormone. These actions appear to allow for osteoclasts to attach to the bone surface and begin bone resorption. Thus, bone-lining cells may have a role in attracting and stimulating osteoclasts to resorb bone (Buckwalter, Glimcher, Cooper, Recker, 1996; Martin, Burr, Sharkey, 1998).

Osteoclasts are bone-resorbing cells. These cells are formed from the fusion of monocytes derived from the hemopoietic portion of bone marrow. Osteoclasts initiate the bone resorption process by first binding to the surface of the bone periosteum. This bondage creates a sealed space

between the cell and the bone matrix. Endosomes containing membrane-bound proton pumps then move to the area of the osteoclast closest to the bone matrix and insert themselves into the cell membrane. This action forms a brush border between the cell and the bone, with the membrane-bound proton pumps transporting hydrogen ions from the cell into the sealed space. The hydrogen ions are generated within the osteoclasts through the action of carbonic anhydrase II (Garner, Anderson, Ambrose, 1996). The transfer of hydrogen ions from the cell to the sealed space decreases the pH from approximately 7 to 4. This pH shift is responsible for demineralizing the adjacent bone. The osteoclast then secretes acid proteases to dissolve the remaining organic matrix, releasing the minerals that make up the matrix into the extracellular fluid (Buckwalter, Glimcher, Cooper, Recker, 1996). Osteoclasts are capable of eroding bone at a rate of tens of micrometers per day (Martin, Burr, Sharkey, 1998). In conjunction with their ability to erode bone, osteoclasts also participate in plasma calcium homeostasis by possessing a receptor for calcitonin. When large amounts of dietary calcium are being absorbed and plasma calcium levels rise, calcitonin is released and acts on osteoclasts by inhibiting their bone resorption, thus decreasing bone calcium levels (Weaver, Heaney, 1999).

Bone Matrix

Bone matrix consists of an organic phase and an inorganic phase. The organic phase contributes to approximately 20% of the wet weight of bone, with the inorganic phase contributing 65% and water contributing approximately 10% (Buckwalter, Glimcher, Cooper, Recker, 1996). The organic phase of bone, which primarily consists of collagen, provides bone its form and its ability to resist tension. The inorganic phase, however, is the component of bone that gives it rigidity and its characteristic ability to resist compression (Heaney, 1999).

The organic matrix of bone is similar to the fibrous matrix present in tendons, ligaments, and joint capsules. Type I collagen is the predominant collagen present in bone, while minor

amounts of types V and XII also exist. Collagen makes up approximately 90% of the organic matrix, with noncollagenous proteins contributing to approximately 10%. The noncollagenous proteins present in bone are either synthesized by osteoblasts or serum derived; these proteins may have a role in influencing the organization of the matrix, the calcification of bone, and/or the activities of bone cells (Buckwalter, Glimcher, Cooper, Recker, 1996). Thrombospondin, fibronectin, bone sialoprotein, osteopontin, proteoglycan I and II, osteonectin, osteocalcin, and matrix gla-protein are some of the noncollagenous proteins included in bone (Garner, Anderson, Ambrose, 1996). Growth-related proteins have also been identified in bone, including the transforming growth factor-β family, insulin-like growth factor-1 and 2, bone morphogenic proteins, platelet-derived growth factors, interleukin-1 and 6, and colony-stimulating factors (Buckwalter, Glimcher, Cooper, Recker, 1996). Although the specific function of these proteins remains uncertain, the fact that they are incorporated into bone suggests that they have an important role in bone.

The inorganic matrix of bone, or the mineral phase, serves as an ion reservoir for the body, containing approximately 99% of the body calcium, 85% of the phosphorus, and 40 to 60% of the total body magnesium and sodium (Buckwalter, Glimcher, Cooper, Recker, 1996). It is through this function as an ion reservoir that bone is able to maintain the extracellular fluid concentration in a range necessary for critical physiological functions. The inorganic phase consists primarily of hydroxyapatite crystals, ($Ca_{10}[PO_4][OH_2]_2$), comprising 60 – 65% of bone weight (Garner, Anderson, Ambrose, 1996). Minor amounts of sodium, potassium, magnesium, citrate, carbonate, fluoride, and other ions have also been shown to substitute or be absorbed onto the crystal surface (Heaney, 1999; Martin, Burr, Sharkey, 1998). A substitution of ions present on hydroxyapatite with other ions is governed by the composition of the extracellular fluid, and in turn, affects the solubility of the mineral phase.

To gain an understanding of the mineral composition in various bones, research has been conducted using several animal models. Table 2.1 and Table 2.2 display a summary of several research studies that have looked at the macro mineral and micro and trace mineral (respectively) composition of femur, vertebra and skull in the rat (Seaborn, Nielsen, 1994; Seaborn, Nielsen, 1994; Seaborn, Nielsen, 2002b; Seaborn, Nielsen, 1994). All values were obtained from rats consuming a synthetic diet containing all of the known nutrients adequate for a rat (National Research Council, US 1978).

Table 2.1. Summary of Rat Bone Macro Mineral Concentrations

Bone	Ca[1]	P[1]	Mg[2]	Na[2]	K[2]
Femur	224[3]; 245[4]; 237.1[5]	104[3]; 117[4]; 115.2[5]	3930[3]; 4110[5]	4190[3]; 5060[4]; 4430[5]	4430[4]
Vertebra	215[4]	107[4]	---	3750[4]; 3470[5]	5910[4]
Skull	194[3]	88[3]	---	4150[3]	611[3]

[1]Values are shown in mg/g dry weight.
[2]Values are shown in μg/g dry weight
[3]Values obtained from Seaborn, C. D., Nielsen, F. H. (1994) Boron and silicon: effects on growth, plasma lipids, urinary cyclic AMP and bone and brain mineral composition of male rats. *Environmental Toxicology and Chemistry* 13: 941-947.
[4]Values obtained from Seaborn, C. D., Nielsen, F. H. (2002b) Dietary silicon and arginine affect mineral element composition of rat femur and vertebra. *Biol. Trace Element Res.* 89: 239-250.
[5]Values obtained from Seaborn, C. D., Nielsen, F. H. (1994) Effects of germanium and silicon on bone mineralization. *Biol. Trace Element Res.* 42: 151-164.

Table 2.2. Summary of Rat Bone Micro and Trace Mineral Concentrations

Bone	Cu[1]	Zn[1]	Fe[1]	Mn[1]	Mo[1]	Si[1]
Femur	1.33[4]; 1.23[5]	116.2[2]; 116[3]; 200[4]; 172.5[5]	49.54[2]; 49.5[3]; 73[4]; 61.2[5]	0.75[4]; 0.61[5]	2.23[4]; 0.94[5]	0.57[5]
Vertebra	1.77[4]	156[4]; 138.25[5]	55.12[5]	0.42[4]; 0.48[5]	1.78[4]; 1.60[5]	0.86[4]
Skull	3.25[3]	94[3]	20.19[2]; 20.2[3]	0.7[3]	6.01[2]	10.98[2]

[1]Values are shown in μg/g dry weight.
[2] Values obtained from Seaborn, C. D., Nielsen, F. H. (1994) High dietary aluminum affects the response of rats to silicon deprivation. *Biol. Trace Element Res* 41: 295-304.
[3] Values obtained from Seaborn, C. D., Nielsen, F. H. (1994) Boron and silicon: effects on growth, plasma lipids, urinary cyclic amp and bone and brain mineral composition of male rats. *Environmental Toxicology and Chemistry* 13: 941-947.
[4]Values obtained from Seaborn, C. D., Nielsen, F. H. (2002b) Dietary silicon and arginine affect mineral element composition of rat femur and vertebra. *Biol. Trace Element Res.* 89: 239-250.
[5]Values obtained from Seaborn, C. D., Nielsen, F. H. (1994) Effects of germanium and silicon on bone mineralization. *Biol. Trace Element Res.* 42: 151-164.

Bone Formation

Although all bones are created by the placement of hydroxyapatite crystals within a collagen matrix, the process by which the collagen matrix is arranged differs depending on the type of bone formation utilized. Two types of bone formation exist: intramembranous and endochondral bone formation (Garner, Anderson, Ambrose, 1996).

Intramembranous bone formation is utilized to form the flat bones of the skull, jaw, and ribs. During this process, mesenchymal cells differentiate into preosteoblasts and then into osteoblasts. The bone tissue formulated by these cells is woven, causing calcification in this tissue to be in irregular patches due to the irregular arrangement of the collagen fibers. As these bones undergo tissue remodeling, the woven bone will be replaced by lamellar bone (Garner, Anderson, Ambrose, 1996).

Endochondral bone formation is utilized to form long bones; this process involves the calcification of cartilaginous structures. The formation of cartilage is performed by chondroblasts, cells that are derived from mesenchymal cells, which differentiate to form prechondroblasts, and then form chondroblasts. The chondrocytes secrete a collagen matrix, which eventually encloses

them into lacunae. Although they are enclosed within these small cavities, the flexibility of the collagen fibers surrounding them allows for the chondrocytes to continue to proliferate and differentiate, expanding the lacunar spaces. The invasion of blood vessels into the cartilage initiates the mineralization process of the organic matrix. The mineralization decreases the ability of nutrients to diffuse through the organic matrix, causing the chondrocytes to begin to die. Only a thin layer of chondrocytes, at each end of the bone, survives the initial mineralization. The remainder of these active chondrocytes allows for bone to continue elongating at this site, a site known as the epiphyseal growth plate (Garner, Anderson, Ambrose, 1996).

Mineralization

The formation of crystals in an aqueous solution, a process necessary for bone mineralization to occur, involves three primary physico-chemical steps: supersaturation, nucleation, and crystal growth or maturation (Perry, Fraser, Hughes, 1991). The supersaturation of an ion occurs when the activity product of the ion exceeds the solubility product, favoring the precipitation of that ion. The nucleation of that precipitated mineral involves the deposition of the mineral onto an active interface, such as that provided by an organic substrate. The growth of the crystal formed is dependant on the supply of additional materials to the newly formed interface; if supply is adequate, growth of the crystal will occur.

Mineralization of bone involves the deposition of hydroxyapatite crystals into cartilage or osteoid (Garner, Anderson, Ambrose, 1996). The mineralization process will continue to occur until the crystals occupy all the available space within the collagen fibrils (Buckwalter, Glimcher, Cooper, Recker, 1996). The exact mechanism of mineralization is not known, however several theories exist as to how it occurs. One theory envisions the mineralization process involving matrix vesicles, membrane-invested particles formed from osteoblasts. This form of mineralization is believed to occur during intramembranous and endochondral bone formation. The

mineralization process involving matrix vesicles is theorized to occur in two distinct phases: initiation of first crystals and regulation of crystal proliferation (Anderson, 1985). In the first phase, calcium is believed to accumulate in the matrix vesicles prior to phosphate due to their attraction to the acid phospholipids concentrated within the vesicle. Phosphate levels then appear to increase in the matrix vesicle via the action of phosphatases, allowing for the deposition of solid-phase calcium phosphate minerals to occur. In phase two, crystal proliferation is believed to be initiated by the exposure of the preformed apatite crystals to extracellular fluid. Crystal proliferation continues to occur until it eventually infiltrates the surrounding matrix. Another theory states that collagen fibrils are the nucleation catalysts of mineralization, containing specific nucleation sites that allow for mineralization to occur (Glimcher, 1985). Phosphoproteins residing within the collagen fibrils are also believed to have an important role in the mineralization process, by possibly binding calcium and phosphate ions, facilitating their conversion to a solid phase.

Inhibitors of crystal proliferation include: inadequate levels of calcium and phosphate; certain organic phosphate compounds, which prevent hydroxyapatite growth, like pyrophosphate and ATP; specific noncollagenous proteins; and γ-carboxyglutamic acid-containing proteins, proteins which have been found to impede hydroxyapatite deposition. Factors seen as promoting crystal proliferation include: elevated calcium and phosphate levels, collagen, and osteonectin (Garner, Anderson, Ambrose, 1996).

Urine and Serum Bone Markers

Urine and serum bone markers are a noninvasive way to assess the rate of bone turnover. Changes in marker status are likely to occur in short time periods, such as over hours or days, however the ability of these markers to reflect the actual turnover of bone remains questionable. Thus, the utilization of several bone markers is necessary to provide the most complete assessment

of bone turnover. These markers can be delineated into two major groups: markers of bone formation and markers of bone resorption (Garner, Anderson, Ambrose, 1996; Lester, 1996).

Markers for bone formation are likely molecules synthesized by osteoblasts, the bone cell responsible for bone formation. Three markers exist for bone formation: alkaline phosphatase (skeletal and total), osteocalcin, and procollagen I extension peptides. All three of these markers are obtained from the plasma. Skeletal alkaline phosphatase is an enzyme produced and released by the osteoblast during bone formation and mineralization. The liver, kidney, and gastro-intestinal tract, however, also produce an alkaline phosphatase isoenzyme, causing the discrimination between total alkaline phosphatase activity and bone-specific activity to be difficult (Garner, Anderson, Ambrose, 1996). Osteocalcin is a noncollagenous protein found in bone and dentin. Although the precise function of osteocalcin is unknown, it is known that it is produced by the osteoblast and either released into circulation or incorporated into the bone matrix. Two major problems exist with utilizing osteocalcin as a bone marker: 1) substantial differences in osteocalcin levels are observed when different assays methods are utilized, and 2) both intact osteocalcin and fragments are released from bone during bone resorption (Lester, 1996). Although alkaline phosphatase and osteocalcin are the two primary bone markers for bone formation, use of procollagen I extension peptides as possible reliable markers have also been tested. Assays have been developed to detect the level of carboxy-terminal and amino-terminal segments of type I procollagen. Both of these procollagen I extension peptides are cleaved from procollagen and released into the extracellular fluid in the same rate as to which collagen is synthesized. Upon examination, however, it appears that either these peptides are preferentially released from the bone or cleared from the plasma at different rates since amino-terminal segments of type I procollagen in the plasma are 100-fold higher than carboxy-terminal type I procollagen (Lester, 1996).

Bone resorption is a product of osteoclastic activity, thus markers for bone resorption are proteins specific to osteoclasts and amino acids released during collagen breakdown. Four markers

exist for bone resorption: hydroxyproline, tartrate-resistant acid phosphatase, hydroxylysine glycosides, and pyridinoline/deoxypyridinoline. Of these four markers, tartrate-resistant acid phosphatase is an osteoclast specific protein, while hydroxyproline, hydroxylysine glycosides, pyridinoline, and deoxypyridinoline are modified amino acids released from collagen during breakdown. Hydroxyproline is measurable in both the plasma and urine. This modified amino acid is a nonspecific index of bone resorption since it reflects the breakdown of collagen from all body tissues, including the breakdown of dietary proteins. Tartrate-resistant acid phosphatase is a plasma lysosomal enzyme synthesized and released by osteoclasts. Although plasma levels of this enzyme increase during periods of increased bone turnover, tartrate-resistant acid phosphatase has not been found to be a more sensitive indicator of bone turnover than hydroxyproline. Hydroxylysine glycosides, specifically galactosyl-hydroxylysine and glucosyl-galactosyl-hydroxylysine are released from collagen and secreted in the urine. The ratio of these urine markers is dependent upon the tissue in which they were derived, thus specificity is attainable with this assay. In order for quantification to occur, however high performance liquid chromatography is required. Pyridinoline and deoxypyridinilone are cross-links found in mature collagen that can be measured in the urine during periods of bone resorption. Although levels of these peptides are increased during the onset of menopause and decreased with hormone replacement therapy, these peptide levels correlate well with bone turnover as determined by histomorphometric analysis of bone biopsy specimens (Lester, 1996).

Collagen

This section briefly introduces the collagen family and identifies the structure of collagen, the types of collagen, and their classifications. A focus on type I collagen is also made in this section because of its prominence in bone. The biosynthesis, intracellular alterations, and extracellular processing of type I collagen will be described.

Collagen Family

Collagen accounts for approximately 30% of the total protein present in mammals, making it the most abundant protein in mammalian tissues (Yamauchi, 1996). Its presence in the extracellular space in nearly all types of connective tissue in the body makes it a key structural protein. Collagen possesses a triple-helical structure, with each polypeptide chain (α chain) consisting of a repetitive sequence of amino acids (glycine-proline-hydroxyproline) (Nimni, 1988). The presence of glycine, the smallest amino acid, in the third position of the repeating sequence is important for the helical structure of collagen because it occupies the center of the helix. Thirty unique alpha chains have been identified. Nineteen unique collagen types have also been identified; each type is distributed in a characteristic tissue with a unique biological function.

Three different classifications exist for the types of collagen: fibril-forming, fibril-associated, and nonfibrillar collagens (Yamauchi, 1996). Types I, II, III, V, and XI are fibril-forming collagens. These collagen types, as their name implies, form fibrils in various tissues in which they are found. They are rod-shaped molecules, packed in parallel lines, staggered longitudinally in respect to one another. This packing arrangement creates areas that have high and low densities of collagen, forming areas known as hole zones (gaps), and overlapping zones (Figure 2.2). The fibril-associated collagens, however, do not form fibrils; these collagen types are believed to function as regulators of the fibril diameter and/or as bridges between fibrils. Types IX, XII, XIV, and possibly XIX are fibril-associated collagens. Several nonfibrillar collagen types have been identified, in addition to the fibril-forming and fibril-associated collagens. Types IV, VI, VII, and X are nonfibrillar collagens.

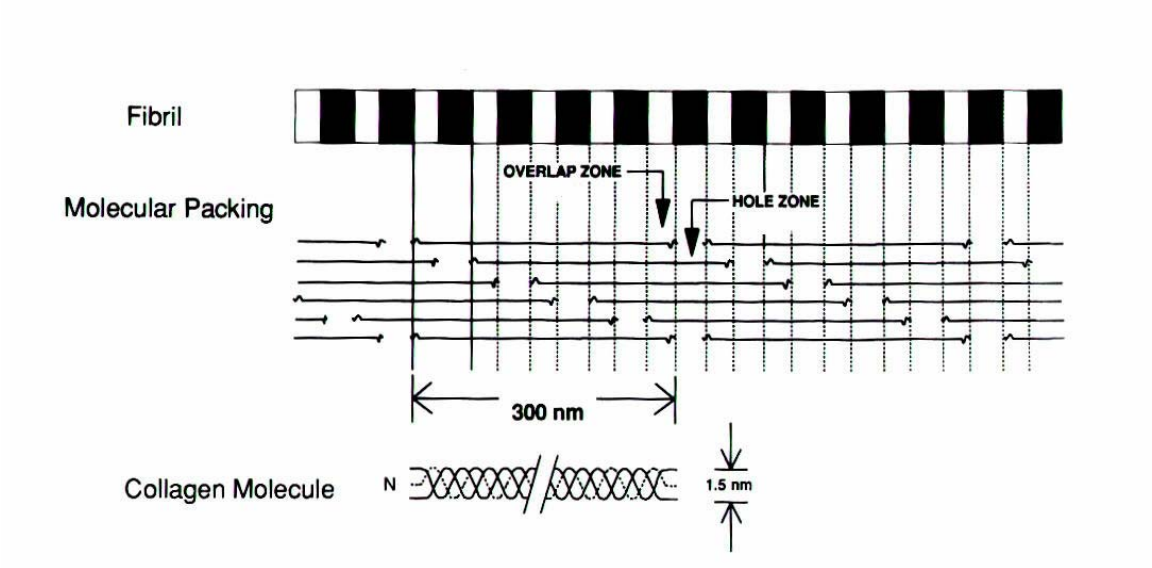

Figure 2.2. A two dimensional diagram of a type 1 collagen fibril. Yamauchi, M. (1996) Collagen: the major matrix molecule in mineralized tissues. In: *Calcium and Phosphorus in Health and Disease*. (Anderson, J.J.B., Garner, S.C., eds.), pp. 129, CRC Press Inc, Boca Raton, Florida.

Synthesis of Type I Collagen

Type I collagen is composed of three alpha chains, two α-1 chains and one α-2 chain (Nimni, 1988). The synthesis of type 1 collagen is a complex, multiple-step process that involves both intracellular and extracellular modifications (Figure 2.3). In order for the development of extracellular collagen fibers, a cell must first synthesize procollagen, a precursor molecule to type 1 collagen. The procollagen molecule consists of three different domains: the NH_2-terminal, the triple helical, and the COOH-terminal domains. The triple helical domain represents approximately 95% of the procollagen molecule (Yamauchi, 1996). Once procollagen is synthesized and released from the cell it is enzymatically cleaved of both of its nonhelical ends, to produce a collagen molecule that spontaneously constructs into fibers in the extracellular fluid.

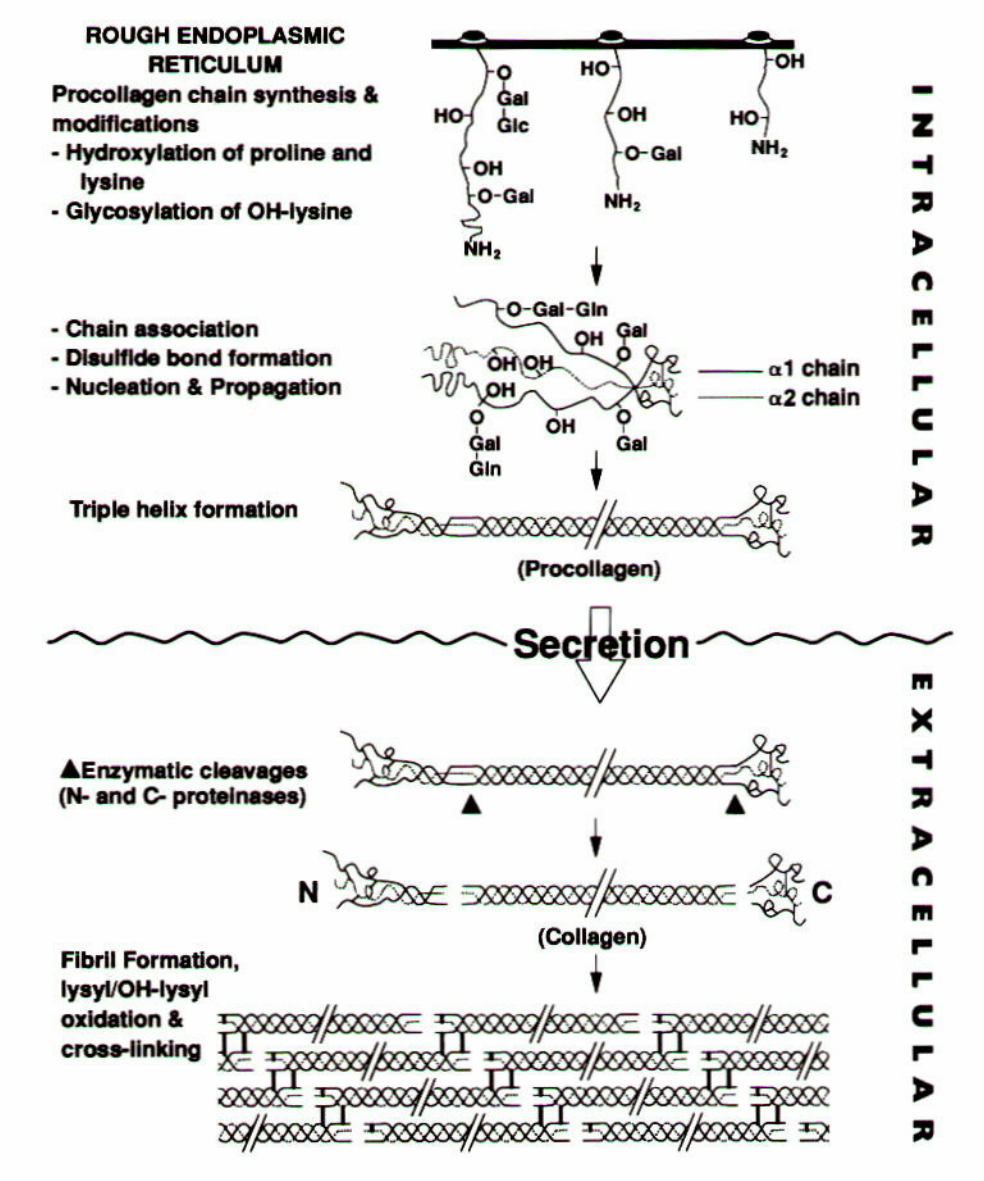

Figure 2.3. A schematic representation of the formation of collagen. Yamauchi, M. (1996) Collagen: the major matrix molecule in mineralized tissues. In: *Calcium and Phosphorus in Health and Disease*. (Anderson, J.J.B., Garner, S.C., eds.), pp. 132, CRC Press Inc, Boca Raton, Florida.

The synthesis of intracellular procollagen is initiated by the transcription of the collagen gene (Nimni, 1988). Specific messenger RNAs are formed for each alpha chain of the collagen molecule and translocated from the nucleus into the cytoplasm. Once in the cytoplasm, the

messenger RNA is translated in the rough endoplasmic reticulum on membrane-bound ribosomes. After the translation of the single pro-alpha chains, the chains are transferred into the lumen of the rough endoplasmic reticulum where essential cotranslational events occur. The hydroxylation of specific proline residues by 3-proline hydroxylase and 4-proline hydroxylase and of lysine by lysyl hydroxylase occurs during this time, forming hydroxyproline and hydroxylysine respectively. This modification occurs prior to the formation of the triple helix, since the enzymes that mediate this reaction are inactive against a triple helical structure (Yamauchi, 1996). These three enzymes also require ferrous iron, ascorbate, and α-ketoglutarate for activity. As the lysyl residues are hydroxylated, sugar residues are also added. Two enzymes, galactosyltransferase and glucosyltransferase, catalyze this glycosylation reaction, with the first enzyme adding galactose to the hydroxylysine residue and the second adding glucose to the galactosylhydroxylysine residue that was formed. These two enzymes, similar to the hydroxylation enzymes, require the pro-alpha chains to be in the nonhelical conformation. A bivalent cation, preferably manganese, is also required to be present during these reactions. Once these modifications and additions are complete, it is essential for pro α chains to properly align for the triple helix to form. The COOH-terminal propeptides initiate the intertwinement of the three pro α chains through the formation of disulfide bonds between the individual pro α chains. This association allows for the spontaneous formation of the triple helical structure, an intertwinement that propagates from the COOH-terminal to the NH_2-terminal. Once the procollagen molecule is formed, it travels from the lumen of the rough endoplasmic retiuclum through the transitional endoplasm to the Golgi apparatus. In the Golgi, procollagen is packaged in saccules, transformed into secretory granules, and extruded into the extracellular space via a cellular process known as exocytosis.

Once released from the cell, extracellular processing is required to transform procollagen into the active fibril-forming type I collagen. The C- and N-terminal propeptide extensions of the procollagen molecule are cleaved by the enzymes procollagen C-proteinase and procollagen N-

proteinase, respectively (Nimni, 1988). Once these two procollagen extensions are cleaved, the type I collagen molecules spontaneously aggregate to form a fibril (Yamauchi, 1996).

Bone Collagen Cross-links

The orientation of the collagen molecules in the fibril consists of a staggered longitudinal pattern of molecules with the multiples having tissue-specific lateral orientations with respect to one another. The cross-linking of bone collagen is initiated by the conversion of a specific peptidyl hydroxylysine to its aldehyde form, hydroxyallysine. This conversion occurs almost immediately after the collagen molecule is synthesized and is catalyzed by lysyl oxidase, a copper-dependent amine oxidase enzyme that requires oxygen and a carbonyl cofactor for activity. The orientation of the hydroxyallysine is near the "hole zone" and reacts with the adjacent hydroxylysine to form a bifunctional cross-link prior to mineralization. These links are able to tautomerize between the iminium and keto forms. This bifunctional cross-link is stereospecific in nature, connecting adjacent molecules laterally, in a sheet-like manner. The cross-links also laterally join neighboring hole regions, forming hole zones with plate-like shapes. It is this nature of cross-links that leads researchers to speculate the dynamic role collagen has in mineralization, regulating the size, shape, and site of mineral crystals within the fibrils (Yamauchi, 1996).

Teeth Biology

This brief overview of teeth biology will focus primarily on the anatomy of teeth, its tissues, and the process of each tissue's formation. A succinct look at the mineral exchange that occurs between the tissues and the extracellular fluid will also be examined.

Anatomy

A tooth consists of an anatomical crown and an anatomical root (Figure 2.4). The anatomical crown consists of three tissues: enamel, dentine, and pulp, while the anatomical root consists of cementum, dentine, and pulp (Bawden et al., 1996). Enamel tissue covers the outer surface of the anatomical crown while a tissue known as cementum encases the anatomical root. The area at which the outer layer of the crown and the outer layer of the root join is known as the cementoenamel junction; this junction typically occurs at the gum line. A tissue known as pulp occupies the innermost layer of the tooth whereas dentine encompasses the central layer of the tooth, in between the layers of enamel and pulp or cementum and pulp.

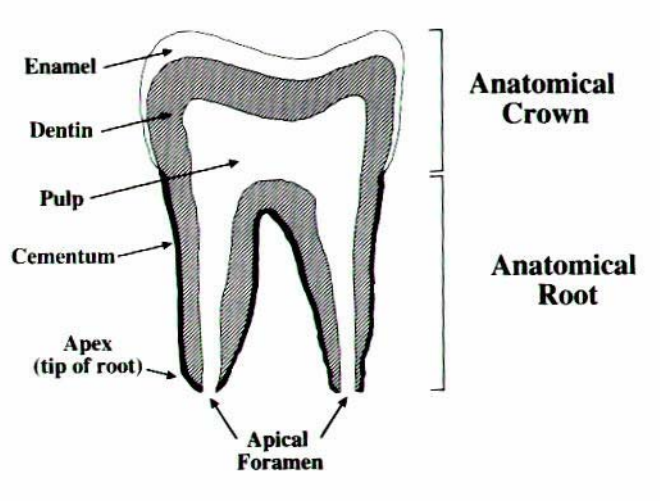

Figure 2.4. An anatomical structure of a mature tooth. Bawden, J. W., Anderson, J. J. B., Garner, S. C. (1996) Dental tissues. In: *Calcium and Phosphorus in Health and Disease*. (Anderson, J.J.B., Garner, S.C., eds.), pp. 121, CRC Press Inc, Boca Raton, Florida.

Teeth Formation

The initiation of tooth formation can be detected in embryos at the very beginning of their development. The formation of the dental ledge, a band of epithelial cells that advance into the underlying mesenchyme around the entire curve of the jaw, indicates the initiation of tooth development (Patten, Carlson, 1974).

Once the dental ledge is formed, local buds arise from the ledge in the positions where individual teeth are intended to form (Patten, Carlson, 1974). These local buds are masses of cells that materialize into the enamel crowns of each tooth; due to this role, they are termed enamel organs. The epithelial cells that line the inside of the enamel organ have a columnar shape and are known as ameloblasts, enamel formers. The epithelial cells that constitute the outer epithelium of the enamel organ are closely packed together, first appearing to be polyhedral in shape but then rapidly flattening with the subsequent growth of the enamel organ. The layer between the outer epithelium and the inner ameloblast region is known as the enamel pulp.

The inside of the enamel organ also contains a mass of mesenchymal cells of neural crest origin, these cells are known as the dental papilla (Patten, Carlson, 1974). The cells of the dental papilla rapidly proliferate, forming a dense cellular aggregation, with the outer cells taking on a columnar shape similar to that of the ameloblasts. These outer cells are now termed odontoblasts, dentine formers, because of their future role in the secretion of dentine (Bawden, Anderson, Garner, 1996). Within the central portion of the dental papilla, vessels and nerves appear, forming the pulp region of the tooth.

The growth of the dental papilla in the direction of the gum line has also begun to occur at this time, crowding the enamel pulp of the enamel organ in the region where the future tooth's crown will form (Patten, Carlson, 1974). This crowding brings the local ameloblasts closer to the small blood vessels that surround the mesenchyme, a circumstance that appears significant since it is here that the ameloblasts first initiate enamel secretion.

Once these preparatory developments are complete, the tooth structures are ready to fabricate the organic matrixes of the dentine and enamel tissues of the tooth. The dentine tissue is first deposited against the inner layer of the enamel organ by the odontoblasts (Patten, Carlson, 1974). These cells extract the raw materials necessary to make the dentine tissue from the small vessels present in the pulp, and then secrete the dentine tissue toward the enamel organ. The

secretion of additional dentine matrix by the odontoblasts forces the odontoblasts to move further from the dentine matrix they first deposited (Bawden, Anderson, Garner, 1996). Since the strands of their cytoplasm are embedded in the dentine tissue first deposited, the formation of dentinal fibers occurs as the odontoblasts move further from this region. Thus, as the dentine tissue continues to be secreted, the dentinal fibers continue to become longer. Once the desired organic matrix thickness is achieved, mineralization commences, following the pulpal direction of matrix deposition. The presence of the dentinal fibers is an important factor for the health of the dentine tissue since these processes maintain the organic matrix of dentine by providing nourishment to this tissue. These processes are also believed to act as intermediaries in transmitting impulses to the local nerve fibers.

The formation of the enamel cap by the ameloblast layer of the enamel organ is also occurring as the dentine tissue layer is secreted by the odontoblasts (Patten, Carlson, 1974). Like the secretion process of the odontoblasts, the ameloblasts utilize the small vessels in the adjacent mesenchyme to provide the raw materials necessary for enamel secretion, while moving away from each subsequent layer of newly secreted enamel. The cytoplasmic extensions of the ameloblasts are also present in the initial layer of deposited enamel, thus delicate fibrous strands known as Tomes processes can be detected from the tips of the ameloblasts to the areas of newly formed enamel. Once the initial layer of enamel is laid down, small crystals of hydroxyapatite also form in this layer, slowly enlarging until the entire thickness of enamel is deposited (Bawden, Anderson, Garner, 1996). Following the completion of mineral deposition, nearly the entire noncollagenous organic matrix secreted by the ameloblasts disappears (Weatherell, Robinson, 1973). Each ameloblast forms a prism of calcareous material beneath itself with the prisms' long axes at approximately right angles to the dentoenamel junction. Collectively these prisms form an extremely rigid cap over the entire crown of the tooth.

Although the first indications of tissue specialization occurs at the base of the dental papilla and extends crownward around the developing tooth, the actual formation of cementum does not occur until the tooth has acquired nearly its full growth and its definitive position in the jaw (Patten, Carlson, 1974). As the tooth erupts it compromises the specialized mesenchymal layer that surrounds the crown, with only the deeper portion of the layer persisting and differentiating into a connective-tissue layer. This layer constitutes the cementoblast layer. The cells of this layer, following the final positioning of the tooth, initiate the deposition of cementum around the dentine of the root. The layer of cementum formed, although initially thin, continues to develop as the tooth matures, gradually thickening with age.

Organic and Inorganic Matrixes

Enamel consists of an organic matrix unique to that of other mineralized tissues in that it is collagen free. This specialized organic matrix consists of two classes of glycoproteins, the amelogenins and the enamelins (Bawden, Anderson, Garner, 1996). Mature enamel is completely free of cytoplasm and only 1% of the enamel mass constitutes organic material. Very large dense crystals of hydroxyapatite make up the inorganic composition of tooth enamel. Absorbed to these hydroxyapatite crystals, in addition to several trace elements, are carbonate, magnesium, sodium, and potassium ions. Approximately 96% of enamel is mineralized, making it the most mineralized tissue in the body (Bawden, Anderson, Garner, 1996; Weatherell, Robinson, 1973).

Unlike enamel, the organic matrixes of dentine and cementum are similar to that of bone in that both are composed of collagen, constituting 20% of these tissues' dry weights. Although the gross composition of dentine is similar to bone, slight differences at the molecular level may explain the tissue organizational differences that exist between dentine and bone and not cementum. Dentine collagen appears to have a relatively high concentration of hydroxylysine, when compared to bone collagen. The increased presence of hydroxylysine results in a more

organized organic matrix due to the extra stabilizing cross-linkages. The inert nature of the dentine organic matrix may also be related to the absence of the resorptive and appositional activities of osteoclasts and osteoblasts, which are present in bone and cementum tissues (Smillie, 1973). The increased concentration of hydroxylysine may also impact the inorganic matrix of dentine, having a possible role in the mineralization process of this tissue. The inorganic matrix constitutes 70% of dentine and cementum masses, with the majority of their masses derived from hydroxyapatite crystals (Weatherell, Robinson, 1973).

Research has addressed the mineral composition of the various tissue layers of teeth, research has been conducted to address this question. Table 2.3 displays a summary of several research studies that have looked at the mineral composition of enamel, dentine and cementum in humans (Bowes, Murray, 1935; Weatherell, Robinson, 1973).

Table 2.3. Summary of the Mineral Composition of Human Enamel, Dentine and Cementum

Tissue	Ca[1]	P[1]	Mg[1]	Na[1]	K[1]	Si[1]
Enamel	37.07[2]; 36.1[3]	17.22[2]; 17.6[3]	0.464[2]; 0.2[3]	0.25[2]	0.05[2]	0.003[4]
Dentine	27.79[2]; 29.4[3]	13.81[2]; 13.6[3]	0.835[2]; 0.8	0.19[2]	0.07[2]	---
Cementum	23[3]	12[3]	---	---	---	---

[1]Values are shown in percentage of dry weight.
[2] Values obtained from Bowes, J. H., Murray, M. M. (1935) The composition of human enamel and dentine. *J. Biol. Chem.* 29: 2721-2727.
[3] Values obtained from Weatherell, J. A. Robinson, C. (1973) The inorganic composition of teeth. In: *Biological Mineralization*. (Zipkin, I., ed.), pp. 43-74, John Wiley & Sons, New York, New York.
[4] Percentage found in whole teeth only.

The pulp cavity differs drastically from the other tissues present in teeth in that it is not mineralized. Pulp is comprised of connective tissue with a profuse supply of nerve fibers, blood vessels, and lymphatics (Guyton, 1991). This cavity provides the primary source of nourishment for the dentine tissue and allows for the exchange of minerals.

Mineral Exchange

Similar to the ability of bone to exchange minerals with the extracellular fluid, new salts are constantly being deposited while others are being reabsorbed from teeth. The extent to which salts are incorporated into teeth tissue depends upon the availability of the ion, the accessibility of the crystallites, and the biological and chemical activity of the tissue (Weatherell, Robinson, 1973). Mature enamel is composed almost completely of crystalline hydroxyapatite, contains no cells, and exhibits no biological or chemical activity. Thus, this tissue appears to be exempt from mineral exchange. Dentine and cementum, however, are biologically and chemically active, possessing small, hydrated crystallites that allow for mineral exchange to occur. These tissues also exhibit signs of cellular activity and growth throughout life.

A difference in the rate of reabsorption and deposition of minerals within dentine and cementum also exists (Guyton, 1991). The rate at which dentine exchanges minerals is approximately one-third that of bone, while the rate cementum tissue exchanges minerals equals that of the surrounding jawbone. Although the mechanism of dentine mineral exchange is not defined, researchers hypothesize the role of dentinal fibers in this exchange. It is probable that these tubular processes allow for the transference of salts to occur, thus providing a physical structure for exchange. The ability of cementum to exchange minerals at a rate equal to that of bone is due to the presence of osteoblasts and osteoclasts within this tissue.

Calcium

Calcium, as discussed in previous sections is a major mineral component of the skeleton, with more than 99% of calcium storage occurring within bones and teeth. This section will focus on the metabolism of Ca, concentrating on its absorption. The experimental affects of Ca on bones when dietary levels are altered will also be discussed, in addition to the interactions calcium has with other minerals. The current dietary recommendations for calcium will also be addressed, stating the requirements for both humans and the rat.

Metabolism

To allow for absorption of Ca to occur in the intestine, ingested Ca products must be released from the salt compounds and remain in their soluble ionized form. (Groff, Gropper, 2000). The amount of ingested Ca inversely correlates with the percentage of Ca absorbed; thus as dietary Ca increases the percentage of absorbed Ca decreases, however the total amount of Ca absorbed is greater (Heaney, Weaver, Fitzsimmons, 1990). Several other factors that are known to affect Ca absorption include intestinal segment length, chyme transit time and Ca bioavailability (Louie, 1996).

Ca absorption in the intestinal tract occurs through two primary pathways, paracellular and transcellular transport. Paracellular transport of Ca is a nonsaturable transfer that occurs between the intestinal epithelium cells (Louie, 1996; Weaver, Heaney, 1999; Groff, Gropper, 2000). This movement of Ca occurs through the process of diffusion, with Ca moving from areas of high calcium concentration to areas of low concentration, with water believed to be the solvent thought to carry Ca along through a process called solvent drag (Karbach, 1992). This passive absorption pathway is believed to account for as much as 90% of the total calcium absorbed in animal models (Nellans, Kimberg, 1978). Transcellular transport of Ca is a saturable transfer that occurs in three separate steps: 1) entry into the intestinal epithelium cells through the brush border, 2) movement through the intracellular cytoplasm, and 3) exiting the cell through the basolateral membrane (Louie, 1996; Groff, Gropper, 2000). The entry of Ca across the brush border is a saturable process that is believed to occur via calcium transporters or channels that move Ca down an electrochemical gradient. Once Ca enters the cell, a Ca-binding protein, known as calbindin, transports the calcium through the cytoplasm to the basolateral membrane of the cell. Calcium then exits the intestinal epithelium cell by action of an ATP-dependent Ca pump, the first step in

transcellular transport that requires energy. The parathyroid – vitamin D pathway, regulates all three steps of transcellular transport.

Dietary calcium that is not absorbed in the intestinal tract is excreted in the feces. Endogenous calcium can also be lost in urine, sweat and feces. Endogenous calcium excretion in the feces results from body calcium that has entered the intestinal tract shed through saliva, mucosal cells, bile, gastric and pancreatic juices (Weaver, Heaney, 1999)

Altering Dietary Levels and Interactions

As discussed in earlier sections and reintroduced in the introduction of this section, bone serves as the body's calcium reservoir, exchanging calcium ions with the extracellular fluids in an attempt to equalize extracellular fluid calcium concentrations when conditions of hypo or hyperavailability of calcium exits (Guyton, 1991). Calcium deficiency, caused by inadequate dietary intake, poor absorption and/or extreme excretion, can then severely impact bone health. Bone conditions that are due, at least in part by inadequate calcium levels are known as rickets, osteomalacia and osteoporosis. Experimentally altering dietary concentrations of calcium to levels seen as inadequate have also been shown to drastically affect bone composition in animal models. Gaster et al. (1967) fed rats a calcium inadequate diet (0.02% - 0.03% calcium) for four weeks, which resulted in significant bone rarefaction and a decrease in bone ash. Alfaro et al. (1988) fed dairy calves varying levels of calcium for four weeks and found that calves receiving the calcium inadequate diet (0.17% calcium) had a significant decrease in the calcium content of their bone ash.

Experimentally altering diets to an excessive calcium level has also been shown in animal models to have a drastic impact. Shackelford et al. (1994) fed female rats diets with excessive levels of calcium (0.75%, 1.00% and 1.25% calcium) and reported that calcium levels in the femur displayed a dose-related linear increase, (166.0 ± 5.2, 170.3 ± 6.1 and 169 ± 4.7 in mg/g fresh, respectively), likely displaying the ability of calcitonin to inhibit osteoclast activity. This study

also indicated that extreme intakes of calcium could cause interference with other cations when fetuses from female rats fed supplemental calcium in excess had dose-related reduction in whole-body concentrations of copper, iron, magnesium and phosphorus. Alfaro et al. (1988) also reported nutrient interactions with calcium in dairy calves when dietary levels were increased to 1.31% and 2.35% calcium. Copper, iron, zinc and manganese concentrations were inversely impacted in certain body tissues when dietary calcium increased, with iron and manganese levels decreasing in the rib, zinc concentrations decreasing in the liver, and copper decreasing in the spleen, heart, and muscle. Alfaro et al. (1988) also indicated that serum phosphorus and magnesium concentrations decreased in calves when dietary calcium equaled 2.35% of the diet. These nutrient interactions are believed to not only occur during absorption at the border of the intestinal cell but also inside the body as well (Groff, Gropper, 2000).

Dietary Recommendations

The National Research Council (1978) has recommended that rats receive an estimated 0.50% calcium for maximum bone calcification during growth, although appropriate levels during the lifespan of the rat have not been recommended for bone maintenance. Due to the essentiality of calcium in the body**,** an adequate intake level for humans has been recommended by the Food and Nutrition Board (Institute of Medicine, 1998). This recommendation covers both genders and is specific to an individual's stage of life, from birth to greater than 70 years of age, an adequate intake of calcium ranges from 210 mg/day to 1200 mg/day, respectively.

Silicon

This section will introduce the ultra trace mineral, silicon, focusing on its metabolism and its perceived role in bones and collagen. The experimental affects of Si when dietary levels are altered will also be discussed, in addition to the interactions silicon has with other minerals. The current estimated dietary recommendations for both humans and rats will also be addressed.

Metabolism

Several forms of silicon are known to exist; silica, tetraethylorthosilicate, monosilicic acid, sodium zeolite A and metasilicate are a few of the dietary forms. The dietary form of silicon appears to have a great affect on the amount of absorption, with one research study reporting a difference in absorption rates in humans from 1 to 70% (Nielsen, 1999). Metasilicate is the most soluble form of silicon; this form is widely utilized in animal studies to investigate silicon's biological functions (Groff, Gropper, 1999; Kayongo-Male, Jia, 1999). The mechanism of intestinal absorption of silicon is poorly understood.

Dietary silicon that is not absorbed in the intestinal tract is excreted in the feces. Endogenous silicon is lost mainly through the urine, with urinary silicon output typically increasing with increased silicon intake (Groff, Gropper, 1999; Nielsen, 1999). There does appear to be a defined limit, however, to the amount of silicon excreted by the kidney, which is not due to the kidney's excretory threshold. Thus, urinary excretion of silicon by the kidney appears to be regulated by the rate and extent of absorbed silicon in the intestinal tract (Nielsen, 1999).

Functional Role and Deficiency

The physiological function of silicon is believed to be related to bone and collagen, with silicon participating in the maturation of bone and formation of connective tissue and cartilage. Silicon was first hypothesized to have a role in bone calcification when Carlisle (1970) reported the localization of silicon in the active growth areas of mice and rat bones. During the early stages of bone mineralization, calcium and silicon levels were low in the osteoid layer of the bone, however as mineralization progressed the silicon and calcium concentrations continued to rise, until calcium levels reached the amount present in bone apatite, and silicon levels dropped significantly. This same phenomenon exists in the metaphysis of young bone. Carlisle's research suggests that the concentrations of silicon in bone are related to the level of bone mineral maturity, with low levels of silicon and high levels of calcium indicating a mature bone. Subsequent in vivo research conducted by Carlisle (1974) also supported the role of Si in bone calcification. When rats were fed diets of varying levels of calcium and silicon (0.08, 0.40, 1.20% Ca and 10, 25, 250 ppm Si), the percentage of tibia ash in the calcium deficient rats were significantly increased by increases in dietary silicon.

The role of silicon in bone formation was further substantiated when animal studies indicated silicon deficiency states were unable to coexist with normal growth and skeletal development. When chicks were fed silicon deficient diets, gross abnormalities in skeletal growth were noticeable after 1-2 weeks. Manifestations included growth retardation, reduced bone circumferences, thinning cortexes, decreased leg bone flexibility and decreased skull size with abnormally shaped and flatter cranial bones, when compared to chicks consuming silicon supplemented diets (Carlisle, 1972). Schwartz and Milne (1972) also reported in this same year the effects silicon deficiency has on bones of the rat. Significant growth retardation and skull and bone architecture disturbances resulted in rats fed silicon deficient diet as opposed to rats consuming silicon supplemented diets.

In addition to the role of silicon in bone, silicon is also involved in the formation of cartilage and connective tissue, with silicon deficiency resulting in abnormalities in articular cartilage and connective tissue development. When chicks were fed silicon deficient diets, gross abnormalities in collagen development were noticeable after 1-2 weeks, with legs appearing thinner and combs appearing smaller, when compared to chicks consuming silicon supplemented diets (Carlisle, 1976). The long-bone tibial joints of chicks fed silicon deficient diets were also decreased in size, with less articular cartilage. Hexosamine content (used to assess cartilage and glycosaminoglycan content) in the articular cartilage and in the comb were also decreased in the silicon deficient chicks. These results indicate a role of silicon in glycosaminoglycan metabolism and were further supported by research indicating silicon to be a component of glycosaminoglycans (Schwartz, 1973). Following the analysis of several connective tissue polysaccharides, Schwartz (1973) found silicon to be component of certain glycosaminoglycans and polyuronides, particularly hyaluronic acid, chondroitin 4-sulfate, dermatan sulfate, heparin sulfate, and pectinic and alginic acids. Silicon was reported to be firmly bound to their carbohydrate matrix, possibly aiding in the structural organization of these molecules, affecting their shape, their size and their ability to link to other polysaccharide chains and proteins. These studies clearly indicate the association of silicon in collagen and glycosaminoglycan formation and suggest a role of silicon in the structural organization of cartilage and connective tissue.

Toxicity

Oral ingestion of silicon is unlikely to result in toxic effects (Nielsen, 1999). However, the development of kidney stones has been shown to be associated with excessive silicon intake. Stewart et al. (1993) fed rats varying levels of silicon (0, 540, and 2700 mg Si/kg of diet) and reported the production of uroliths in rats consuming 2700 mg Si/kg of diet. Analysis of the

uroliths produced indicated that silicon was the principle inorganic component of the stone, comprising 91 – 96% of the ash.

Dietary Interactions

Experimentally altering dietary silicon levels in animal studies have shown dietary silicon to interact with several minerals, specifically zinc, copper and molybdenum. Emerick and Kayongo-Male (1990) fed rats varying levels of copper, zinc and silicon (1 and 5 mg Cu/kg, 2 and 12 mg Zn/kg and 5 and 270 mg Si/kg, respectively). An antagonistic relationship between silicon and zinc was reported, with plasma zinc concentrations decreasing with the supplemental silicon diet only in those animals fed zinc-inadequate diets. Najda et al. (1992) also indicated an antagonistic relationship between silicon and zinc when he fed rats increasing doses of silicon over eighteen weeks (0.1 mg Si/g body weight for the first 6 weeks, 0.2 mg Si/g body weight for the second 6 weeks, then 0.4 mg Si/g body weight for the last 6 weeks). Silicon supplementation decreased concentrations of zinc in serum and organs. Silicon supplementation also interacted with copper. Copper concentrations increased in the liver, aorta walls and in the serum with increasing dietary silicon. Carlisle (1979) reported a silicon-molybdenum interaction when chicks were fed normal dietary levels of silicon and molybdenum. Dietary silicon intake decreased molybdenum retention in tissues and plasma.

Dietary Recommendations

Although several researchers have proposed the essentiality of silicon, an adequate intake level has not been recommended by the Food and Nutrition Board (Institute of Medicine, 1998). Current estimates for human silicon requirements range from 2 to 20 mg/day (Carlisle, 1979; Nielsen, 1999; Seaborn, Nielsen, 1993). Although several animal studies provide evidence for the addition of silicon to the list of essential elements for laboratory animals, the National Research

Council (1978) does not have a recommended intake for rats. Dietary levels ranging from 4.5 – 35 mg/kg silicon have been shown to adequately prevent the signs of silicon deficiency in the rat, which may be indicative of adequate intake for silicon in the rat (Nielsen, 1999).

Summary

Many aspects of the role of silicon in the body remain uncertain. Of the studies that have attempted to investigate the involvement of silicon in bone and collagen formation, researchers have used excessive levels of dietary silicon. Additional research where moderate levels of dietary silicon are utilized is required to gain further evidence to support the role of silicon in bone mineralization and collagen metabolism. An understanding of the excessive levels of dietary silicon would also be of importance, to determine if pharmacological effects of silicon on bone exist.

CHAPTER THREE

MATERIALS AND METHODS

Animals and treatments

Sixty weanling male Sprague-Dawley (Sasco, Omaha, NE) rats (age 21 days) were weighed upon arrival and housed three per all-plastic cage measuring 50 x 24 x 16 cm and located inside a laminar air flow rack (Lab Products, Maywood NJ) (Nielsen, Bailey, 1979). Rats were randomly assigned to one of nine treatment groups with no significant differences in weight (mean of 39 g) in a two factor, central composite, response surface design. There were six rats for each rotatable point and twelve for the central point (see Table 3.1). The two factors were either dietary Si as sodium meta-silicate and dietary Ca as calcium carbonate. The silicon and calcium supplements were reagent grade (J.T. Baker, Phillipsburg, NJ). Dietary concentrations of silicon were based on a logarithmic scale (0, 3.5, 35, 350, and 870 µg/g diet) to increase the range of concentrations that could be tested; whereas dietary concentrations of calcium were increased incrementally (0.15%, 0.25%, 0.50%, 0.75% and 0.85% of the diet).

Table 3.1. Number of Animals Delegated to Each Response Surface Point

	0.0 µg/g Si	**3.5 µg/g Si**	**35 µg/g Si**	**350 µg/g Si**	**870 µg/g Si**
0.15% Ca	---	---	6	---	---
0.25% Ca	---	6	---	6	---
0.50% Ca	6	---	12	---	6
0.75% Ca	---	6	---	6	---
0.85% Ca	---	---	6	---	---

The composition of the casein-based basal diet is shown in Table 3.2. Analysis indicated that the basal diet contained 0.6 µg Si/g. Fresh food in plastic cups was provided ad libitum each day. The diets were mixed one week before the start of the experiment. The diets were not pellated and were stored at -16 °C in tightly capped plastic containers. The rats were fed deionized

water (Super Q system, Millipore Corporation, Bedford, MA) in plastic cups. Absorbent paper under the false-bottom cages was changed daily. Room temperature was maintained at 23 °C. Room lighting was controlled automatically to provide 12 h each of light and dark. Animals were weighed and provided clean cages weekly. The rats were fed their respective diets for 9 weeks.

Table 3.2. Composition of Basal Diet

Ingredient	g/kg diet
Casein, low trace element[1, 2]	120.00
Ground corn, acid washed[1, 3]	760.00
Corn oil[4]	75.00
dl-α-tocopherol[1]	0.20
Choline chloride[5]	0.75
Calcium phosphate[5]	5.00
Potassium chloride[5]	7.00
Arginine[6]	5.00
Methionine[6]	2.50
Vitamin mix[7]	4.55
Mineral mix[8]	20.00
Calcium carbonate[5, 9]	Varied

[1]ICN Pharmaceutical, Cleveland, OH.
[2]Deionized water was vacuum filtered through the casein and then the casein was freeze-dried. This procedure decreased Si content of the casein tenfold.
[3]Corn was acid washed by a described procedure (Nielsen, Myron, Givand, Zimmerman, Ollerich, 1975)
[4]Best Foods, Englewood Cliffs, NJ.
[5]JT Baker, Phillipsburg, NJ.
[6]Ajinomoto, Teaneck, NJ.
[7]Composition of vitamin mix, ingredient (g/kg diet): Vitamin A palmitate (1,000,000 IU/g), 0.008; cholecalciferol mix (Vitamin D_3 powder in corn endosperm carrier, 400,000 IU/g), 0.0038; biotin, 0.001; dl-pantothenic acid, 0.048; thiamin HCl, 0.01; pyridoxine HCl, 0.015; vitamin B-12 (0.1% triturate), 0.05; glucose, 4.2992 (ICN, Cleveland, OH); menadione, 0.001 g; folic acid, 0.002; *i*-inositol, 0.050; niacin, 0.03; riboflavin, 0.027; *p*-aminobenzoic acid, 0.005 (GIBCO, Grand Island, NY).
[8]Composition of mineral mix, ingredient (g/kg diet): $NaH_2PO_4 \cdot H_2O$, 9.0; Mg $(C_2H_3O_2)_2 \cdot 4H_2O$, 3.5; $Na_2HAsO_4 \cdot 7H_2O$, 0.005; ("Reagent" grade, JT Baker, Phillipsburg, NJ), Mn $(C_2H_3O_2) \cdot 4H_2O$, 0.225; (EM Industries, Inc., Cherry Hill, NJ), Zn $(C_2H_3O_2) \cdot 2H_2O$, 0.05; Cr $(C_2H_3O_2) \cdot 3H_2O$, 0.002; ("Purified" grade, Fisher Scientific, Fair Lawn, NJ), iron powder dissolved in HCl, 0.04 g; $CuSO_4 \cdot 5H_2O$, 0.03 g; NaF, 0.002; $(NH_4)_6 Mo_7O_{24} \cdot 4H_2O$, 0.0004; H_3BO_3, 0.006; NH_3VO_3, 0.0003; ("Puratronic" grade, Johnson Matthey Chemicals, Limited, England), KI, 0.004; Na_2SeO_3, 0.0003; $NiCl_2 \cdot 3H_2O$, 0.002; (Alfa, Danvers, MA) and corn, acid washed, 7.1366.
[9]Calcium carbonate was added to increase calcium, 0.15%, no addition; 0.25%, 20 g; 0.50%, 70 g; 0.75%, 120g; 0.85%, 140 g.

Collection and analysis of samples

Following a 16-h fast, animals were weighed and decapitated subsequent to ether anesthesia and cardiac exsanguination with a heparin-coated syringe and needle. The lumbar vertebra, right hind and fore legs, and head (containing skull and upper incisor teeth) were removed and frozen until further processing. Alkaline phosphatase concentrations in plasma were measured by colorimetric method (Sigma Chemical Co., St. Louis, MO).

To determine the DNA concentration of bone, the humerus bone was cleaned of adhering tissue, demarrowed, lyophilized in a freeze dryer, and pulverized. DNA was extracted by shaking the aliquot of the pulverized bone with 0.1 N NaOH for 24 h. DNA of an aliquot spotted in falcon tubes was determined colorimetrically using 3,5-diaminobenzoic acid (Gurney, Gurney, 1989). Results were expressed as μg/g dry wt.

An aliquot of pulverized humerus was analyzed for hydroxyproline to assess bone collagen content (Podenphat, Larsen, Christiansen, 1984). Briefly, the aliquot was hydrolyzed in 6 N HCl at 105°C after dilution. The hydroxyproline was extracted by using a strong acidic cation exchange resin (Amberlite, Sigma, catalog I-6641, St. Louis, MO). An acetate-citrate buffer was used to release the hydroxyproline from the resin. Oxidation of hydroxyproline was initiated by choloramine T (with addition of borate buffer and 1 N HCl) followed by a reaction with Ehrlich's reagent (p-dimethylaminobenzaldehyde solution containing concentrated HCl and 2-propranol), which was timed for 15 min at 60°C. The mixture was cooled to room temperature, mixed with 6 N NaOH, and then extracted with toluene followed by an additional extraction with 0.003 N HCl. The extract was measured colorimetrically at 555 nm against standards containing 0.025 to 0.150 mg hydroxyproline/assay. Hydroxyproline was expressed per g dry weight of humeri bone.

The femur, L4 lumbar, skull, and one incisor tooth were freed from excess tissues, cleaned to the periosteal surface with cheese cloth, and dried in a freeze-dry system (Labconco, Kansas City, MO). These tissues were ashed in platinum crucibles utilizing a lithium-boron fusion technique (Lichte, Hopper, Osborn, 1980). Mineral contents of the femur, L4 lumbar, skull, and

incisor teeth were determined by inductively coupled argon plasma atomic emission spectrometry. Standard reference materials (National Institute of Standards and Technology, Gaithersburg, MD) #1572 Citrus Leaves and #1577A Bovine Liver were used as quality control materials in the analyses of minerals.

Statistical Analyses

Data were analyzed using the response surface and regression analyses of PC/SAS (SAS Incorporated Cary, N.C). The primary assumption of response surface designs is that the measured response can be approximated, over the region of interest, by a polynomial in the levels of the treatments factors. The polynomials used included all linear, quadratic, and cross-product terms as potential predictors. An example of a full model, where y is the measured response and b_0 through b_5 are the estimated regression coefficients, is:

$$y = b_0 + b_1 \cdot Si + b_2 \cdot Ca + b_3 \cdot Si^2 + b_4 \cdot Ca^2 + b_5 \cdot Si \cdot Ca$$

The models were reduced by removing statistically non-significant factors, with the criteria that if a quadratic term was significant, the corresponding linear term was included in the model, also. The reduced models were used to predict the dietary intakes of Si and Ca at which the maximum, minimum, or saddle point occurred for each measured response.

CHAPTER FOUR

RESULTS

Sixty weanling male Sprague-Dawley rats were randomly assigned to one of nine treatment groups in a two factor, central composite, response surface design and fed their respective diets for nine weeks. Response surface and regression analyses were utilized to analyze the data. The primary assumption of this analysis is that the measured response can be approximated, over the region of interest, by a polynomial in the levels of the treatments factors. There were no differences in mean body weight between the groups.

Femur Analysis

Table 4.1 and Appendix Figures 1 and 2 display the femur Ca and P response to dietary Ca and Si. There was a significant quadratic response to dietary Ca on the retention of femur Ca and P, with levels of femur Ca and P increasing as dietary Ca levels increased. At higher levels of dietary Ca, femur Ca and P decreased. But at the very highest dietary Ca level, Ca and P femur concentrations increased. For maximum femur Ca deposition, a dietary level of 0.65% Ca was required; maximum femur P deposition required a dietary level of 0.62% Ca. Dietary Si did not affect femur Ca and P concentrations.

Table 4.1 and Appendix Figure 3 display the femur Mg response to dietary Ca and Si. There was a significant quadratic femur Mg response due to dietary Ca. Dietary Ca increased femur Mg retention to a point, and then decreased retention with the two highest levels of dietary Ca. For maximum femur Mg concentration, a dietary level of 0.50% Ca was required. There was no indication that dietary Si had any effect on femur Mg concentrations.

Table 4.1. Macro Mineral Analysis of Femur from Rats Fed Graded Levels of Calcium and Silicon for Nine Weeks

Diet		Ca	P	Mg	Na	K
Si (µg/g)	Ca (% diet)	(mg/g dry weight)	(mg/g dry weight)	(µg/g dry weight)	(µg/g dry weight)	(µg/g dry weight)
0	0.50	239.2 ± 2.9[1]	113.6 ± 0.9	3838 ± 105	3855 ± 96	2843 ± 133
3.5	0.25	215.6 ± 3.3	97.2 ± 2.3	3510 ± 64	3777 ± 152	2822 ± 149
3.5	0.75	229.2 ± 3.3	103.3 ± 2.1	3466 ± 88	4384 ± 106	2697 ± 185
35.0	0.15	170.5 ± 4.2	83.0 ± 1.7	2956 ± 43	3290 ± 146	3674 ± 203
35.0	0.50	232.1 ± 2.7	108.6 ± 1.3	3851 ± 61	4275 ± 65	2689 ± 45
35.0	0.85	242.9 ± 4.8	111.6 ± 1.7	3204 ± 127	4338 ± 74	2502 ± 57
350.0	0.25	223.8 ± 5.2	103.3 ± 1.7	3607 ± 49	3811 ± 146	2844 ± 141
350.0	0.75	229.5 ± 2.6	105.2 ± 1.2	3395 ± 96	3985 ± 87	2499 ± 101
870.0	0.50	226.9 ± 3.4	106.4 ± 1.9	3765 ± 44	4051 ± 55	2677 ± 126
Mean ± Pooled SD		224.6 ± 13.7	104.4 ± 6.0	3556 ± 215	4000 ± 291	2800 ± 358
Response Surface Regression Analysis Model						
Intercept		234.5[6]	109.4[6]	3841[6]	4275[6]	2683[6]
Si		---[2]	---	---	0.1	---
Ca		21.5[6]	8.6[6]	18	401[6]	-371[6]
Si x Si		---	---	---	-284[4]	---
Ca x Si		---	---	---	-206	---
Ca x Ca		-24.7[6]	-12.6[6]	-730[6]	-398[5]	291[3]
R^2		0.60	0.60	0.63	0.53	0.35
F value		43.69[6]	44.06[6]	50.33[6]	12.64[6]	15.72[6]
Maximum Si response (µg/g)		---	---	---	18.0	---
Maximum Ca response (%)		0.65	0.62	0.50	0.69	0.72
Predicted (min, max, or saddle)		239.2 maximum	110.8 maximum	3840 maximum	4387 maximum	2564 minimum

[1]Means ± SEM.
[2] (---) indicates when reduced to simplest model, this term was eliminated.
[3] $p < 0.05$.
[4] $p < 0.01$.
[5] $p < 0.001$.
[6] $p < 0.0001$.

Table 4.1 and Appendix Figure 4 illustrate the femur Na response to graded levels of dietary Ca and Si. A small but significant quadratic Na response to Si existed, with the highest femur Na concentrations at the intermediate levels of dietary Si. There was also a quadratic response due to dietary Ca on the retention of Na in the femur, with increasing levels of dietary Ca increasing the retention of Na in the femur to a point, and then decreasing retention until the highest levels of dietary Ca were administered. For maximum femur Na concentration, a dietary Ca level of 0.69% and a dietary Si level of 18 μg/g diet were predicted.

Table 4.1 and Appendix Figure 5 display the femur K response to dietary Ca and Si. A significant, although not readily obvious, quadratic K response to dietary Ca existed. Increasing levels of Ca from 0.15% to 0.25% dramatically decreased the concentration of femur K. Femur K then moderately decreased with each sequential increase of dietary Ca. For minimum femur K concentration, a Ca dietary level of 0.72% was required. Dietary Si had no effect on femur K concentrations.

Table 4.2 and Appendix Figure 6 illustrate the femur Cu response to graded levels of dietary Ca and Si. There was a quadratic femur Cu concentration response due to dietary Si. When dietary Si was absent, Cu concentrations were high, decreasing to a minimum and then increasing to the logarithmic increases in dietary Si. For the minimum femur Cu concentration, the regression analysis indicates that 28 μg Si/g diet was required. Dietary Ca did not have any effect on femur Cu concentrations.

Table 4.2 displays the femur Zn response to dietary Ca and Si. Although the Ca x Si interaction was significant at a $p<0.05$ level, a response surface regression analysis model of the femur Zn response could not be determined.

Table 4.2 and Appendix Figure 7 illustrate the femur Fe response to dietary Ca and Si. There was a significant quadratic Fe response due to dietary Ca. As levels of Ca increased, the

Table 4.2. Micro and Trace Mineral Analysis of Femur from Rats Fed Graded Levels of Calcium and Silicon for Nine Weeks

Diet		Cu	Zn	Fe	Mn	Mo	Si
Si (μg/g)	Ca (% diet)	(μg/g dry wt)	(μg/g dry wt)	(μg/g dry wt)	(μg/g dry wt)	(μg/g dry wt)	(μg/g dry wt)
0	0.50	4.22 ± 0.11[1]	152.6 ± 3.3	64.6 ± 3.6	0.90 + 0.02	4.22 ± 0.10	4.48 ± 0.52
3.5	0.25	2.49 ± 0.40	144.9 ± 4.6	103.0 ± 9.1	1.79 ± 0.06	3.91 ± 0.09	4.30 ± 1.03
3.5	0.75	2.34 ± 0.13	156.9 ± 4.0	70.2 ± 2.8	0.70 ± 0.02	3.84 ± 0.10	4.41 ± 0.52
35.0	0.15	3.21 ± 0.33	149.4 ± 5.4	173.4 ± 7.9	2.36 ± 0.13	3.78 ± 0.21	4.14 ± 0.89
35.0	0.50	2.82 ± 0.19	157.0 ± 3.3	72.8 ± 3.2	0.88 ± 0.04	4.19 ± 0.11	6.90 ± 0.77
35.0	0.85	2.00 ± 0.20	154.6 ± 6.3	54.8 ± 5.4	0.67 ± 0.01	3.58 ± 0.16	5.42 ± 0.46
350.0	0.25	3.37 ± 0.18	157.3 ± 4.0	114.6 ± 10.4	2.27 ± 0.13	4.37 ± 0.13	5.86 ± 0.50
350.0	0.75	3.93 ± 0.19	148.5 ± 2.0	56.8 ± 4.3	0.77 ± 0.02	4.25 ± 0.12	5.60 ± 0.64
870.0	0.50	3.44 ± 0.24	152.2 ± 4.6	67.0 ± 5.7	0.83 ± 0.02	4.24 ± 0.11	5.57 ± 0.46
Mean ± Pooled SD		3.11 ± 0.76	153.1 ± 10.8	84.8 ± 17.9	1.20 ± 0.20	4.06 ± 0.35	5.33 ± 1.85
Response Surface Regression Analysis Model							
Intercept		2.62[6]	153.1[6]	67.4[6]	0.92[6]	4.26[6]	6.89[6]
Si		0.15	0.7	---	0.07	0.14[3]	0.76[3]
Ca		---[2]	1.9	-45.4[6]	-0.88[6]	-0.09	0.29
Si x Si		1.16[6]	---	---	---	---	-1.79[4]
Ca x Si		---	-10.3[3]	---	-0.23[4]	---	---
Ca x Ca		---	---	43.2[6]	0.69[6]	-0.50[6]	-2.04[4]
R^2		0.27	0.10	0.78	0.91	0.29	0.22
F value		10.37[5]	2.05	102.9[6]	148.77[6]	7.67[5]	3.90[4]
Maximum Si response (μg/g)		28.0		---	0.0	871.0[7]	68.0
Maximum Ca response (%)		---		0.68	0.61	0.47	0.53
Predicted (min, max, or saddle)		2.6 minimum	Model not statistically significant	55.5 minimum	0.72 minimum	4.4 maximum	6.99 maximum

[1] Means ± SEM.
[2] (---) indicates when reduced to simplest model, this term was eliminated.
[3] $p < 0.05$.
[4] $p < 0.01$.
[5] $p < 0.001$.
[6] $p < 0.0001$.
[7] Si was included in model as a linear factor only, so Si was arbitrarily set at the maximum value in the response surface analysis.

retention of femur Fe decreased. The most dramatic decreases occurred as dietary Ca changed from 0.15 to 0.25%. For minimum femur Fe concentration, a dietary level of 0.68% Ca was required. Dietary Si appeared to have no effect on femur Fe concentrations.

Table 4.2 and Appendix Figure 8 display the femur Mn response to dietary Ca and Si. There was a small but significant Ca x Si interaction on femur Mn, with increasing dietary Si increasing femur Mn concentrations at high and low levels of dietary Ca. There was also a quadratic response due to dietary Ca on femur Mn concentrations. Increasing dietary Ca levels decreased femur Mn retention. The most dramatic decrease occurred as Ca increased from 0.25% to 0.50%. For minimum femur Mn concentrations, the regression analysis indicates that 0.61% dietary Ca was required.

Table 4.2 and Appendix Figure 9 illustrate the femur Mo response to graded levels of Ca and Si. A small but significant linear relationship between dietary Si and femur Mo concentrations existed. Increasing dietary Si increased the retention of Mo in the femur. There was also a significant quadratic response to dietary Ca on the retention of femur Mo, with the levels of Mo increasing to a plateau in response to increased Ca, and then decreasing at the highest levels of dietary Ca. For maximum femur Mo concentrations, a dietary level of 0.47% Ca was required when dietary Si was arbitrarily set to the maximum.

Table 4.2 and Appendix Figure 10 display the femur Si response to dietary Ca and Si. There was a quadratic response to dietary Si and Ca on femur Si concentrations, with the highest levels of femur Si found at the intermediate dietary levels of Si and Ca. For maximum femur Si concentration, a dietary Ca level of 0.53% and a dietary Si level of 68 μg/g diet were predicted.

Vertebra Analysis

Table 4.3 and Appendix Figures 11 and 12 display the vertebra Ca and P response to graded levels of Ca and Si. Unlike the femur response, a significant linear relationship existed

Table 4.3. Macro Mineral Analysis of Vertebra from Rats Fed Graded Levels of Calcium and Silicon for Nine Weeks

Diet		Ca	P	Mg	Na	K
Si (µg/g)	Ca (% diet)	(mg/g dry wt)	(mg/g dry wt)	(µg/g dry wt)	(µg/g dry wt)	(µg/g dry wt)
0	0.50	169.9 ± 5.1[1]	80.2 ± 2.4	2770 ± 82	5145 ± 153	5293 ± 250
3.5	0.25	158.3 ± 7.3	74.3 ± 3.4	2809 ± 126	3863 ± 119	5858 ± 231
3.5	0.75	156.7 ± 9.9	72.0 ± 4.5	2549 ± 158	4030 ± 47	4828 ± 164
35.0	0.15	134.6 ± 7.3	61.9 ± 4.0	2542 ± 111	3447 ± 109	7156 ± 276
35.0	0.50	184.1 ± 2.8	85.6 ± 1.1	3092 ± 52	4118 ± 58	4714 ± 112
35.0	0.85	190.2 ± 7.1	87.7 ± 2.8	2789 ± 153	4213 ± 118	4867 ± 252
350.0	0.25	173.5 ± 7.2	80.9 ± 3.2	3034 ± 85	3824 ± 69	5692 ± 306
350.0	0.75	195.1 ± 3.8	90.5 ± 1.7	3028 ± 102	4279 ± 118	5018 ± 161
870.0	0.50	184.0 ± 7.7	86.0 ± 3.3	3080 ± 122	4229 ± 97	4846 ± 289
Mean ± Pooled SD		172.9 ± 17.4	80.5 ± 8.1	2880 ± 275	4141 ± 337	5303 ± 598
Response Surface Regression Analysis Model						
Intercept		180.7[6]	84.5[6]	3014[6]	4117[6]	4873[6]
Si		12.3[5]	5.5[4]	199[5]	-212[4]	---
Ca		17.8[6]	7.9[6]	18	297[6]	-874[6]
Si x Si		---[2]	---	---	467[5]	---
Ca x Si		---	---	---	---	---
Ca x Ca		-18.1[4]	-9.6[5]	-332[5]	-425[4]	1063[6]
R^2		0.45	0.45	0.31	0.57	0.58
F value		15.05[6]	15.02[6]	8.14[6]	18.50[6]	39.10[6]
Maximum Si response (µg/g)		871.0[7]	871.0[7]	871.0[7]	72.0	---
Maximum Ca response (%)		0.82	0.64	0.51	0.62	0.64
Predicted (min, max, or saddle)		197.4 maximum	91.7 maximum	3213 maximum	4146 saddle	4692 minimum

[1]Means ± SEM.
[2] (---) indicates when reduced to simplest model, this term was eliminated.
[3] $p < 0.05$.
[4] $p < 0.01$.
[5] $p < 0.001$.
[6] $p < 0.0001$.
[7]Si was included in model as a linear factor only, so Si was arbitrarily set at the maximum value in the response surface analysis.

between dietary Si and vertebra Ca and P retention. Increasing dietary Si increased retention of Ca and P in the vertebra. There was also a quadratic Ca and P response due to increasing dietary Ca, with Ca and P concentrations increasing to a point, decreasing, and then increasing at the higher levels of dietary Ca. For maximum vertebra Ca deposition, a dietary level of 0.82% Ca was required; maximum vertebra P deposition required a dietary level of 0.64% Ca. Si was included in the response surface analysis models of Ca and P as a linear factor only, arbitrarily being set at 871 μg/g diet.

Table 4.3 and Appendix Figure 13 illustrate the vertebra Mg response to dietary Ca and Si. There was a linear relationship between dietary Si and vertebra Mg concentrations, with increasing levels of dietary Si increasing vertebra Mg retention. A significant quadratic response to dietary Ca also existed. As dietary Ca increased, vertebra Mg levels increased to a plateau and then decreased at the higher percentages of dietary Ca. For maximum vertebra Mg concentration, a dietary level of 0.51% Ca was required. A Si level of 871 μg/g diet was included in the model as a linear factor only, set at its maximum value in this analysis.

Table 4.3 and Appendix Figure 14 display the vertebra Na response to graded levels of Ca and Si. A significant quadratic response existed between dietary Si and vertebra Na retention. Increasing dietary Si levels initially decreased Na concentrations, with the lowest retentions at the intermediate levels of dietary Si. At the highest dietary Si levels, Na concentrations slightly increased, but not to the levels found with the 0 μg Si/g diet intake. There was also a quadratic response between dietary Ca and vertebra Na deposition, with increasing dietary Ca levels increasing vertebra Na concentrations. The highest deposition of vertebra Na was at the intermediate levels of dietary Ca. For the saddle point of vertebra Na concentration, a Si dietary level of 72 μg/g and a Ca dietary level of 0.62% were required.

Table 4.3 and Appendix Figure 15 illustrate the vertebra K response to dietary Ca and Si. The K response to dietary Ca in the vertebrae was similar to the femur K response. A significant

quadratic K response to dietary Ca existed. As levels of Ca increased, the retention of vertebra K decreased. Increasing levels of Ca from 0.15% to 0.25% produced the most dramatic decreases in concentration, with further decreases occurring at the higher percentages of dietary Ca. For minimum vertebra K concentration, the regression analysis indicated that 0.64% of dietary Ca was required. Dietary Si had no effect on vertebra K concentrations.

Table 4.4 displays the vertebra Cu response to graded levels of Ca and Si. Although the Si x Si interaction was significant at a $p<0.05$ level, a response surface regression analysis model of the vertebra Cu response could not be determined.

Table 4.4 and Appendix Figure 16 illustrate the vertebra Zn response to dietary Ca and Si. A small, but significant quadratic Zn response to Si existed. Increasing levels of dietary Si increased Zn deposition in the vertebrae, which reaches a plateau at 350 μg Si/g. For a maximum vertebra Zn concentration, the regression analysis indicates that 175 μg Si/g diet was required. Dietary Ca did not have any effect on vertebra Zn concentrations.

Table 4.4 and Appendix Figures 17 and 18 display the vertebra Fe and Mn response to graded levels of Ca and Si. Vertebra Fe responded similarly to the response that occurred in the femur, while the Mn response differed between these two bones. There was a significant quadratic response to dietary Ca on the retention of vertebra Fe and Mn, with levels of Fe and Mn decreasing as dietary Ca percentages increased. The decreases in deposition occurred most dramatically at low to intermediate levels of dietary Ca, forming a plateau at the higher percentages of dietary Ca. For minimum vertebra Fe deposition, a dietary level of 0.69% Ca was required; minimum vertebra Mn deposition required a dietary level of 0.74% Ca. Dietary Si did not affect vertebra Fe and Mn concentrations.

Table 4.4. Micro and Trace Mineral Analysis of Vertebra from Rats Fed Graded Levels of Calcium and Silicon for Nine Weeks

Diet		Cu	Zn	Fe	Mn	Mo	Si
Si (µg/g)	Ca (% diet)	(µg/g dry wt)	(µg/g dry wt)	(µg/g dry wt)	(µg/g dry wt)	(µg/g dry wt)	(µg/g dry wt)
0	0.50	3.83 ± 0.07[1]	108.1 ± 2.5	77.0 ± 3.9	0.80 ± 0.03	3.93 ± 0.16	3.31 ± 0.36
3.5	0.25	3.54 ± 0.17	127.2 ± 5.4	117.1 ± 7.5	1.79 ± 0.21	4.40 ± 0.18	4.31 ± 1.12
3.5	0.75	2.93 ± 0.12	130.8 ± 3.9	72.9 ± 3.1	0.69 ± 0.02	4.05 ± 0.10	4.14 ± 0.55
35.0	0.15	3.51 ± 0.23	136.4 ± 7.4	180.0 ± 6.0	2.15 ± 0.09	4.41 ± 0.35	3.25 ± 0.64
35.0	0.50	3.24 ± 0.17	134.3 ± 3.3	80.8 ± 4.2	0.84 ± 0.05	4.23 ± 0.14	3.57 ± 0.21
35.0	0.85	3.12 ± 0.16	130.1 ± 7.8	65.7 ± 5.1	0.69 ± 0.02	3.97 ± 0.22	2.76 ± 0.56
350.0	0.25	3.63 ± 0.26	137.8 ± 5.5	126.6 ± 7.9	1.92 ± 0.13	4.46 ± 0.31	0.68 ± 0.33
350.0	0.75	3.56 ± 0.18	135.3 ± 5.2	74.3 ± 7.0	0.73 ± 0.04	4.56 ± 0.31	1.58 ± 0.48
870.0	0.50	3.71 ± 0.47	137.3 ± 2.8	82.0 ± 5.0	1.15 ± 0.41	4.53 ± 0.28	3.23 ± 1.33
Mean ± Pooled SD		3.43 ± 0.58	130.7 ± 12.7	95.8 ± 15.8	1.16 ± 0.38	4.28 ± 0.57	3.07 ± 1.75
Response Surface Regression Analysis Model							
Intercept		3.24[6]	135.2[6]	78.8[6]	0.94[6]	4.27[6]	3.04[6]
Si		0.01	10.4[5]	---	---	0.26[3]	-1.06[4]
Ca		---[2]	---	-45.6[6]	-0.77[6]	---	---
Si x Si		0.48[3]	-10.3[3]	---	---	---	---
Ca x Si		---	---	---	---	---	---
Ca x Ca		---	---	41.5[6]	0.55[6]	---	---
R^2		0.10	0.29	0.82	0.66	0.08	0.13
F value		3.07	11.38[6]	128.4[6]	56.42[6]	4.89[3]	8.79[4]
Maximum Si response (µg/g)			175.0	---	---		
Maximum Ca response (%)			---	0.69	0.74		
Predicted (min, max, or saddle)		Model not statistically significant	137.8 maximum	66.3 minimum	0.67 minimum	Linear model (x = Si)	Linear model (x = Si)

[1] Means ± SEM.
[2] (---) indicates when reduced to simplest model, this term was eliminated.
[3] $p < 0.05$.
[4] $p < 0.01$.
[5] $p < 0.001$.
[6] $p < 0.0001$.

Table 4.4 and Appendix Figure 19 illustrate the vertebra Mo response to dietary Ca and Si. A significant linear relationship existed between dietary Si and vertebra Mo, with Mo deposition increasing as dietary Si levels increased. Dietary Ca had no effect on vertebra Mo concentrations.

Table 4.4 and Appendix Figure 20 display the vertebra Si response to graded levels of Ca and Si. There was a significant linear Si response to dietary Si in the vertebrae. As dietary Si levels increased, the retention of vertebra Si decreased. Dietary Ca appeared to have no effect on vertebra Si concentrations.

Skull Analysis

Table 4.5 and Appendix Figures 21, 22, and 23 illustrate the skull Ca, P and Mg responses to dietary Ca and Si. There was a significant quadratic response to dietary Si and Ca on skull Ca, P, and Mg concentrations. The highest deposition of skull Ca, P and Mg occurred at the intermediate levels of dietary Si and Ca. For maximum skull Ca concentration, a dietary Ca level of 0.62% and a dietary level of 36 μg Si/g diet were predicted. For maximum skull P concentration, a dietary Ca level of 0.59% and a dietary level of 45 μg Si/g diet were predicted. For maximum skull Mg concentration, a dietary Ca level of 0.54% and a dietary level of 39 μg Si/g diet were predicted.

Table 4.5 and Appendix Figure 24 display the skull Na response to graded levels of Ca and Si. A significant inverse linear relationship between dietary Si and Na retention in the skull existed, with increasing levels of Si decreasing skull Na deposition. There was also a Na quadratic response to dietary Ca. As dietary Ca levels increased, Na retention increased to 5322 μg Na/g dry weight of skull, decreased, and then increased at the highest percentage of dietary Ca. For the maximum skull Na concentration, the regression analysis indicates that 0.59% Ca was required. A

Table 4.5. Macro Mineral Analysis of Skull from Rats Fed Graded Levels of Calcium and Silicon for Nine Weeks

Diet		Ca	P	Mg	Na	K
Si (µg/g)	Ca (% diet)	(mg/g dry wt)	(mg/g dry wt)	(µg/g dry wt)	(µg/g dry wt)	(µg/g dry wt)
0	0.50	212.8 ± 4.5[1]	91.1 ± 2.3	3638 ± 91	5322 ± 155	4043 ± 291
3.5	0.25	182.5 ± 3.8	80.8 ± 1.6	3385 ± 79	4490 ± 128	4777 ± 235
3.5	0.75	218.8 ± 2.6	97.8 ± 3.0	3679 ± 54	4589 ± 89	3200 ± 119
35.0	0.15	135.1 ± 2.8	67.0 ± 1.9	2605 ± 55	3596 ± 45	5433 ± 196
35.0	0.50	226.5 ± 3.9	110.6 ± 2.2	4231 ± 95	4921 ± 98	3312 ± 125
35.0	0.85	217.9 ± 4.9	99.8 ± 2.7	3264 ± 196	4915 ± 44	3622 ± 259
350.0	0.25	186.7 ± 5.6	87.1 ± 2.4	3334 ± 115	4215 ± 50	4278 ± 259
350.0	0.75	214.7 ± 5.9	96.8 ± 2.2	3488 ± 98	4501 ± 120	3152 ± 226
870.0	0.50	212.3 ± 3.0	96.9 ± 1.5	3887 ± 58	4585 ± 170	3396 ± 193
Mean ± Pooled SD		203.4 ± 12.9	97.8 ± 6.5	3577 ± 284	4631 ± 352	3871 ± 565
Response Surface Regression Analysis Model						
Intercept		226.5[6]	110.6[6]	4231[6]	4911[6]	3485[6]
Si		0.2	2.6	30	-259[5]	-285[4]
Ca		32.1[6]	12.9[6]	245[6]	398[6]	-928[6]
Si x Si		-10.9[3]	-15.6[6]	-412[5]	---	---
Ca x Si		---[2]	---	---	---	---
Ca x Ca		-46.5[6]	-26.1[6]	-1223[6]	-737[6]	930[6]
R^2		0.82	0.80	0.73	0.60	0.62
F value		60.95[6]	53.7[6]	37.02[6]	28.59[6]	30.80[6]
Maximum Si response (µg/g)		36.0	45.0	39.0	1.0[7]	871.0[7]
Maximum Ca response (%)		0.62	0.59	0.54	0.59	0.67
Predicted (min, max, or saddle)		232.1 maximum	112.3 maximum	4244 maximum	5223 maximum	2969 minimum

[1] Means ± SEM.
[2] (---) indicates when reduced to simplest model, this term was eliminated.
[3] $p < 0.05$.
[4] $p < 0.01$.
[5] $p < 0.001$.
[6] $p < 0.0001$.
[7] Si was included in model as a linear factor only, so Si was arbitrarily set to either the minimum or the maximum value in the response surface analysis.

Si level of 1 μg Si/g diet was included in the model as a linear factor only, set at its minimum value in this analysis.

Table 4.5 and Appendix Figure 25 illustrate the skull K response to dietary Ca and Si. There was a linear response due to dietary Si on skull K retention, with skull K levels decreasing as dietary Si increased. A quadratic response to dietary Ca also existed for skull K. As dietary Ca levels increased, K levels decreased until the highest percentage of dietary Ca was administered, causing a slight increase in retention. For the minimum skull K concentration, a dietary level of 0.67% Ca was required. Si was included in the response surface analysis model of K as a linear factor only, arbitrarily being set at the maximum of 871 μg Si/g diet.

Table 4.6 and Appendix Figure 26 display the skull Cu response to graded levels of Ca and Si. A significant linear relationship between dietary Si and skull Cu existed, with increasing dietary Si levels decreasing skull Cu retention. A linear relationship between dietary Ca and skull Cu also existed. As dietary Ca levels increased, skull Cu retention decreased.

Table 4.6 and Appendix Figure 27 illustrate the skull Zn response to dietary Ca and Si. There was a linear response due to dietary Si on skull Zn deposition with increasing levels of dietary Si increasing skull Zn concentrations. Calcium had no effect on skull Zn concentrations. A linear model, where x = Si, was the predicted response surface regression analysis model.

Table 4.6 and Appendix Figures 28 and 29 display the skull Fe and Mn responses to graded levels of Ca and Si. The skull Fe and Mn responses to dietary Ca was very similar to the responses found in the vertebrae for these two trace minerals. A significant quadratic response to dietary Ca on skull Fe and Mn concentrations existed. As dietary Ca levels increased, the concentrations of skull Fe and Mn decreased, with the most pronounced concentration changes occurring at the low to intermediate levels of dietary Ca. The concentrations of skull Fe and Mn

Table 4.6. Micro and Trace Mineral Analysis of Skull from Rats Fed Graded Levels of Calcium and Silicon for Nine Weeks

Diet		Cu	Zn	Fe	Mn	Mo	Si
Si (µg/g)	Ca (% diet)	(µg/g dry wt)	(µg/g dry wt)	(µg/g dry wt)	(µg/g dry wt)	(µg/g dry wt)	(µg/g dry wt)
0	0.50	4.83 ± 0.22[1]	116.3 ± 3.2	44.5 ± 1.9	0.99 ± 0.05	6.16 ± 0.18	3.35 ± 0.50
3.5	0.25	5.87 ± 1.19	129.7 ± 2.5	92.5 ± 7.5	2.57 ± 0.24	6.23 ± 0.26	3.87 ± 1.23
3.5	0.75	4.03 ± 0.29	132.1 ± 4.5	46.1 ± 1.5	1.06 ± 0.08	6.25 ± 0.33	5.79 ± 0.79
35.0	0.15	4.76 ± 0.62	122.5 ± 9.8	146.1 ± 6.8	2.99 ± 0.32	5.22 ± 0.23	4.97 ± 0.42
35.0	0.50	4.31 ± 0.20	133.3 ± 3.2	52.1 ± 2.3	1.33 ± 0.17	6.27 ± 0.42	5.67 ± 0.52
35.0	0.85	4.61 ± 0.33	136.9 ± 7.2	42.5 ± 3.7	0.98 ± 0.03	6.22 ± 0.15	4.68 ± 1.28
350.0	0.25	4.87 ± 0.37	146.6 ± 6.1	93.5 ± 5.3	2.95 ± 0.13	6.66 ± 0.21	3.38 ± 0.68
350.0	0.75	2.88 ± 0.04	130.4 ± 2.3	47.2 ± 8.0	0.84 ± 0.04	5.62 ± 0.20	1.58 ± 0.52
870.0	0.50	3.22 ± 0.17	132.7 ± 4.6	51.6 ± 4.4	0.96 ± 0.04	5.69 ± 0.22	3.05 ± 3.05
Mean ± Pooled SD		4.38 ± 1.12	130.9 ± 13.9	66.8 ± 13.0	1.59 ± 0.47	6.07 ± 0.88	4.22 ± 2.21
Response Surface Regression Analysis Model							
Intercept		4.37[6]	131.2[6]	49.1[6]	1.21[6]	6.26[6]	5.10[6]
Si		-0.75[4]	7.6[6]	---	---	-0.15	-0.82
Ca		-0.69[4]	---	-42.2[6]	-1.14[6]	0.07	---
Si x Si		---[2]	---	---	---	-0.17	-2.23[4]
Ca x Si		---	---	---	---	-0.52	---
Ca x Ca		---	---	43.5[6]	0.94[6]	-0.35	---
R^2		0.25	0.11	0.86	0.75	0.07	0.17
F value		9.24[5]	7.49[4]	173.2[6]	88.67[6]	0.79	5.89
Maximum Si response (µg/g)				---	---		19.0
Maximum Ca response (%)				0.67	0.71		---
Predicted (min, max, or saddle)		Linear model (x=Si, y=Ca)	Linear model (x=Si)	38.82 minimum	0.87 minimum	Model not statistically significant	5.18 maximum

[1]Means ± SEM.
[2] (---) indicates when reduced to simplest model, this term was eliminated.
[3] $p < 0.05$
[4] $p < 0.01$.
[5] $p < 0.001$.
[6] $p < 0.0001$.

then appeared to stabilize as dietary Ca levels increased from intermediate to high levels. For minimum skull Fe concentrations, a dietary level of 0.67% Ca was required; minimum skull Mn concentrations required a dietary level of 0.71% Ca. Dietary Si did not affect skull Fe and Mn concentrations.

Table 4.6 illustrates the skull Mo response to dietary Ca and Si. A significant response surface analysis model could not be predicted for the skull Mo response.

Table 4.6 and Appendix Figure 30 display the skull Si response to graded levels of dietary Ca and Si. There was a significant quadratic response to dietary Si on skull Si deposition. The highest deposition of skull Si occurred at the low to intermediate levels of dietary Si. For the maximum skull Si concentration, the regression analysis indicates that 19 μg Si/g diet was required. Dietary Ca appeared to have no effect on skull Si concentrations.

Teeth Analysis

Table 4.7 and Appendix Figure 31 illustrate the teeth Ca response to dietary Ca and Si. There was a quadratic response to dietary Si and Ca on teeth Ca concentrations, with the highest retention of Ca occurring with low dietary Si and 0.50% dietary Ca. For the saddle point of teeth Ca concentration, a Si dietary level of 165 μg/g and a Ca dietary level of 0.64% were required.

Table 4.7 and Appendix Figure 32 display the teeth P response to graded levels of Ca and Si. A significant quadratic response to dietary Si existed for teeth P concentrations. As dietary Si levels increased, teeth P concentrations decreased. Increasing levels of dietary Si from 0 to 3.5 μg Si/g diet produced the most dramatic decreases in concentration, with the concentrations almost stabilizing at the higher levels of dietary Si. For minimum teeth P concentration, the regression

Table 4.7. Macro Mineral Analysis of Teeth from Rats Fed Graded Levels of Calcium and Silicon for Nine Weeks

Diet		Ca	P	Mg	Na	K
Si (µg/g)	Ca (% diet)	(mg/g dry wt)	(mg/g dry wt)	(µg/g dry wt)	(µg/g dry wt)	(µg/g dry wt)
0	0.50	273.9 ± 2.8[1]	139.9 ± 9.2	5520 ± 332	5254 ± 143	2621 ± 113
3.5	0.25	251.7 ± 3.6	127.1 ± 2.0	6090 ± 380	4684 ± 123	2694 ± 156
3.5	0.75	263.3 ± 3.3	130.7 ± 1.4	5584 ± 284	4879 ± 137	2295 ± 141
35.0	0.15	238.1 ± 5.5	122.9 ± 2.9	6476 ± 423	4567 ± 154	3052 ± 104
35.0	0.50	253.6 ± 1.8	126.8 ± 1.1	5741 ± 214	4964 ± 83	2372 ± 52
35.0	0.85	251.0 ± 3.8	123.3 ± 2.3	5014 ± 207	4885 ± 75	2339 ± 140
350.0	0.25	244.9 ± 3.4	122.7 ± 1.3	5808 ± 364	4743 ± 220	2335 ± 124
350.0	0.75	256.0 ± 1.3	126.7 ± 0.9	5595 ± 529	5048 ± 236	2229 ± 159
870.0	0.50	250.3 ± 1.8	125.3 ± 0.8	5568 ± 46	4882 ± 126	2326 ± 106
Mean ± Pooled SD		253.6 ± 8.0	127.7 ± 10.1	5709 ± 796	4896 ± 364	2473 ± 309
Response Surface Regression Analysis Model						
Intercept		253.6[6]	124.3[6]	5703[6]	5024[6]	2380[6]
Si		-8.5[6]	-5.4[4]	---	---	-158[4]
Ca		7.1[6]	---	-496[4]	165[3]	-267[6]
Si x Si		8.8[4]	7.5[3]	---	---	---
Ca x Si		---[2]	---	---	---	---
Ca x Ca		-8.7[4]	---	---	-322[4]	212[3]
R^2		0.58	0.19	0.13	0.17	0.33
F value		18.87[6]	6.72[4]	9.23[4]	5.88[4]	9.19[6]
Maximum Si response (µg/g)		165.0	111.0		---	871.0[7]
Maximum Ca response (%)		0.64	---		0.59	0.72
Predicted (min, max, or saddle)		253 saddle	123.3 minimum	Linear model (x = Ca)	5045 maximum	2138 minimum

[1] Means ± SEM.
[2] (---) indicates when reduced to simplest model, this term was eliminated.
[3] $p < 0.05$.
[4] $p < 0.01$.
[5] $p < 0.001$.
[6] $p < 0.0001$.
[7] Si was included in model as a linear factor only, so Si was arbitrarily set at the maximum value in the response surface analysis.

analysis indicates that 111 μg Si/g diet was required. Dietary Ca had no effect on teeth P concentrations, which is unique to this tissue.

Table 4.7 and Appendix Figure 33 illustrate the teeth Mg response to dietary Ca and Si. There was a significant linear relationship between dietary Ca and teeth Mg concentrations, with increasing levels of dietary Ca decreasing teeth Mg concentrations. A linear model, where x = Ca, was the predicted response surface regression analysis model for the teeth Mg response. Dietary Si appeared to have no effect on teeth Mg concentrations.

Table 4.7 and Appendix Figure 34 display the teeth Na response to graded levels of Ca and Si. A quadratic Na response to dietary Ca existed. As dietary Ca percentages increased, teeth Na retention increased. The highest retentions of teeth Na occurred at the intermediate to high percentages of dietary Ca. For maximum teeth Na retention, a dietary level of 0.59% Ca was predicted. There was no indication that dietary Si had any effect on teeth Na concentrations.

Table 4.7 and Appendix Figure 35 illustrate the teeth K response to dietary Ca and Si. A small but significant linear relationship between dietary Si and teeth K deposition existed, with increasing levels of dietary Si decreasing K deposition. There was also a significant, although not readily obvious, quadratic response to dietary Ca on the deposition of teeth K. As dietary Ca increased, K deposition decreased. The decreases in K occurred most dramatically as dietary Ca percentages increased from low to intermediate, with only moderate decreases occurring as Ca percentages increased to the high levels. For minimum teeth K deposition, a dietary level of 0.72% Ca was required. A Si level of 871 μg/g was included in the model as a linear factor only, set at its maximum value in this analysis.

Table 4.8 and Appendix Figure 36 display the teeth Cu response to graded levels of Ca and Si. There was a linear relationship between dietary Si and teeth Cu concentrations, with increasing levels of dietary Si decreasing teeth Cu concentrations. The predicted response surface

Table 4.8. Micro and Trace Mineral Analysis of Teeth from Rats Fed Graded Levels of Calcium and Silicon for Nine Weeks

Diet		Cu	Zn	Fe	Mn	Mo	Si
Si (µg/g)	Ca (% diet)	(µg/g dry wt)	(µg/g dry wt)	(µg/g dry wt)	(µg/g dry wt)	(µg/g dry wt)	(µg/g dry wt)
0	0.50	5.49 ± 0.31[1]	91.5 ± 4.7	112.2 ± 8.9	1.56 ± 0.08	6.33 ± 0.30	5.36 ± 0.53
3.5	0.25	4.89 ± 0.64	97.0 ± 3.5	145.3 ± 6.3	3.90 ± 0.20	6.14 ± 0.36	5.78 ± 0.56
3.5	0.75	4.61 ± 0.26	100.1 ± 4.6	125.1 ± 5.5	1.46 ± 0.11	6.09 ± 0.23	4.01 ± 0.17
35.0	0.15	5.48 ± 0.43	101.7 ± 4.9	195.5 ± 7.7	6.27 ± 0.38	6.58 ± 0.35	5.32 ± 0.39
35.0	0.50	5.16 ± 0.24	102.2 ± 1.9	119.9 ± 4.2	1.78 ± 0.13	6.18 ± 0.20	5.67 ± 0.62
35.0	0.85	5.01 ± 1.09	97.6 ± 4.8	114.5 ± 3.2	1.29 ± 0.02	5.63 ± 0.06	3.57 ± 0.18
350.0	0.25	4.11 ± 0.34	101.9 ± 4.8	142.9 ± 8.5	4.69 ± 0.26	5.86 ± 0.29	5.86 ± 0.35
350.0	0.75	4.41 ± 0.55	98.5 ± 4.8	124.8 ± 11.3	1.69 ± 0.26	5.72 ± 0.48	8.42 ± 0.66
870.0	0.50	3.75 ± 0.25	97.5 ± 4.8	117.3 ± 5.8	1.44 ± 0.05	5.41 ± 0.19	5.58 ± 0.99
Mean ± Pooled SD		4.84 ± 1.23	98.8 ± 10.5	131.2 ± 19.2	2.60 ± 0.55	6.03 ± 0.73	5.47 ± 1.69
Response Surface Regression Analysis Model							
Intercept		4.81[6]	102.2[6]	116.4[6]	1.69[6]	6.01[6]	5.52[6]
Si		-0.62[4]	2.2	---	---	-0.34[3]	0.75[3]
Ca		---[2]	-1.1	-27.1[6]	-2.21[6]	---	-0.34
Si x Si		---	-6.8	---	---	---	---
Ca x Si		---	-3.3	---	---	---	2.03[4]
Ca x Ca		---	-1.3	37.4[6]	2.19[6]	---	---
R^2		0.10	0.09	0.58	0.90	0.09	0.20
F value		6.44[3]	1.11	40.55[6]	261.7[6]	5.50[3]	4.70[4]
Maximum Si response (µg/g)				---	---		
Maximum Ca response (%)				0.63	0.68		
Predicted (min, max, or saddle)		Linear model (x = Si)	Model not statistically significant	111.4 minimum	1.14 minimum	Linear model (x = Si)	Unable to be determined

[1] Means ± SEM.
[2] (---) indicates when reduced to simplest model, this term was eliminated.
[3] $p < 0.05$.
[4] $p < 0.01$.
[5] $p < 0.001$.
[6] $p < 0.0001$.

regression analysis model was a linear model where x = Si. Dietary Ca did not affect teeth Cu concentrations.

Table 4.8 illustrates the teeth Zn response to dietary Ca and Si. A significant response surface analysis model could not be determined for the teeth Zn response.

Table 4.8 and Appendix Figures 37 and 38 display the teeth Fe and Mn response to graded levels of Ca and Si. The teeth Fe and Mn response was also similar to the responses found in the vertebrae and skull tissues. A quadratic Fe and Mn response to dietary Ca existed, with increasing dietary Ca levels decreasing Fe and Mn retention in the teeth. The retention of teeth Fe and Mn then appeared to stabilize as dietary levels of Ca increased from intermediate to high. For minimum teeth Fe retention, a dietary Ca level of 0.63% was required; minimum teeth Mn retention required a dietary Ca level of 0.68%. Dietary Si did not affect teeth Fe and Mn retention.

Table 4.8 and Appendix Figure 39 illustrate the teeth Mo response to dietary Ca and Si. A linear relationship between teeth Mo and dietary Si existed. As dietary Si levels increased, the deposition of teeth Mo decreased. A linear model, where x = Si, was the predicted response surface regression analysis model for the teeth Mo response. Dietary Ca appeared to have no effect on Mo deposition in the teeth.

Table 4.8 and Appendix Figure 40 display the teeth Si response to graded levels of Ca and Si. There was a significant linear relationship between dietary Si and teeth Si concentrations. As dietary Si levels increased, teeth Si concentrations increased. A significant Ca x Si interaction on teeth Si also existed. High levels of dietary Ca decreased teeth Si concentrations when dietary Si levels were low; high dietary Si levels, however, prevented this decrease. A response surface analysis model, however, was unable to be determined.

Humeri and Blood Plasma Analysis

Table 4.9 and Appendix Figure 41 illustrate the humeri hydroxyproline response to dietary Ca and Si. A significant quadratic humeri hydroxyproline response to dietary Si existed. As dietary Si increased, hydroxyproline concentrations increased to a plateau and then decreased at the higher levels of dietary Si. For maximum humeri hydroxyproline concentration, a dietary level of 59 μg Si/g diet was required. There was no indication that dietary Ca had any effect on humeri hydroxyproline concentrations.

Table 4.9 and Appendix Figures 42 and 43 display the humeri DNA and plasma alkaline phosphatase responses to graded levels of Ca and Si. Both possessed significant quadratic responses to dietary Ca, decreasing as dietary Ca percentages increased. The most dramatic decreases in humeri DNA and plasma alkaline phosphatase occurred as dietary Ca increased from 0.15% to 0.25%. Concentration levels of DNA and alkaline phosphatase then stabilized at the intermediate percentages of dietary Ca, with increases in concentration occurring as dietary Ca increased to the highest percentage. For minimum humeri DNA concentration, a dietary level of 0.62% Ca was required; minimum plasma alkaline phosphatase concentration required a dietary level of 0.66% Ca. Dietary Si appeared to have no effect on humeri DNA and plasma alkaline phosphatase concentrations.

Table 4.9. Hydroxyproline and DNA Analysis of Humeri and Plasma Alkaline Phosphatase of Rats Fed Graded Levels of Calcium and Silicon for Nine Weeks

Diet		Hydroxyproline	DNA	Alkaline Phosphatase[7]
Si (µg/g)	Ca (% diet)	(mg/g dry wt)	(µg/g dry wt)	
0	0.50	26.51 ± 0.46[1]	4567 ± 315	0.78 ± 0.06
3.5	0.25	30.89 ± 2.45	7590 ± 189	0.92 ± 0.08
3.5	0.75	30.37 ± 2.14	5477 ± 304	0.82 ± 0.12
35.0	0.15	32.79 ± 1.78	10418 ± 167	1.21 ± 0.09
35.0	0.50	31.44 ± 1.14	5126 ± 141	0.90 ± 0.05
35.0	0.85	32.86 ± 1.20	5509 ± 286	0.87 ± 0.07
350.0	0.25	31.28 ± 2.28	6614 ± 202	0.93 ± 0.10
350.0	0.75	29.28 ± 0.52	4875 ± 228	0.81 ± 0.08
870.0	0.50	30.91 ± 1.13	5421 ± 207	0.95 ± 0.09
Mean ± Pooled SD		30.74 ± 3.95	5965 ± 771	0.91 ± 0.21
Response Surface Regression Analysis Model				
Intercept		32.22[6]	4921[6]	0.85[6]
Si		1.16	---	---
Ca		---[2]	-1873[6]	-0.12[4]
Si x Si		-3.49[4]	---	---
Ca x Si		---	---	---
Ca x Ca		---	2762[6]	0.14
R^2		0.14	0.81	0.17
F value		4.53[3]	112.2[6]	6.03[4]
Maximum Si response (µg/g)		59.0	---	---
Maximum Ca response (%)		---	0.62	0.66
Predicted (min, max, or saddle)		32.32 maximum	4604 minimum	0.82 minimum

[1]Means ± SEM.
[2](---) indicates when reduced to simplest model, this term was eliminated.
[3]$p < 0.05$.
[4]$p < 0.01$.
[5]$p < 0.001$.
[6]$p < 0.0001$.
[7]Units are µmoles of *p*-nitrophenol formed/min/mL plasma x 10.

CHAPTER FIVE

DISCUSSION

Conclusions

Evidence suggests that the effect of silicon on bone mineralization is affected by the amount of dietary calcium (Carlisle, 1986). The objective of this experiment was to determine the effects of varying concentrations of dietary silicon on bone mineralization when there were incremental increases in dietary calcium. A second objective was to determine if pharmacological effects on bone would be evident at very high levels of dietary silicon (350 to 870 μg Si/g diet). An advantage of the response surface experimental design is the ability to predict the dietary intake of silicon or calcium necessary to see minimum or maximum mineralization responses.

Dietary silicon affects bone mineral content but these effects may vary depending on the bone tissue. A mineral that exemplifies this variation is copper. In the vertebrae and femur, both silicon deficiency and excess increased copper concentrations. These results are similar to that of Najda et al. (1992) who reported a synergistic increase in tissue copper in response to higher intakes of silicon (0.1-0.4 mg Si/g body wt). In contrast to vertebrae and femur copper findings in the present study, dietary silicon decreased copper concentrations in the skull and teeth. This finding may indicate less need for copper in bone formation enzymatic processes as the animal ages. Calcium also affected the copper concentrations in the skull, an effect unique to this tissue of those examined. Incremental increases in dietary calcium decreased skull copper concentrations; this possibly occurred through an effect upon the uptake and utilization of copper. Shackelford et al. (1994) noted the presence of a calcium-copper antagonism in fetuses of female rats fed supplemental calcium in excess.

In qualitative studies, copper is consistently associated with the organic fraction of bone (Ellis, 1964). Spadaro et al. (1970) hypothesized that copper is directly involved in the

organization of the organic matrix of bone or indirectly involved through control of enzymatic activity. In our study, the minimum copper content of the vertebra and femur was achieved by 25 and 28 µg Si/g diet, respectively; with increases in copper occurring with both silicon deficiency and silicon excess. Changes in copper were opposite those of the hydroxyproline concentrations of the humeri, with both low and high dietary silicon decreasing the hydroxyproline or collagen content. The finding of less collagen in conjunction with retained copper when silicon is deficient or in excess suggests that adequate silicon has a direct effect on collagen organization or an indirect effect on enzymatic functioning. It is possible that the cross-linking of collagen by the copper-dependent lysyl oxidase is decreased when silicon is not optimal, which could lead to reduction in mechanical strength with copper deficiency as reported by Medeiros et al. (1997). In the present study the predicted amount of dietary silicon for maximum collagen production in humeri bone is 59 µg Si/g diet.

Accumulating research findings point to possible overlapping nutritional effects for silicon, copper and zinc in the biosynthesis or structural integrity of connective tissues (Emerick, Kayongo-Male, 1990). Both copper and zinc are found in the insoluble organic fraction of bone (despite extensive demineralization); this suggests that these ions are strongly bound to the collagen matrix playing a role in bone calcification. In this study, incremental increases in dietary silicon increased zinc concentrations in the skull. Najda et al. (1992), however, found that silicon supplementation decreased the concentrations of zinc in serum and organs of rats. Emerick et al. (1990) indicated that zinc blood plasma concentrations were negatively affected by silicon supplementation only in those animals fed zinc-inadequate diets. Shackelford et al. (1994) indicated that kidney concentrations of zinc decreased in response to increased dietary calcium. Our data does not strongly support the contention that silicon or calcium intake decrease zinc retention in the femur, vertebra, or teeth; thus suggesting the presence of tissue specific responses to dietary calcium and silicon manipulation.

Carlisle (1974) found silicon to be localized in the active growth areas of tibia in mice and rats 0 to 28 days old. The amount of silicon apparently is related to the "maturity" of the bone mineral. In the earliest stages of calcification, silicon and calcium content are low, however, as mineralization progresses, silicon and calcium contents rise congruently. Later, as calcium approaches the predicted proportion in bone apatite, silicon is present in very low concentrations; thus, the more "mature" the bone, the smaller the amount of detectable silicon. The femur and skull, in the present study, retained silicon when dietary silicon was low to intermediate, but retention decreased when dietary silicon increased. In vertebrae, as dietary silicon increased, silicon concentrations decreased. These findings are consistent with Carlisle's findings; as silicon retention in these bones was decreasing, the concentrations of calcium and phosphorus were increasing, thus indicating the presence of a more mature bone.

A relationship between dietary silicon intake and percent bone ash has also been found, which suggests that higher dietary intakes of silicon increases major mineral concentrations in bone (Elliot, Edwards, 1991). In the present study, increasing dietary silicon linearly increased calcium, phosphorus and magnesium concentrations in the vertebra and skull. At the highest dietary silicon intakes, however, concentrations of calcium, phosphorus and magnesium decreased in the skull. The highest skull concentration of calcium, phosphorus and magnesium occurred at the predicted values of 36, 45, 39 μg Si/g diet, respectively.

The teeth mineralization response to dietary silicon was unique to that of other mineralized tissues analyzed in this study. The highest calcium and phosphorus concentrations in teeth occurred when dietary silicon was low in the basal diet and decreased with the addition of silicon to the diet. This was also the only tissue where each subsequent increase in dietary silicon increased the silicon concentrations.

The mineralization changes in teeth may be influenced by the mineral metabolism properties of the three mineralized layers present in the tooth. The presence of osteoblasts and

osteoclasts in cementum allows this tissue to exchange minerals in a manner similar to that of bone. Because the mineralization effects in the tooth are unique, the contradictory effects of dietary silicon in decreasing calcium and phosphorus concentrations apparently are related to alterations in either the dentine or enamel tissue. Alterations in diet have been shown to modify the overall composition of dentine tissue due to its continued metabolic activity throughout life (Weatherell, Robinson, 1973). Although mature enamel is chemically and physically stable, it is also inhomogenous. When portions of the enamel surface are removed by wear, considerable changes in the inorganic nature of enamel can result. An analysis of the various tooth layers would be appropriate to determine the specific effect of dietary silicon on the tooth.

An increased incidence of caries has been associated with higher concentrations of enamel copper (Curzon, Losee, 1978). Our finding of lower copper concentrations when Si was adequate may indicate a beneficial role of adequate dietary silicon intake. The decrease in potassium and molybdenum as well as copper suggests that there is a decrease in the organic components of the bone.

Dietary calcium affected bone mineralization in predictable ways. Calcium, phosphorus, magnesium, and sodium were incrementally increased in the femur, vertebra, and skull as dietary calcium concentrations increased. Mineralization, however, apparently slightly decreased in the presence of excess dietary calcium. The response surface analysis model indicates that the maximum calcium deposition occurred at 0.65% and 0.62% for the femur and skull, but at 0.82% for the vertebra. The higher predicted maximum for the vertebra corresponds to data indicating that higher calcium intakes benefit vertebra mineralization (Dawson-Hughes et al., 1990). Our results indicate that maximum calcium deposition occurred at dietary calcium intakes that are higher than the current recommendations for a rat diet (0.50%) (National Research Council, US, 1978).

Manganese was also affected by dietary calcium, with increasing dietary calcium, manganese concentrations decreased in the femur, vertebra, skull, and teeth. Manganese is important for the glycosylation of bone proteins. As mineralization progresses, the role of manganese for the glycosylation of bone proteins may no longer be required. Dietary calcium also affected iron retention in the femur, vertebra, skull and teeth; iron retention decreased as dietary Ca increased. This finding is consistent with the calcium-iron antagonist relationship reported by Cook et al. (1991). A similar dietary calcium effect occurred with plasma alkaline phosphatase, DNA and potassium. These results indicate that as calcification increased, organic material, reflected in DNA and cellular potassium, decreased. The decrease in plasma alkaline phosphatase parallels the decrease in bone DNA and cellular potassium this indicates that the mineralization process has slowed down.

Summary

In summary, dietary silicon impacts bone mineralization in ways that can be generally regarded as positive, because it increases calcium, phosphorus, and magnesium concentrations. These effects may be the result of alterations in the organic matrix, reflected by the changes in copper concentrations. Regardless of the mechanism, silicon has such a strong impact on bone maturation and mineralization that is should be considered a mineral of concern in human nutrition.

Limitations

When using response surface analysis, the researcher is required to decide the normal level for each of the two variables and concentrate the number of animals in that group (in this study the estimated requirement for silicon and calcium, 35 µg/g Si and 0.50% Ca respectively). If, however, an assumption is incorrect and the levels are unduly favoring one side, the response surface analysis could miss a response that is occurring at a lower or higher level. Adequate literature

exists regarding the recommended calcium intake for the rat, however this is not the case for silicon. The response surface analysis method can then be a limitation if the actual requirement for the rat is lower than 35 μg/g silicon. The use of an animal model is also a limitation to the study. Animal models allow researchers to investigate topics that are not ethically possible to investigate in humans, however, the data from animals is not directly applicable to humans although it can still provide valuable insight to the function silicon has to bone mineral composition.

Recommendations

Although the dietary calcium level utilized in this study ranged from 0.15 – 0.85%, this level was not low enough to show the benefit of supplementary silicon on bone ash as shown by Carlisle (1986) when 0.08% dietary calcium was used in the rat. Future research studies might use response surface analysis to test the benefit of dietary silicon with low levels of dietary calcium to determine the mechanism by which silicon acts when low concentrations of calcium are fed.

Due to the effect of increasing copper concentrations in the vertebra and femur when dietary silicon levels were deficient or in excess, analysis of lysyl oxidase activity would be of benefit to determine if silicon is affecting the enzymatic function of this protein. Future research studies might investigate lysyl oxidase activity in conjunction with altering levels of dietary silicon in an attempt to ascertain the mechanism of silicon on bone copper.

Although the teeth mineral composition data displayed very interesting results, the inability to distinguish between which layers of the tooth were changing in relationship to altering dietary levels of calcium and silicon made interpretation of the teeth results difficult. Future research studies might investigate the teeth response to altering levels of calcium and silicon by sectioning the tooth into its various layers: enamel, dentine and cementum, prior to analysis.

CHAPTER SIX

REFERENCES

Alfaro, E., Neathery, M. W., Miller, M, J., Crowe, C. T., Gentry, R. P., Fielding, A. S., Pugh, D. G., Blackmon, D. M. (1988) Influence of a wide range of calcium intakes on tissue distribution of macroelements and microelements in dairy calves. *J. Dairy Sci.* 71: 1295-1300.

Anderson, H. C. (1985) Normal biological mineralization: role of cells, membranes, matrix vesicles, and phosphatase. In: *Calcium in Biological Systems.* (Rubin, R. P., Weiss, G. B., Putney, J. W., eds.), pp. 599-606, Plenum Press, New York City, New York.

Bawden, J. W., Anderson, J. J. B., Garner, S. C. (1996) Dental tissues. In: *Calcium and Phosphorus in Health and Disease*. (Anderson, J.J.B., Garner, S.C., eds.), pp. 119-126, CRC Press Inc, Boca Raton, Florida.

Bowes, J. H., Murray, M. M. (1935) The composition of human enamel and dentine. *J. Biol. Chem.* 29: 2721-2727.

Brossart, B. Shuler, T.R., & Nielsen, F.H. (1990) Effect of silicon deficiency on the mineral composition of bone. *North Dakota Academy of Science Proceedings.* 44: 95.

Buckwalter, J.A., Glimcher, M.J., Cooper, R.R., Recker, R. (1996) Bone biology I: structure, blood supply, cells, matrix, and mineralization. *Instr. Course Lect.* 45: 371-386.

Carlisle, E. M. (1970) Silicon: a possible factor in bone calcification. *Science* 167: 279-280.

Carlisle, E. M. (1972) Silicon an essential element for the chick. *Science* 178: 619-621.

Carlisle, E. M. (1974) Silicon as an essential element. *Fed. Proc.* 33: 1758-1766.

Carlisle, E. M. (1979) A silicon-molybdenum interrelationship in vivo. *Fed Proc.* 38: 553.

Carlisle, E.M. (1986) Silicon as an essential trace element in animal nutrition. In: *Silicon Biochemistry,* (Evered, D., O'Conner, M., eds.), pp 123-139, John Wiley and Sons, New York, New York.

Carlisle, E.M. (1986) Silicon as an essential trace element in animal nutrition. *Ciba. Found Symp.* 121: 123-139.

Carlisle, E. M. (1997) Silicon. In: *Handbook of Nutritionally Essential Mineral Elements,* (O'Dell, B. L. Sunde, R. A., eds), pp 603-618, Marcel Dekker, New York, New York.

Cook, J., Dassenko, S. & Whittaker, P. (1991) Calcium supplementation: effect on iron absorption. *Am. J. Clin. Nutr.* 53: 106-111.

Curzon, M.J. Losee, F.L. (1977) Dental caries and trace element composition of whole human enamel: Eastern United States. *J. Am. Dent. Assoc.* 94: 1146-1150.

Dawson-Hughes, B., Dallal, G.E., Krall, E.A., Sadowski, L., Sahyoun, N. Tannenbaum, S. (1990) A controlled trial of the effect of calcium supplementation on bone density in postmenopausal women. *N. Engl. J. Med.* 323: 878-883.

Elliot, M. A. Edwards, J. M. Jr. (1991) The effect of silicon on the growth and skeletal development of chickens. *J. Nutr.* 121: 201-207.

Ellis, E. H. (1964) The fluorescence of bone. Thesis, Syracuse University.

Emerick, R. J. Kayongo-Male, H. (1990) Interactive effects of dietary silicon, copper, and zinc in the rat. *J. Nut. Biochem.* 1: 35-40.

Garner, S.C., Anderson, J.J.B., Ambrose, W.W. (1996) Skeletal tissues and mineralization. In: *Calcium and Phosphorus in Health and Disease*. (Anderson, J.J.B., Garner, S.C., eds.), pp. 97-117, CRC Press Inc, Boca Raton, Florida.

Gaster, D., Havivi, E., Guggenheim, K. (1967) Differential effects of low calcium diets on the bones of mice and rats. *Nutr. Dieta.* 9: 200-207.

Glimcher, M. J. (1985) The role of collagen and phosphoproteins in the calcification of bone and other collagenous tissues. In: *Calcium in Biological Systems.* (Rubin, R. P., Weiss, G. B., Putney, J. W., eds.), pp. 607-616, Plenum Press, New York City, New York.

Groff, J. L, Gropper, S. S. (2000) Macrominerals. In: *Advanced Nutrition and Human Metabolism*, 3rd ed, pp. 371-400, Wadsworth/Thomson Learning, Belmont, California.

Gurney, T. Gurney, E. G. (1989) Nucleic acids. In: *Methods in Molecular Biology*, vol. 2, (Walker, J. M., ed.), pp. 5-11, Clifton: Humana.

Guyton, A. C. (1991) Parathyroid hormone, calcitonin, calcium and phosphate metabolism, vitamin D, bone, and teeth. In: *Textbook of Medical Physiology*, 8th ed, pp. 868-884, WB Saunders Company, Philadelphia, Pennsylvania.

Heaney, R. P. (1999) Bone biology in health and disease: a tutorial. In: *Modern Nutrition in Health and Disease*, 9th ed. (Shils, M. E., Olson, J. A., Shike, M., Ross, A. C., eds.), pp. 1327-1338, Williams & Wilkins, Baltimore, Maryland.

Heaney, R.P., Weaver, C. M., Fitzsimmons, M. L. (1990) Influence of calcium load on absorption fraction. *J. Bone Miner. Res.* 5: 1135-1138.

Institute of Medicine, Food and Nutrition Board, National Academy of Sciences. (1998) Dietary Reference Intakes. National Academy Press, Washington, District of Columbia.

Kayongo-Male, H., Jia, X. (1999) Silicon bioavailability studies in young rapidly growing rats and turkeys fed semipurified diets. *Biol. Trace Element Res.* 67: 173-186

Karbach, U. (1992) Paracellular calcium transport across the small intestine. *J. Nutr.* 122: 672-677.

Lester, G. E. (1996) Serum and urine markers of bone turnover. In: *Calcium and Phosphorus in Health and Disease*. (Anderson, J.J.B., & Garner, S.C., eds.), pp. 147-154, CRC Press Inc, Boca Raton, Florida.

Lichte, F. E., Hopper, S. Osborn, T. W. (1980) Determination of Si and Al in biological matrices by ICP-ES. *Anal. Chem.* 52: 120-124.

Louie, D. (1996) Intestinal Bioavailability and absorption of calcium. In: *Calcium and Phosphorus in Health and Disease*. (Anderson, J.J.B., Garner, S.C., eds.), pp. 45-60, CRC Press Inc, Boca Raton, Florida.

Marks, S.C., Hermey, D.C. (1996) The structure and development of bone. In: *Principles of Bone Biology*. (Bilezikian, J. P., Rodan, G. A., Raisz, L. G.), pp. 3-14, Academic Press Inc, Orlando, Florida.

Martin, R.B., Burr, D.B., Sharkey, N.A. (1998) Skeletal biology. In: *Skeletal Tissue Mechanics*. Springer-Varlag New York Inc, New York City, New York.

Medeiros, D. M., Illich, J., Ireton, J., Velimir, M., Shiry, L., Wildman R. (1997) Femurs from rats fed diets deficient in copper or iron have decreased mechanical strength and altered mineral composition. *J. Trace Elem. Exp. Med.* 10: 197-203.

Najda, J., Fminski, J., Drozdz, M., Danch, A. (1992) The interrelations of inorganic silicon (Si) with systemic iron (Fe), zinc (Zn), and copper (Cu) pools in the rat. *Biological Trace Element Research.* 34: 185-195.

National Research Council (U.S.) Subcommittee on Laboratory Animal Nutrition. (1978) Nutrient requirements of the laboratory rat. In: *Nutrient Requirements of Laboratory Animals: rat, mouse, gerbil, guinea, pig, hamster, vole, fish*, 3rd ed., pp.7-37, National Academy of Sciences, Washington.

Nellans, H. N., Kimberg, D. V. (1978) Cellular and paracellular calcium transport in rat ileum: effects of dietary calcium. *Am. J. Physiol.* 235: E726-E737.

Nielsen, F. H. (1999) Ultratrace minerals. In: *Modern Nutrition in Health and Disease*, 9th ed. (Shils, M. E., Olson, J. A., Shike, M., Ross, A. C., eds.), pp. 283-303, Williams & Wilkins, Baltimore, Maryland.

Nielsen, F. H., Bailey, B. (1979) The fabrication of plastic cages for suspension in mass air flow racks. *Lab. Anim. Sc.* 29: 502-506.

Nielsen, F.H., Myron, S.H., Givand, S.H., Zimmerman, T.J., Ollerich, D.A. (1975) Nickel deficiency in rats. *J. Nutr.* 105: 1607-1630.

Nimni, M. E. (1988) *Collagen: Biochemistry*, vol. 1, CRC Press Inc, Boca Raton, Florida.

Patten, B. M., Carlson, B. M. (1974) The face and oral region. In: *Foundations of Embryology*, 3rd ed., pp. 439-457, McGraw-Hill Book Company, New York, New York.

Perry, C. C., Fraser, M. A., Hughes, N. P. (1991) Macromolecular assemblages in controlled biomineralization. In: *Surface Reactive Peptides and Polymers*. pp. 316-339, American Chemical Society, Washington DC.

Podenphat, J., Larsen, N. E., Christiansen, C. (1984) An essay and reliable method for determination of urinary hydroxyproline. *Clinica. Chimica. Acta*. 142: 145-148.

Schwartz, K., Milne, D. B. (1972) Growth promoting effects of silicon in rats. *Nature* 239: 333-334.

Schwartz, K. (1973) A bound form of silicon in glycosaminoglycans and polyuronides. *Proc. Nat. Acad. Sci.* 70: 1608-1612.

Seaborn, C. D., Nielsen, F. H. (1993) A nutritional beneficence for bones, brains, and blood vessels. *Nutr. Today* 13-18.

Seaborn, C. D., Nielsen F. H. (1994) High dietary aluminum affects the response of rats to silicon deprivation. *Biol. Trace Element Res* 41: 295-304.

Seaborn, C. D., Nielsen F. H. (1994) Boron and silicon: effects on growth, plasma lipids, urinary cyclic amp and bone and brain mineral composition of male rats. *Environmental Toxicology and Chemistry* 13: 941-947.

Seaborn, C. D., Nielsen, F. H. (1994) Effects of germanium and silicon on bone mineralization. *Biol. Trace Element Res.* 42: 151-164.

Seaborn, C. D., Nielsen, F. H. (2002a) Silicon deprivation decreases collagen formation in wounds and bone, and ornithine transaminase enzyme activity in liver. *Biol. Trace Element Res.* 89: 251-261.

Seaborn, C. D., Nielsen, F. H. (2002b) Dietary silicon and arginine affect mineral element composition of rat femur and vertebra. *Biol. Trace Element Res.* 89: 239-250.

Shackelford, M. E., Collins, T. F. X., Black, T. N., Ames, M. J., Dolan, S., Sheikh, N. S., Chi R. K., O'Donnell, M. W. (1994) Mineral interactions in rats fed AIN-76A diets with excess calcium. *Fd. Chem. Toxic.* 32: 255-263.

Smillie, A. C. (1973) The inorganic composition of teeth. In: *Biological Mineralization*. (Zipkin, I., ed.), pp. 139-163, John Wiley & Sons, New York, New York.

Spadaro, J. A., Becker, R. O., Bachman, C. H. (1970) The distribution of trace metal ions in bone and tendon. *Calc. Tiss. Res.* 6: 49-54.

Stewart, S. R., Emerick, R. J., Kayongo-Male, H. (1993) Silicon-zinc interactions and potential roles for dietary zinc and copper in minimizing silica urolithiasis in rats. *J. Anim. Sci.* 71: 946-954.

Weatherell, J. A., Robinson, C. (1973) The inorganic composition of teeth. In: *Biological Mineralization*. (Zipkin, I., ed.), pp. 43-74, John Wiley & Sons, New York, New York.

Weaver, C. M., Heaney, R. P. (1999) Calcium. In: *Modern Nutrition in Health and Disease,* 9th ed. (Shils, M.E., Olson, J.A., Shike, M., Ross, A.C., eds.), pp. 141-155, Williams & Wilkins, Baltimore, Maryland.

Yamauchi, M. (1996) Collagen: the major matrix molecule in mineralized tissues. In: *Calcium and Phosphorus in Health and Disease*. (Anderson, J.J.B., Garner, S.C., eds.), pp. 127-145, CRC Press Inc, Boca Raton, Florida.

APPENDIX

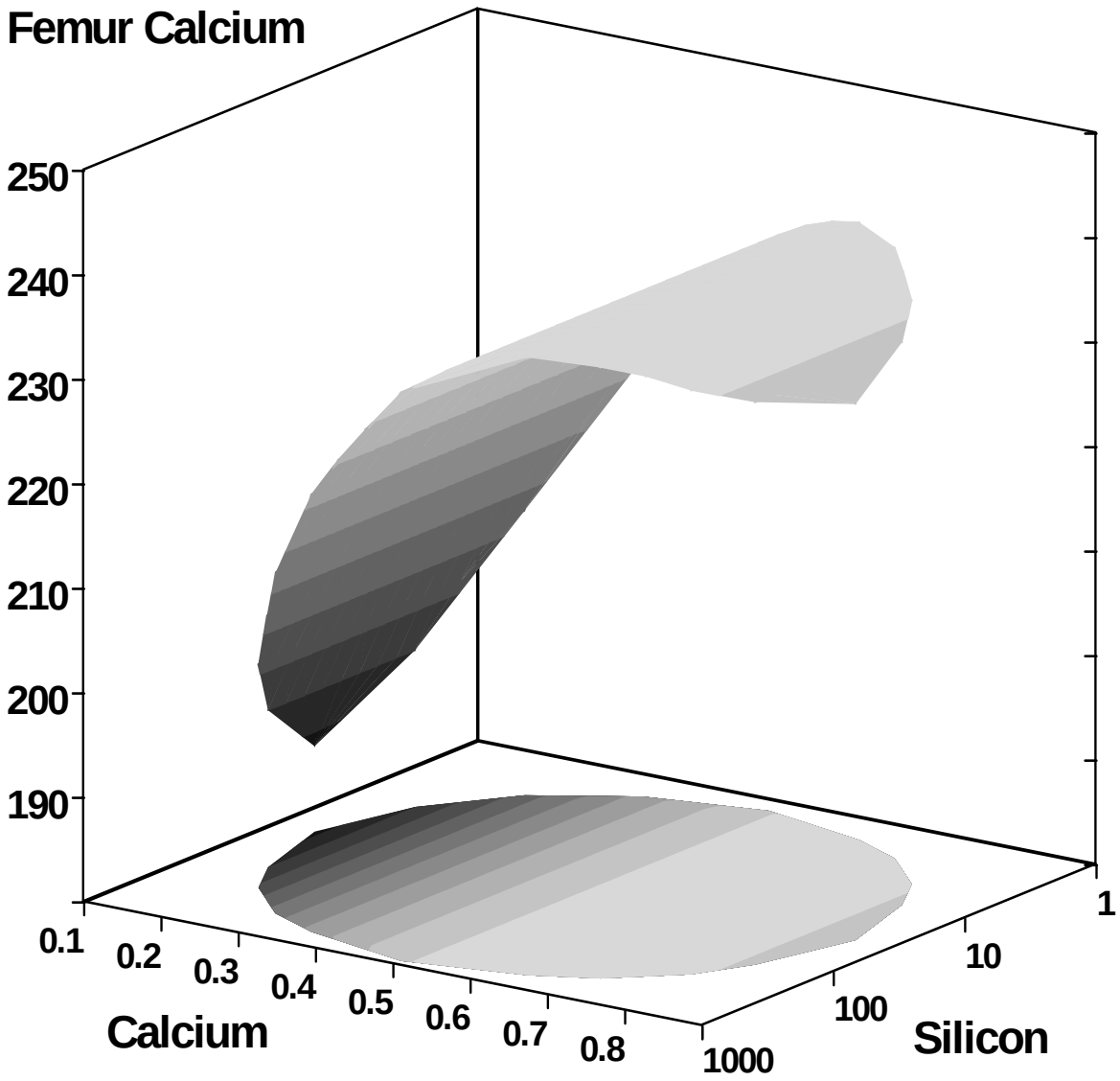

Appendix Figure 1. Response surface plot of femur Ca. Femur calcium is expressed in my/g dry weight. Dietary calcium is expressed as percent of diet. Dietary silicon is expressed as μg/g diet.

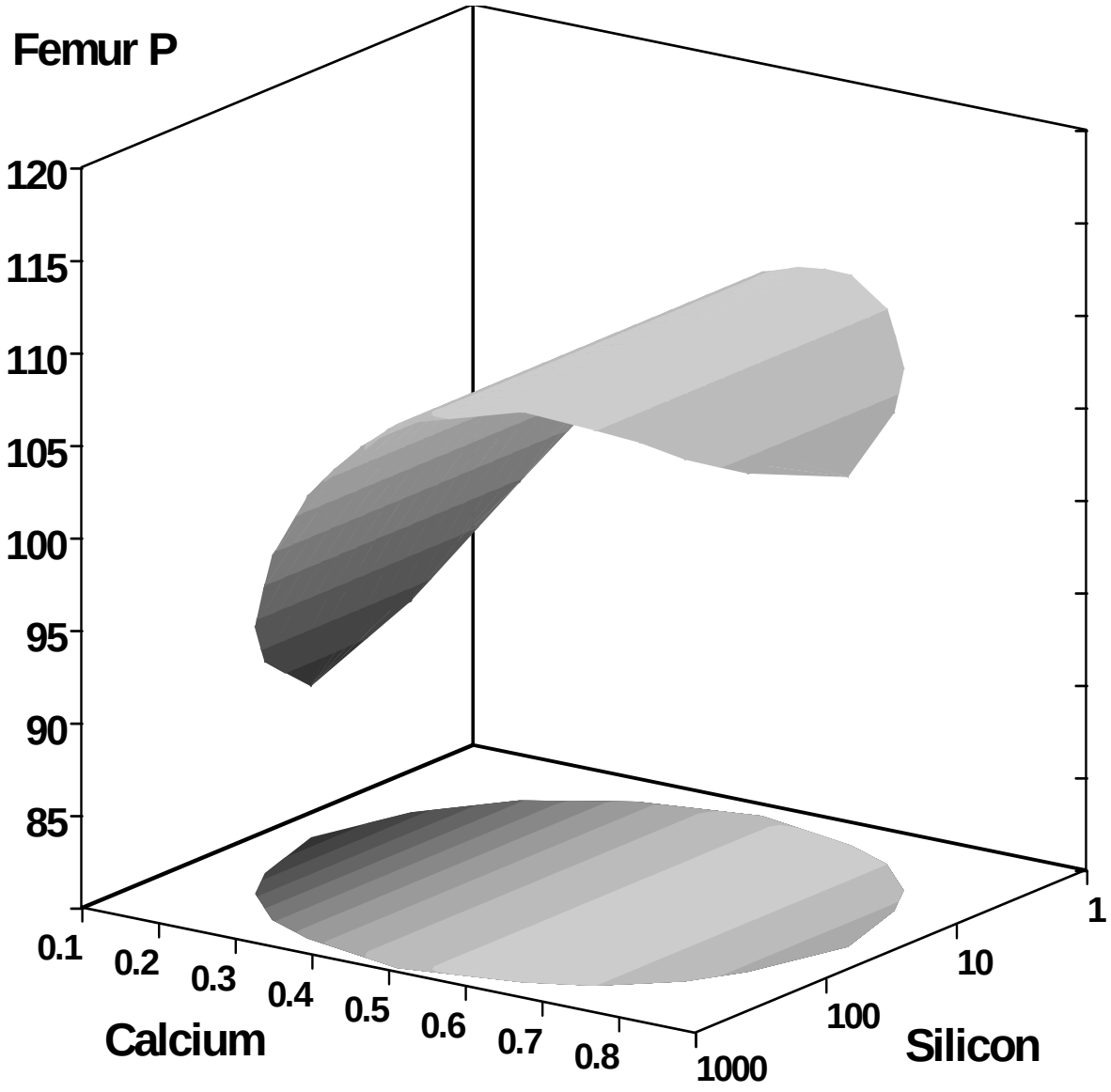

Appendix Figure 2. Response surface plot of femur P. Femur phosphorus is expressed in mg/g dry weight. Dietary calcium is expressed as percent of diet. Dietary silicon is expressed as μg/g diet.

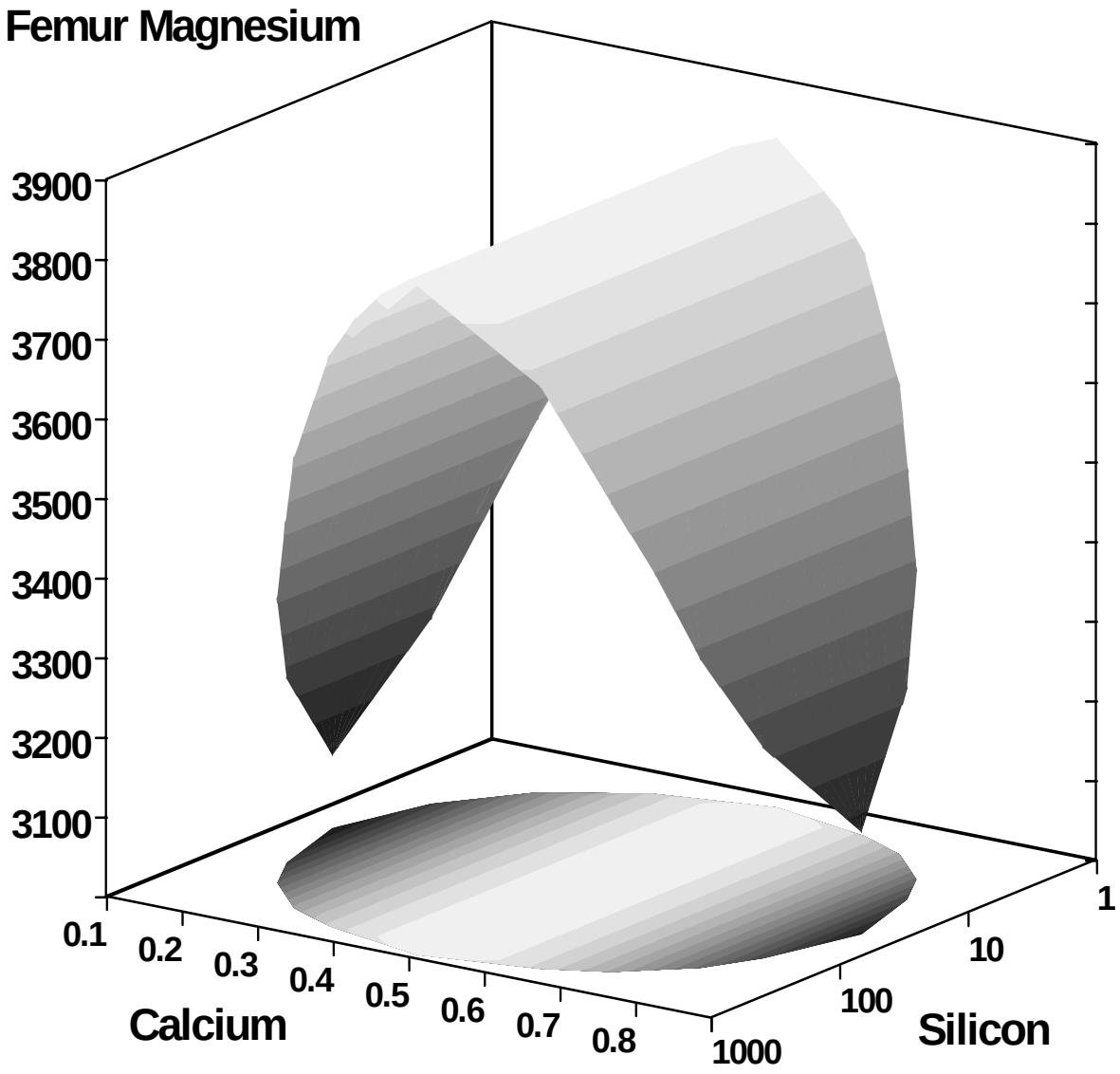

Appendix Figure 3. Response surface plot of femur Mg. Femur magnesium is expressed in μg/g dry weight. Dietary calcium is expressed as percent of diet. Dietary silicon is expressed as μg/g diet.

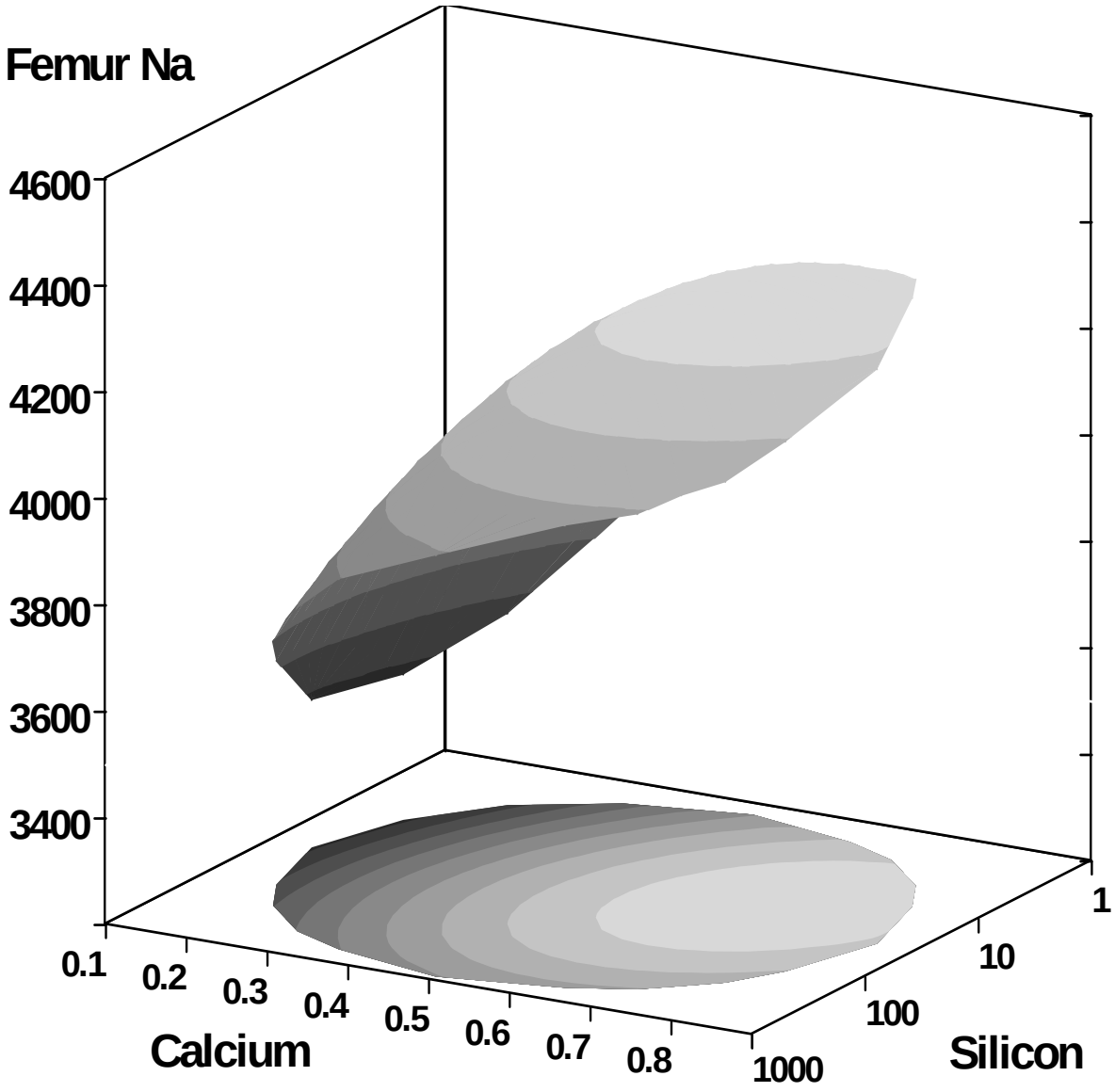

Appendix Figure 4. Response surface plot of femur Na. Femur sodium is expressed in μg/g dry weight. Dietary calcium is expressed as percent of diet. Dietary silicon is expressed as μg/g diet.

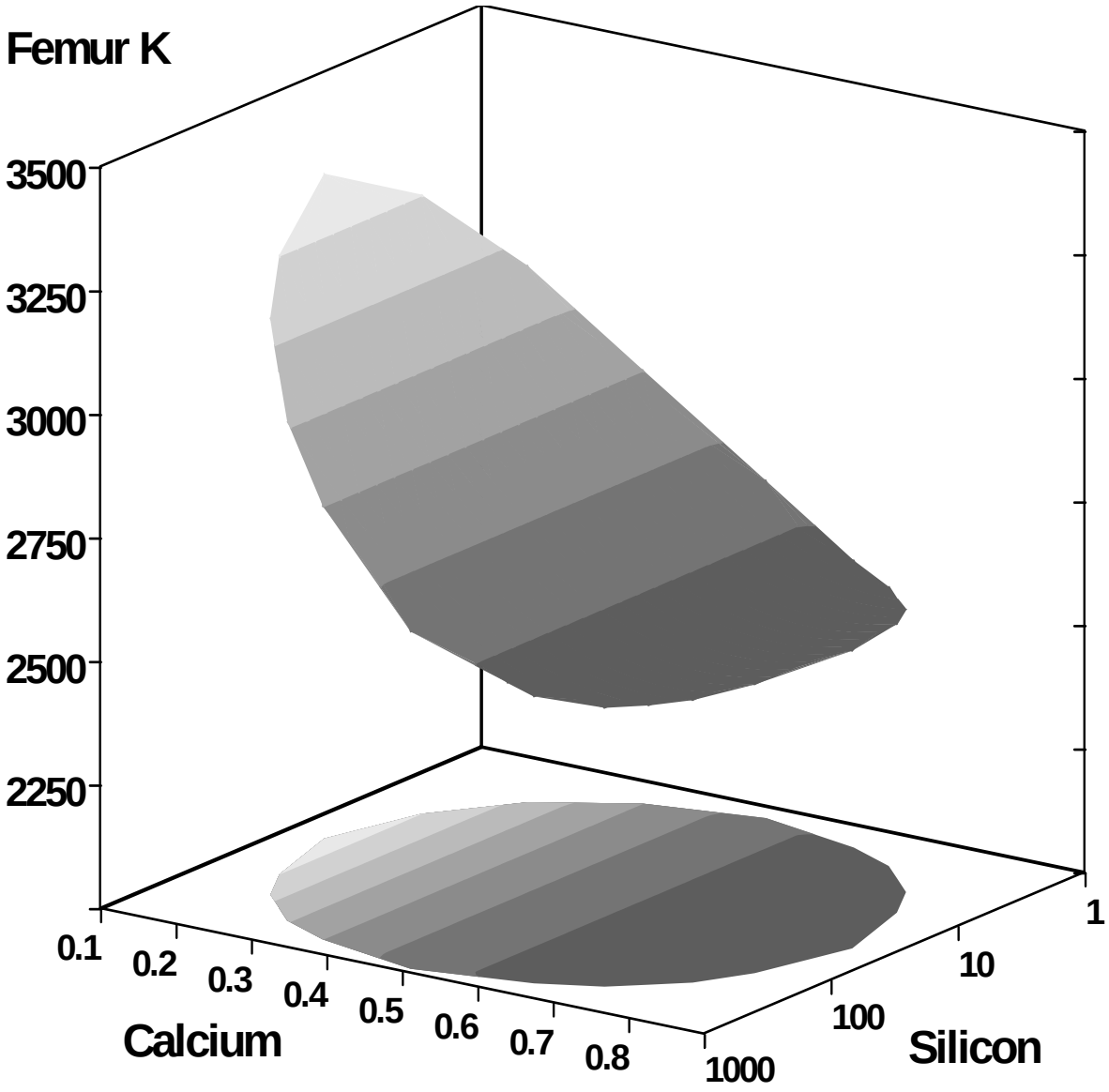

Appendix Figure 5. Response surface plot of femur K. Femur potassium is expressed in μg/g dry weight. Dietary calcium is expressed as percent of diet. Dietary silicon is expressed as μg/g diet.

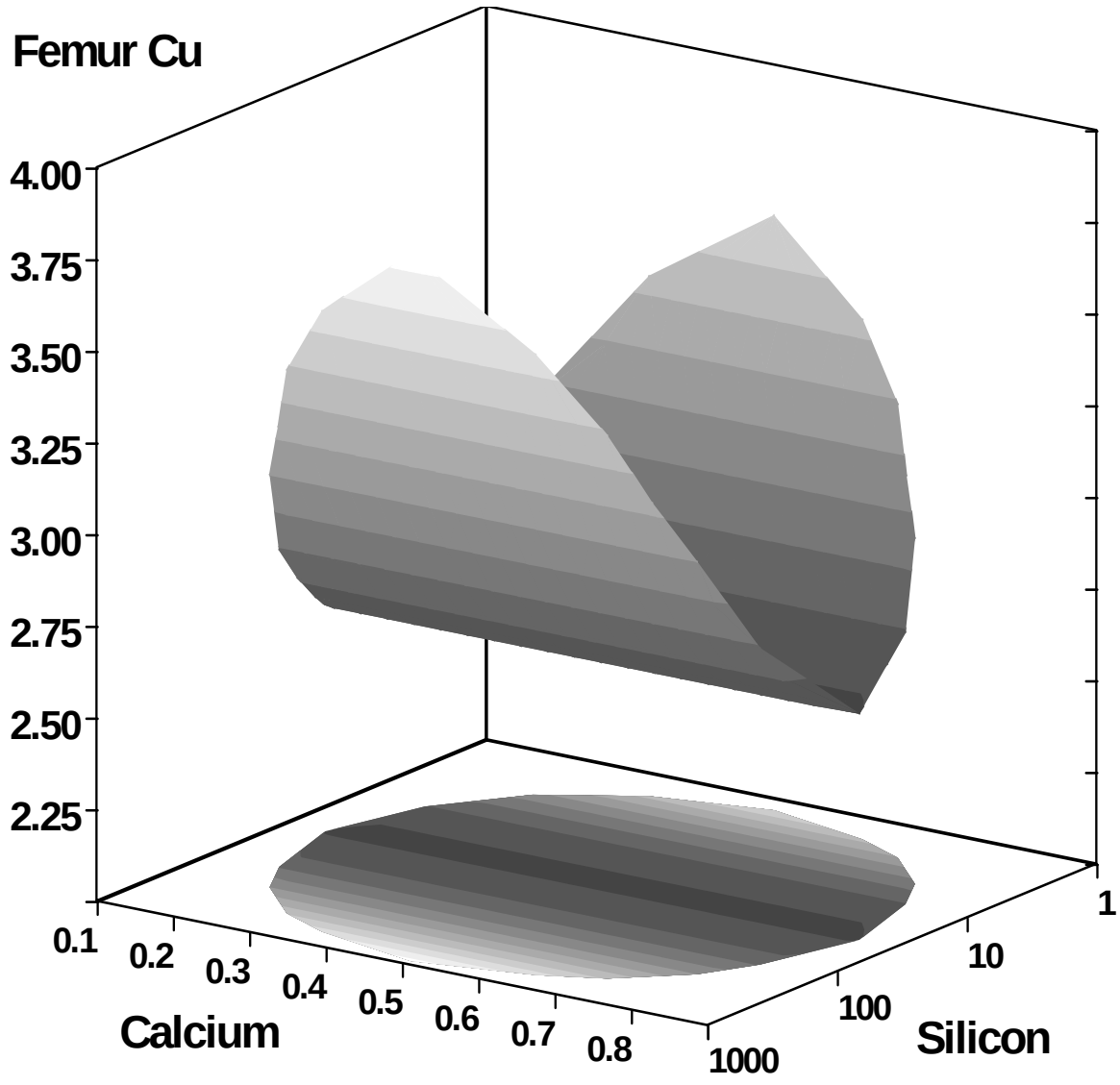

Appendix Figure 6. Response surface plot of femur Cu. Femur copper is expressed in μg/g dry weight. Dietary calcium is expressed as percent of diet. Dietary silicon is expressed as μg/g diet.

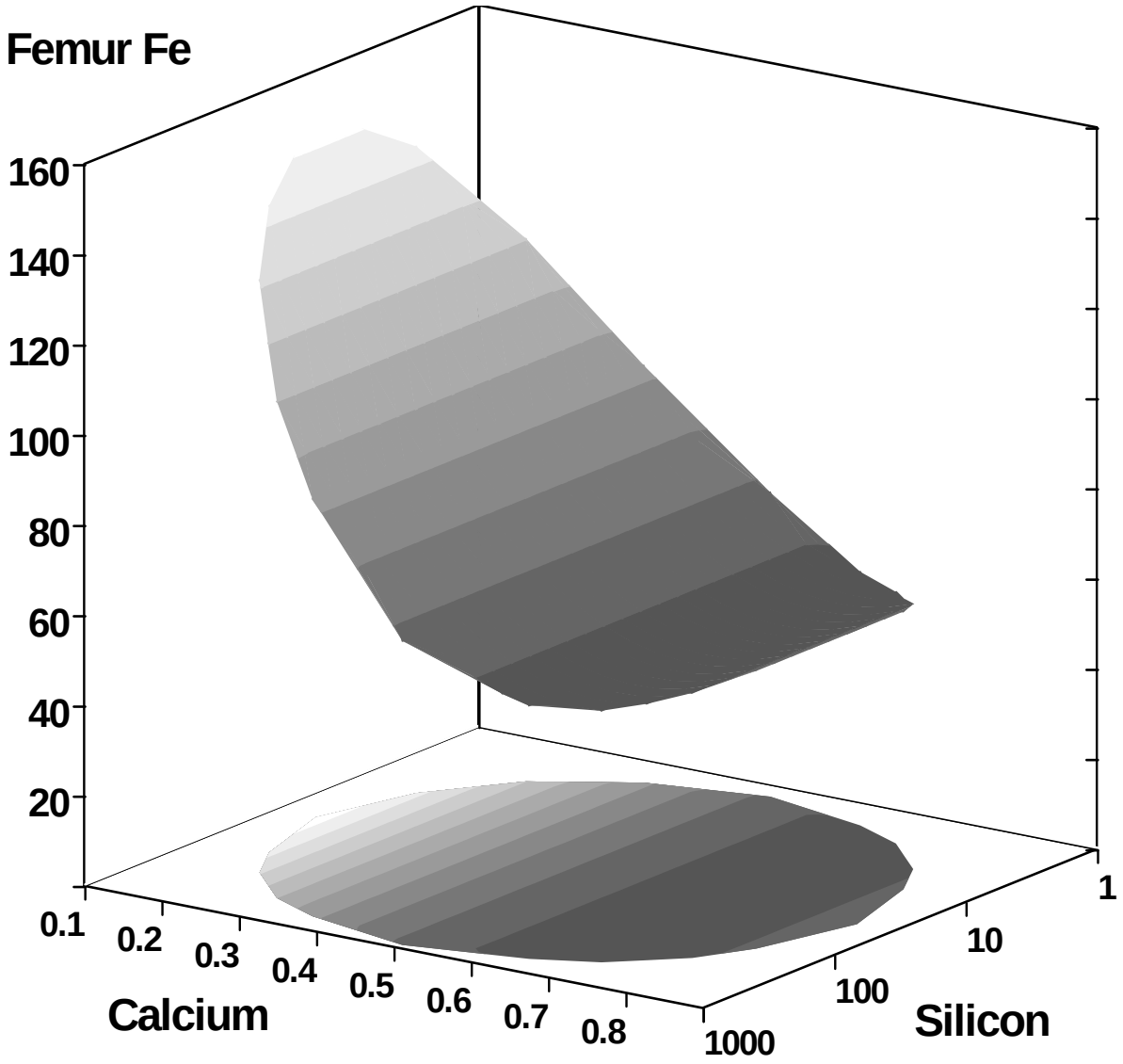

Appendix Figure 7. Response surface plot of femur Fe. Femur iron is expressed in μg/g dry weight. Dietary calcium is expressed as percent of diet. Dietary silicon is expressed as μg/g diet.

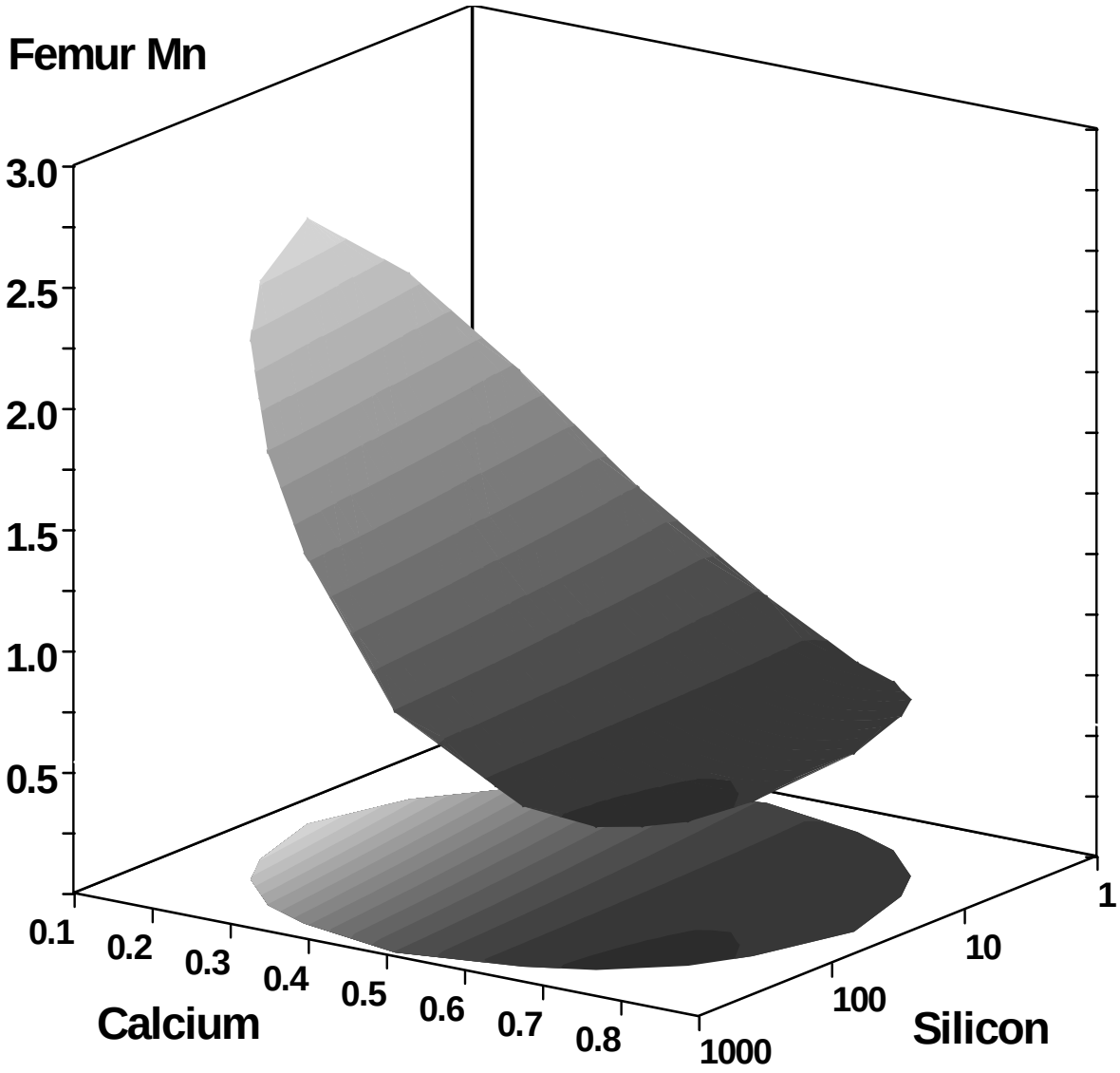

Appendix Figure 8. Response surface plot of femur Mn. Femur manganese is expressed in μg/g dry weight. Dietary calcium is expressed as percent of diet. Dietary silicon is expressed as μg/g diet.

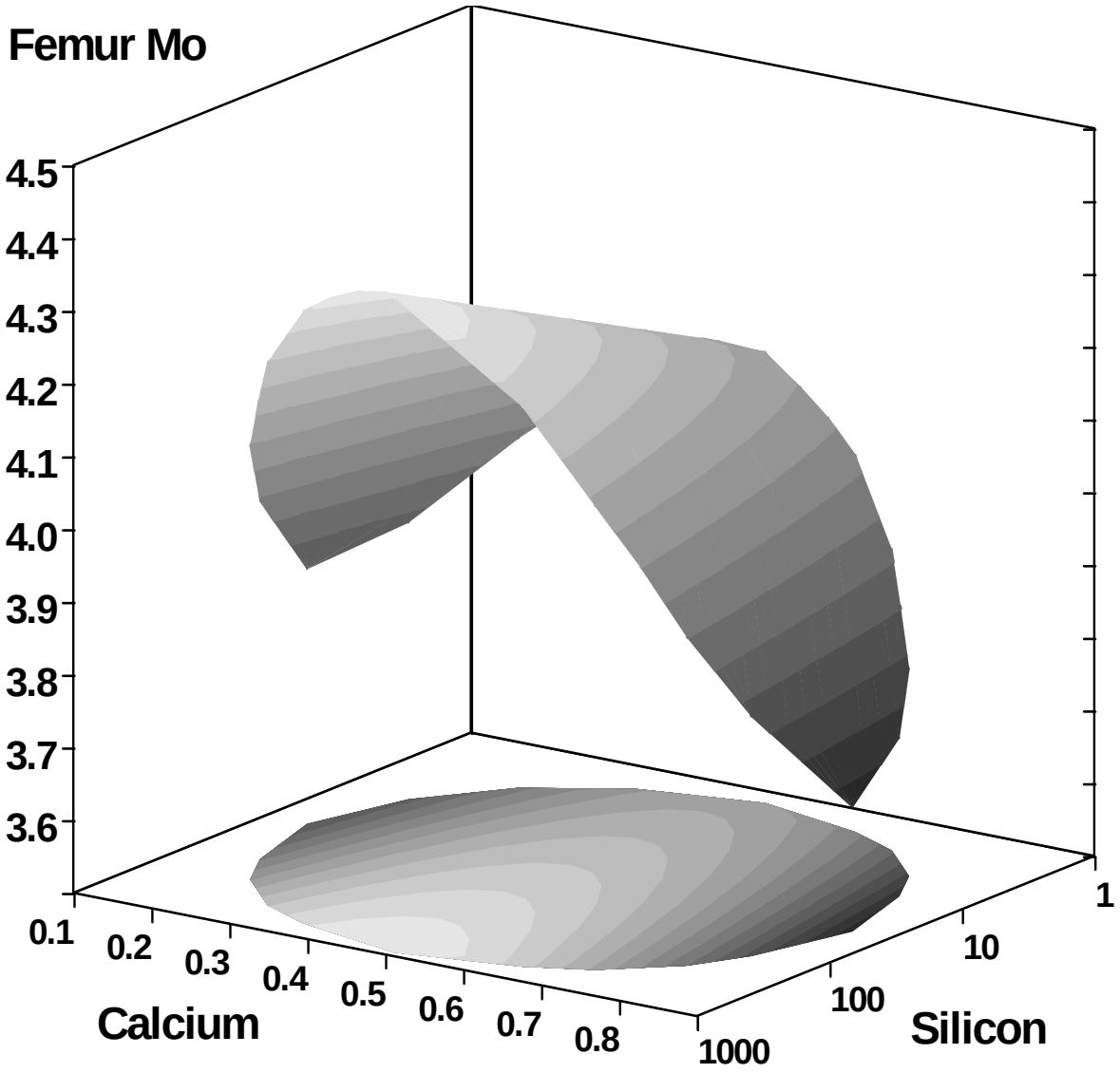

Appendix Figure 9. Response surface plot of femur Mo. Femur molybdenum is expressed in μg/g dry weight. Dietary calcium is expressed as percent of diet. Dietary silicon is expressed as μg/g diet.

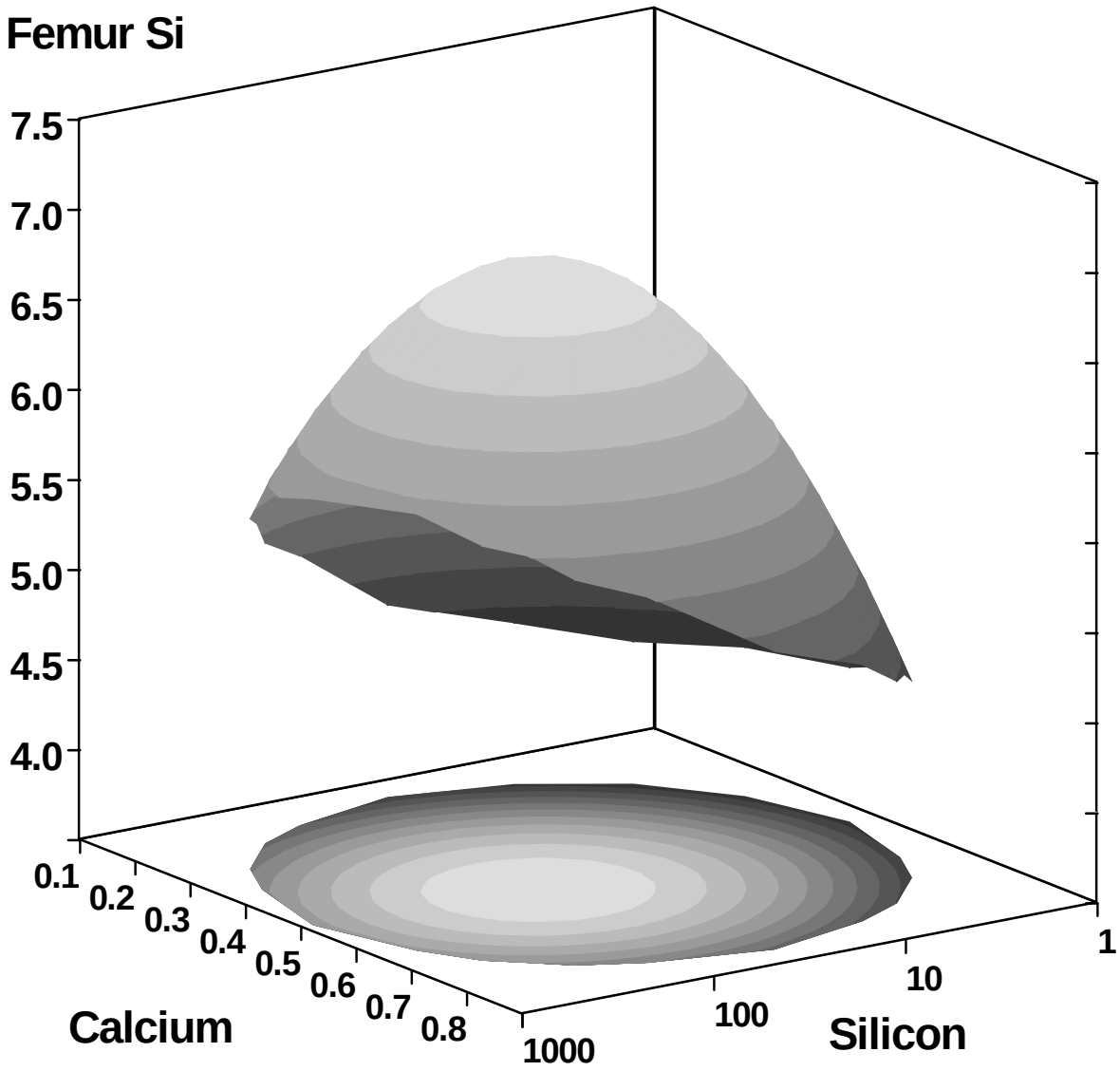

Appendix Figure 10. Response surface plot of femur Si. Femur silicon is expressed in μg/g dry weight. Dietary calcium is expressed as percent of diet. Dietary silicon is expressed as μg/g diet.

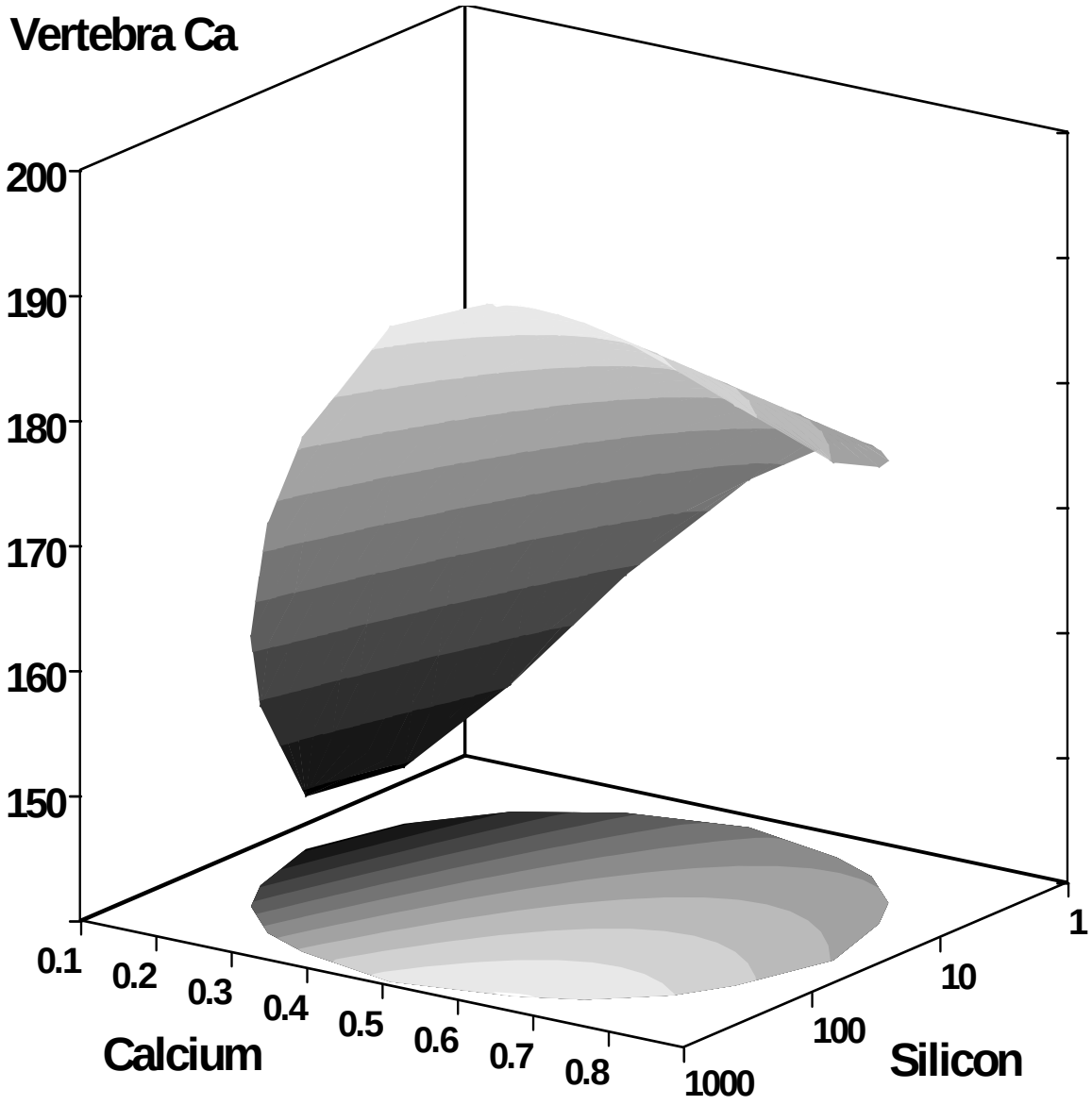

Appendix Figure 11. Response surface plot of vertebra Ca. Vertebra calcium is expressed in mg/g dry weight. Dietary calcium is expressed as percent of diet. Dietary silicon is expressed as μg/g diet.

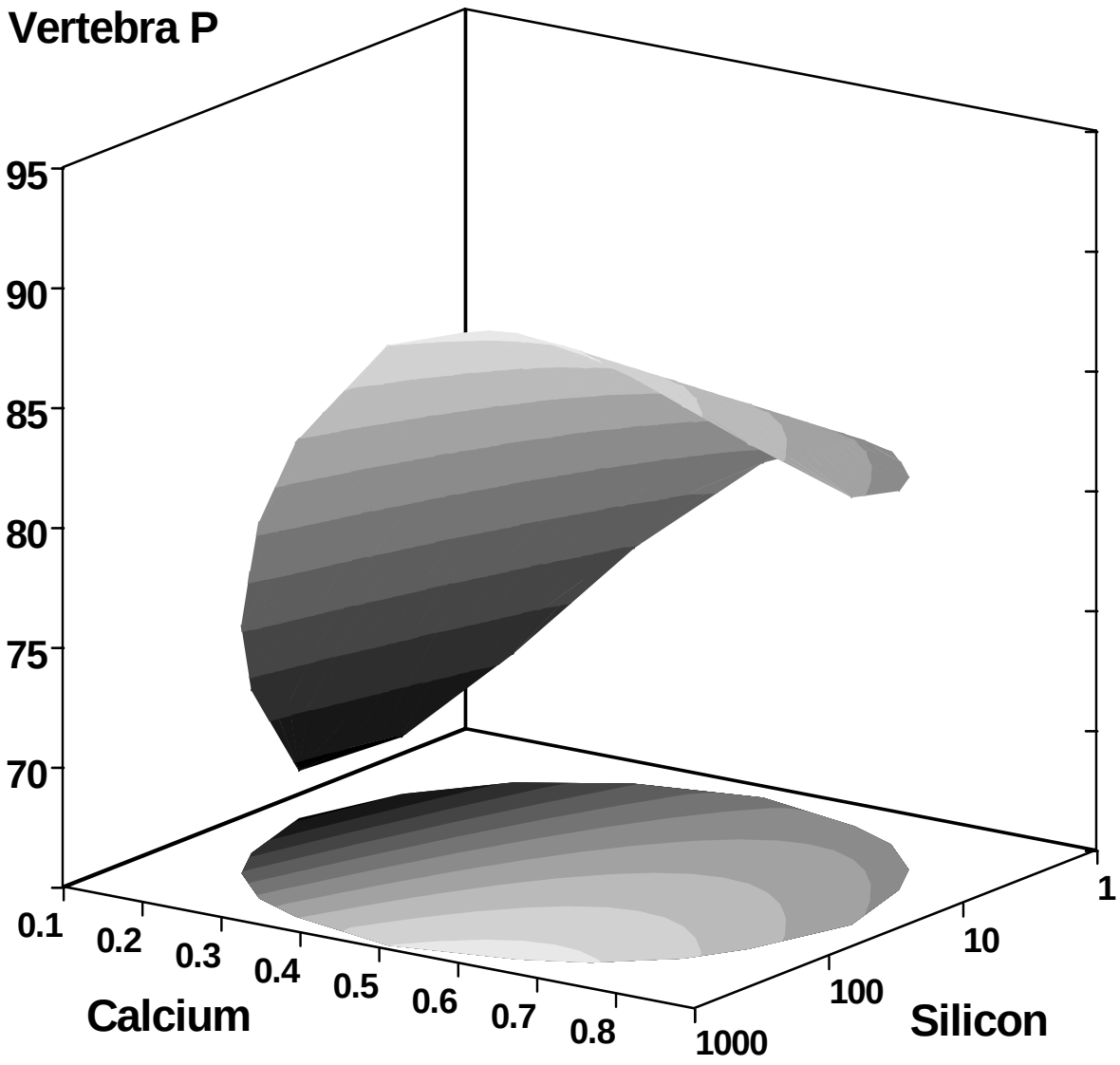

Appendix Figure 12. Response surface plot of vertebra P. Vertebra phosphorus is expressed in mg/g dry weight. Dietary calcium is expressed as percent of diet. Dietary silicon is expressed as μg/g diet.

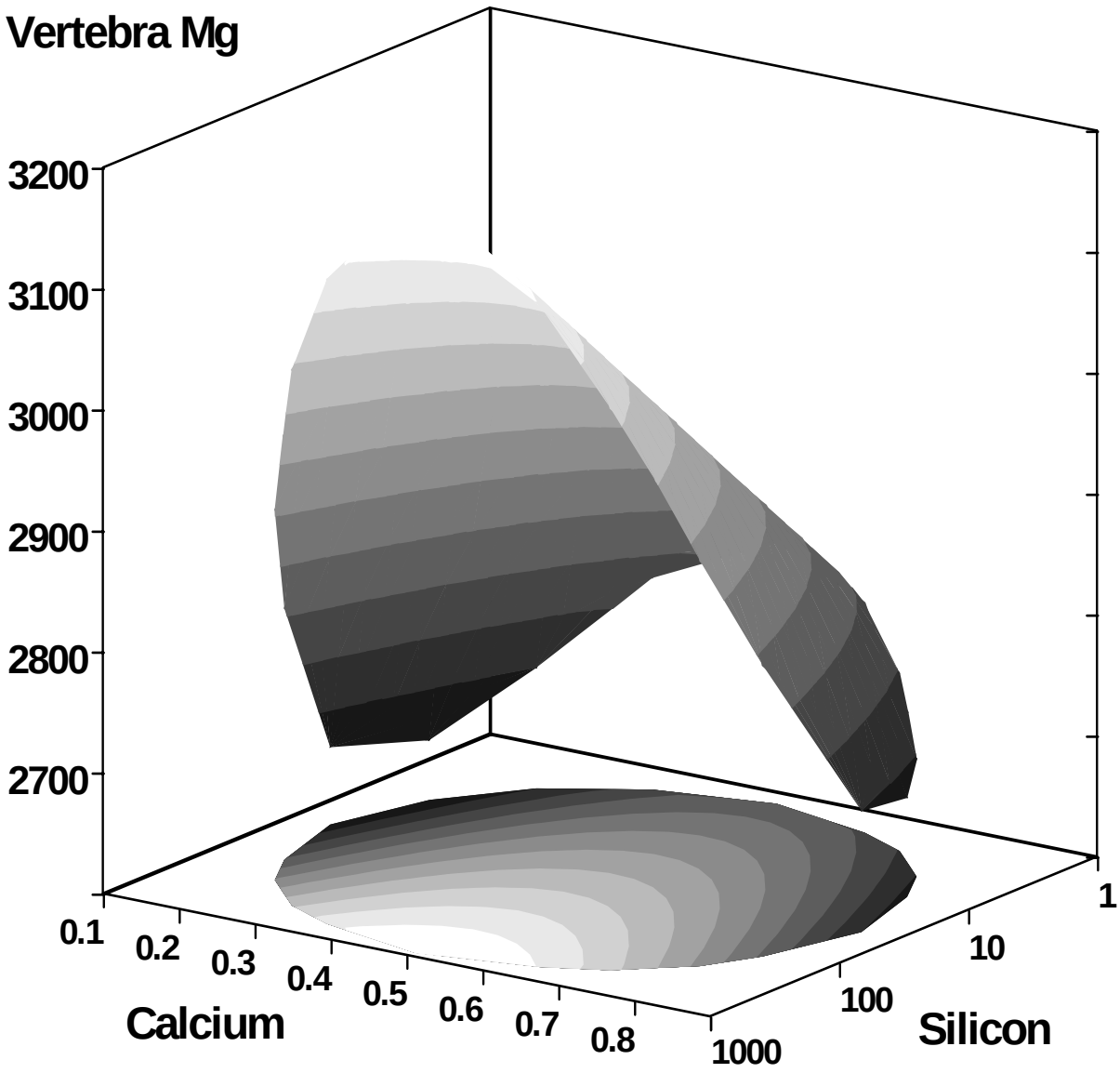

Appendix Figure 13. Response surface plot of vertebra Mg. Vertebra magnesium is expressed as μg/g dry weight. Dietary calcium is expressed as percent of diet. Dietary silicon is expressed as μg/g diet.

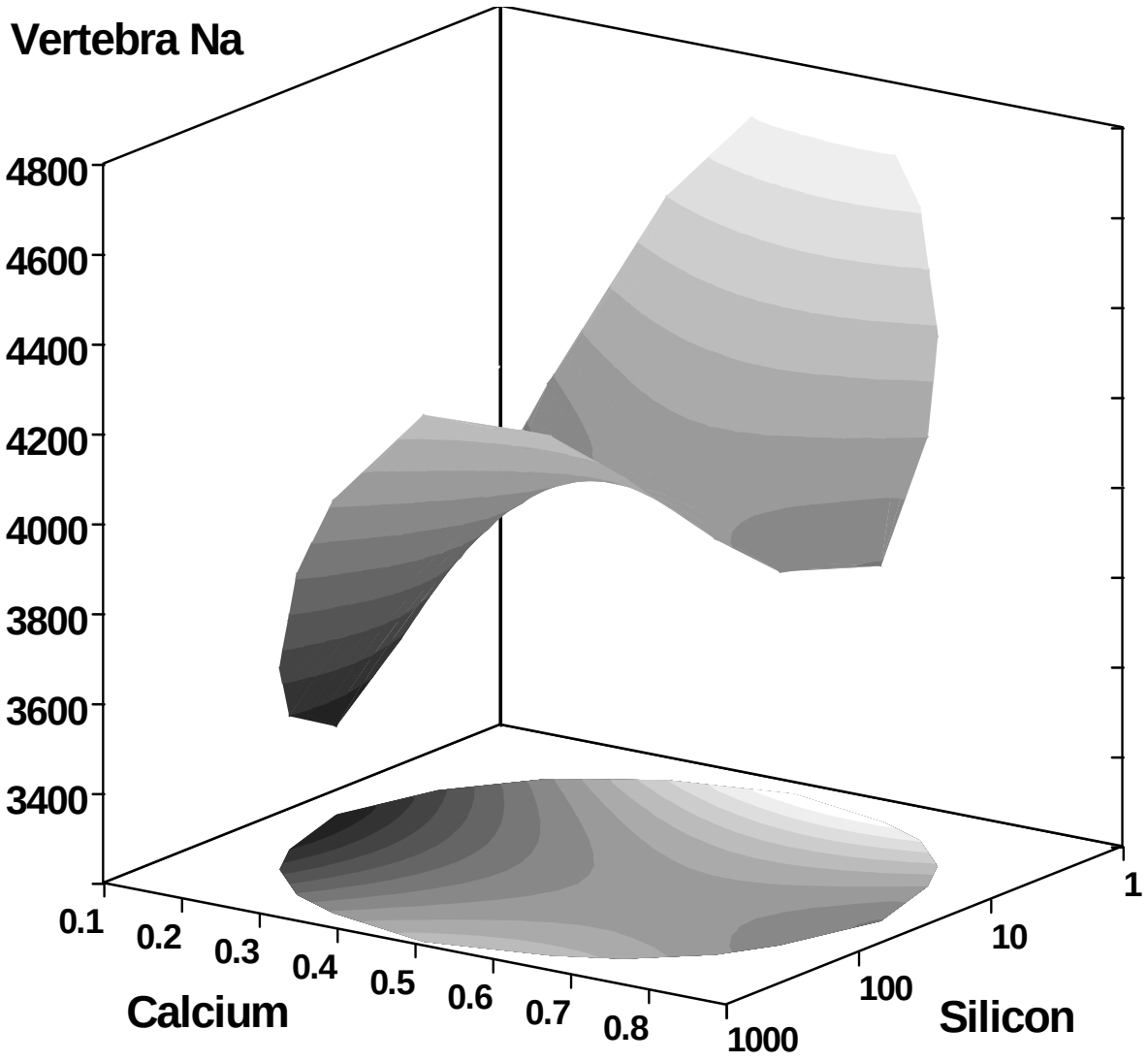

Appendix Figure 14. Response surface plot of vertebra Na**.** Vertebra sodium is expressed in μg/g dry weight. Dietary calcium is expressed as percent of diet. Dietary silicon is expressed as μg/g diet.

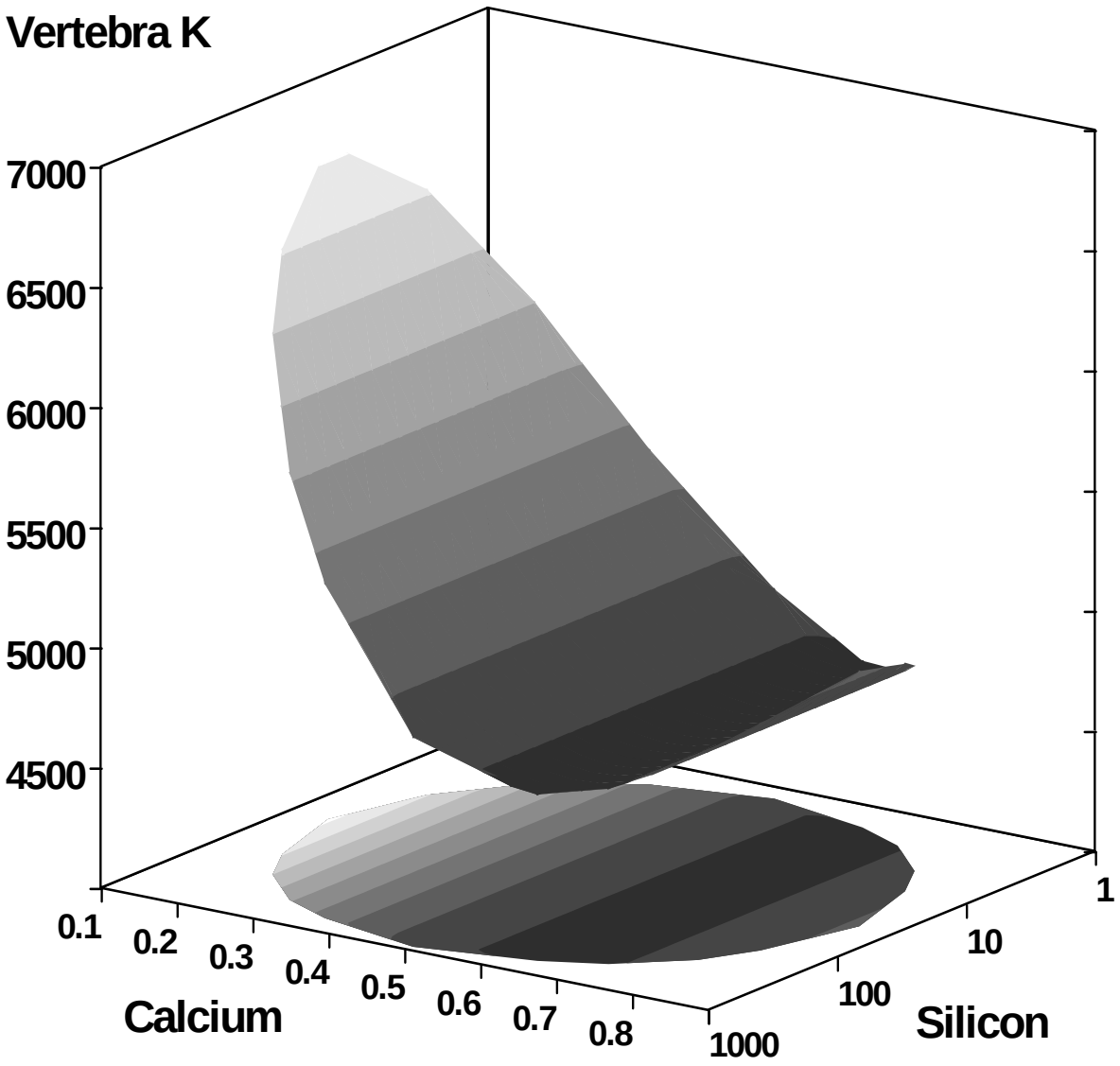

Appendix Figure 15. Response surface plot of vertebra K. Vertebra potassium is expressed in μg/g dry weight. Dietary calcium is expressed as percent of diet. Dietary silicon is expressed as μg/g diet.

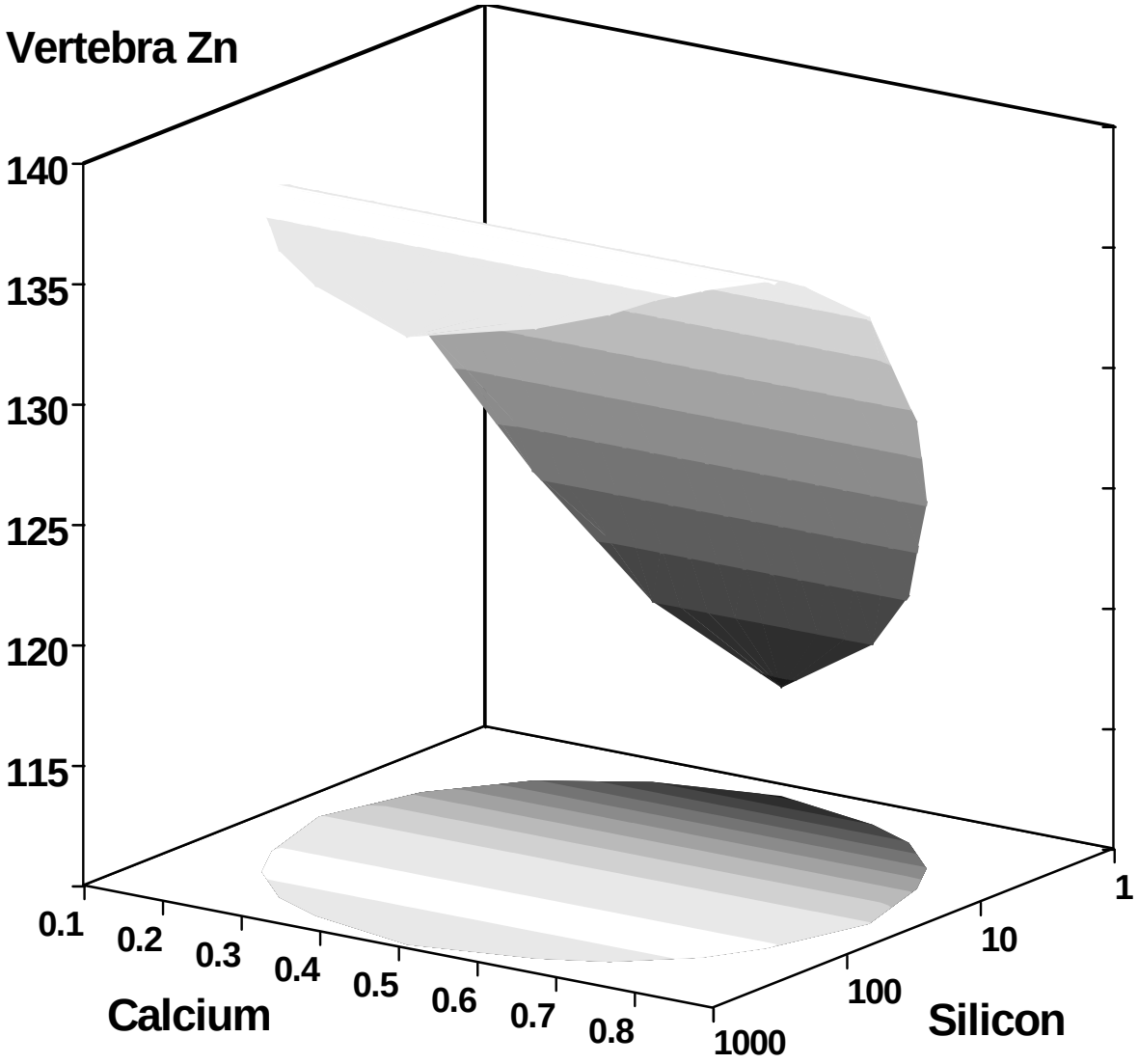

Appendix Figure 16. Response surface plot of vertebra Zn. Vertebra zinc is expressed in μg/g dry weight. Dietary calcium is expressed as percent of diet. Dietary silicon is expressed as μg/g diet.

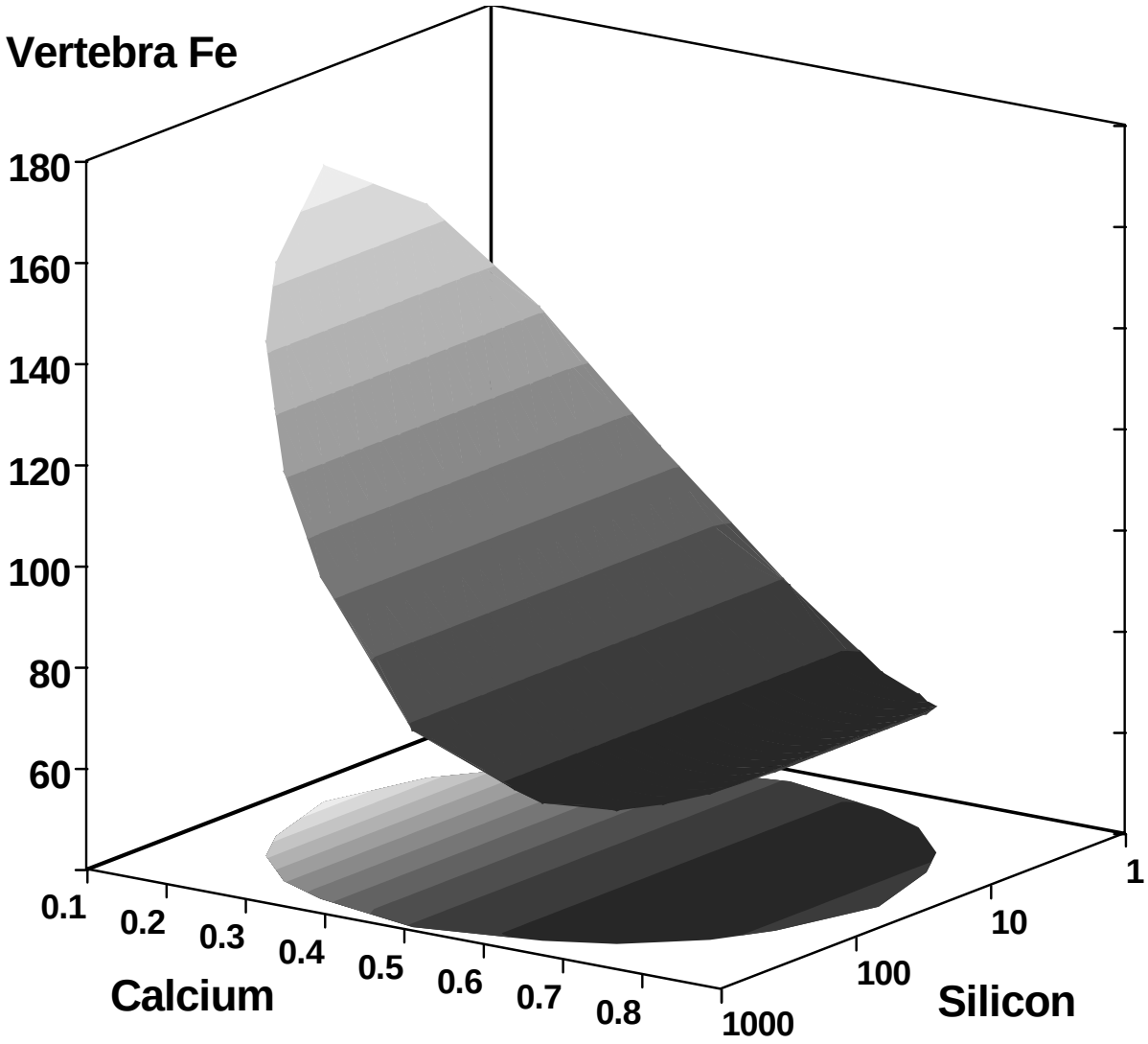

Appendix Figure 17. Response surface plot of vertebra Fe. Vertebra iron is expressed in μg/g dry weight. Dietary calcium is expressed as percent of diet. Dietary silicon is expressed as μg/g diet.

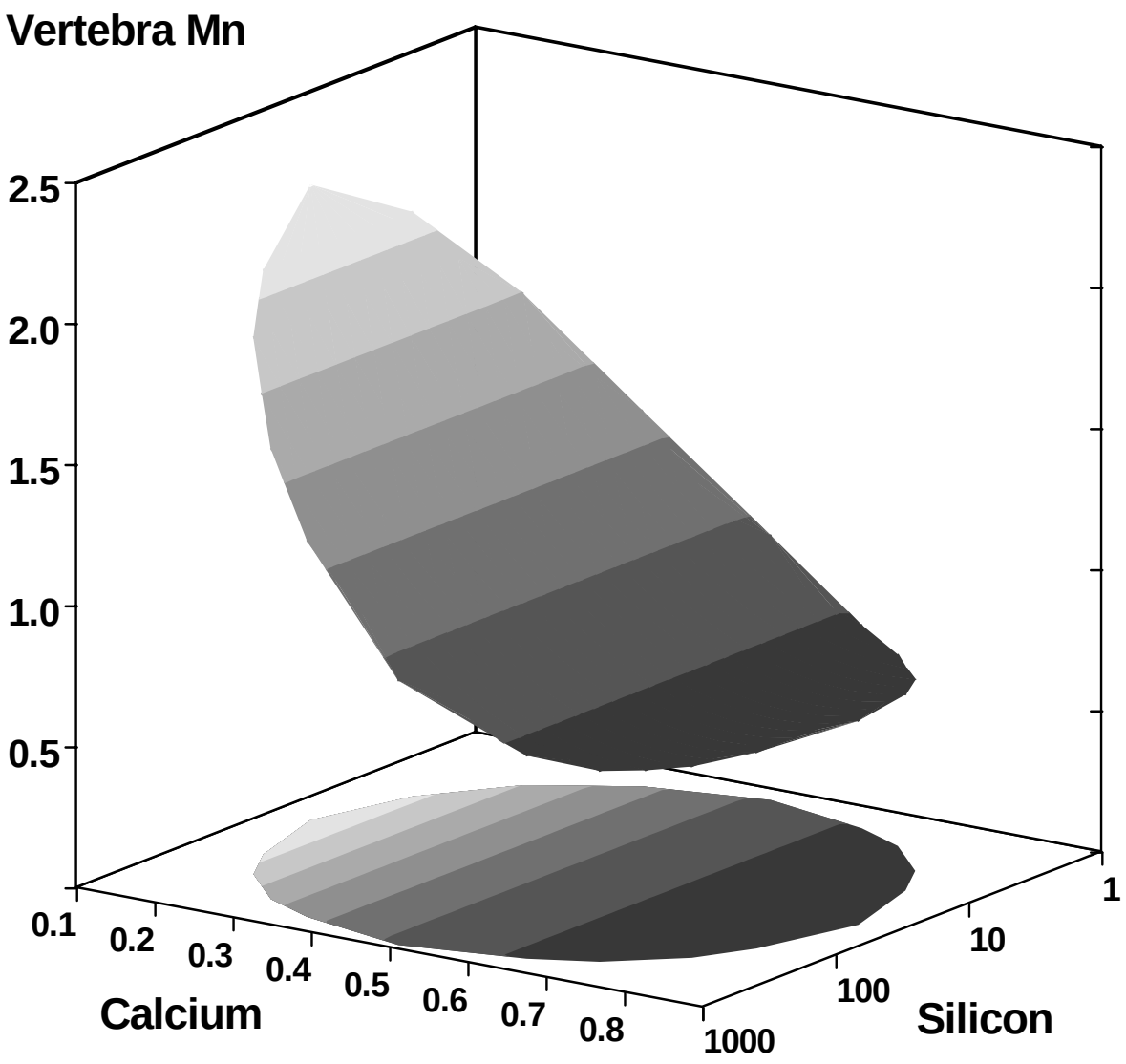

Appendix Figure 18. Response surface plot of vertebra Mn. Vertebra manganese is expressed in μg/g dry weight. Dietary calcium is expressed as percent of diet. Dietary silicon is expressed as μg/g diet.

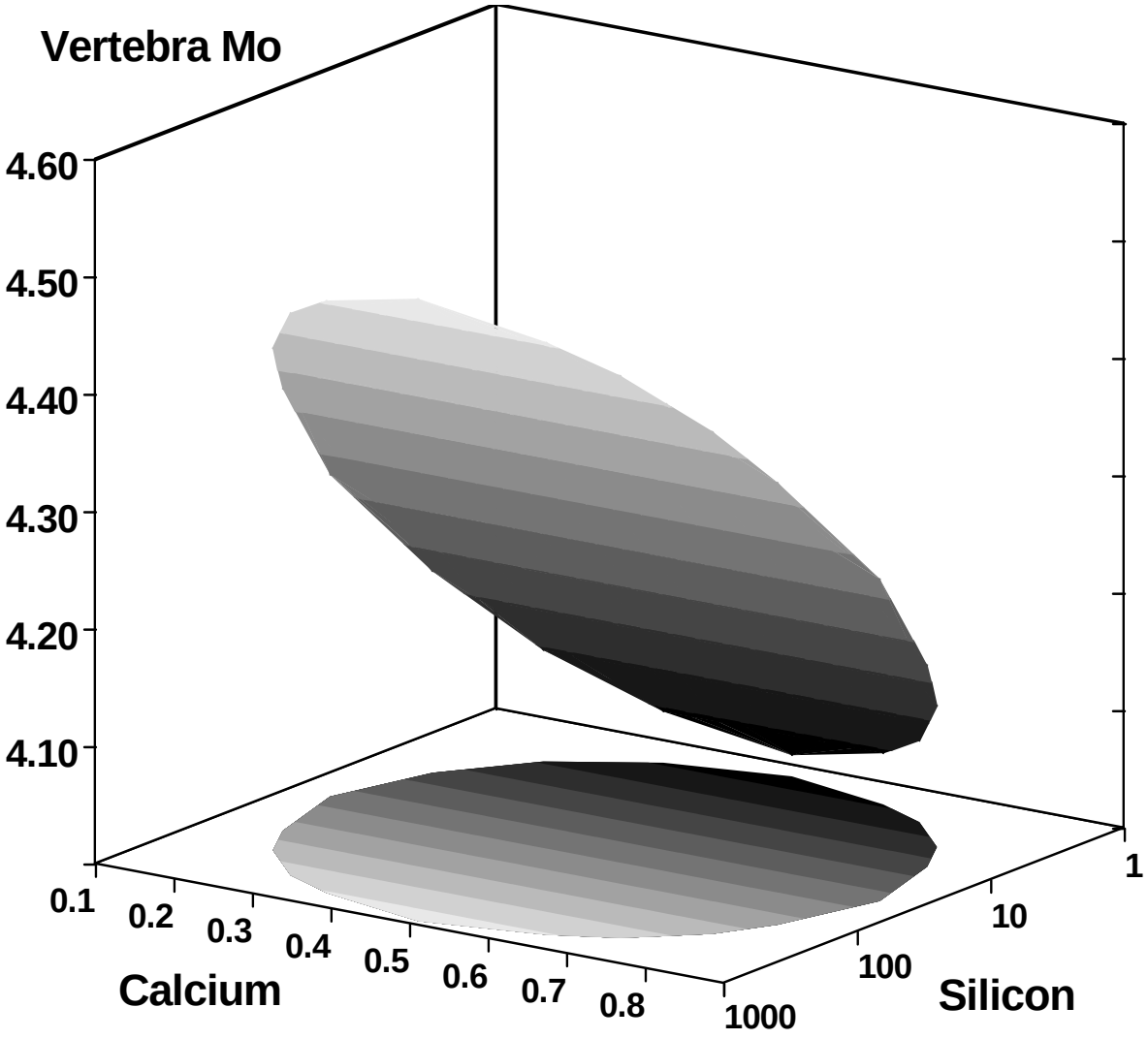

Appendix Figure 19. Response surface plot of vertebra Mo. Vertebra molybdenum is expressed in μg/g dry weight. Dietary calcium is expressed as percent of diet. Dietary silicon is expressed as μg/g diet.

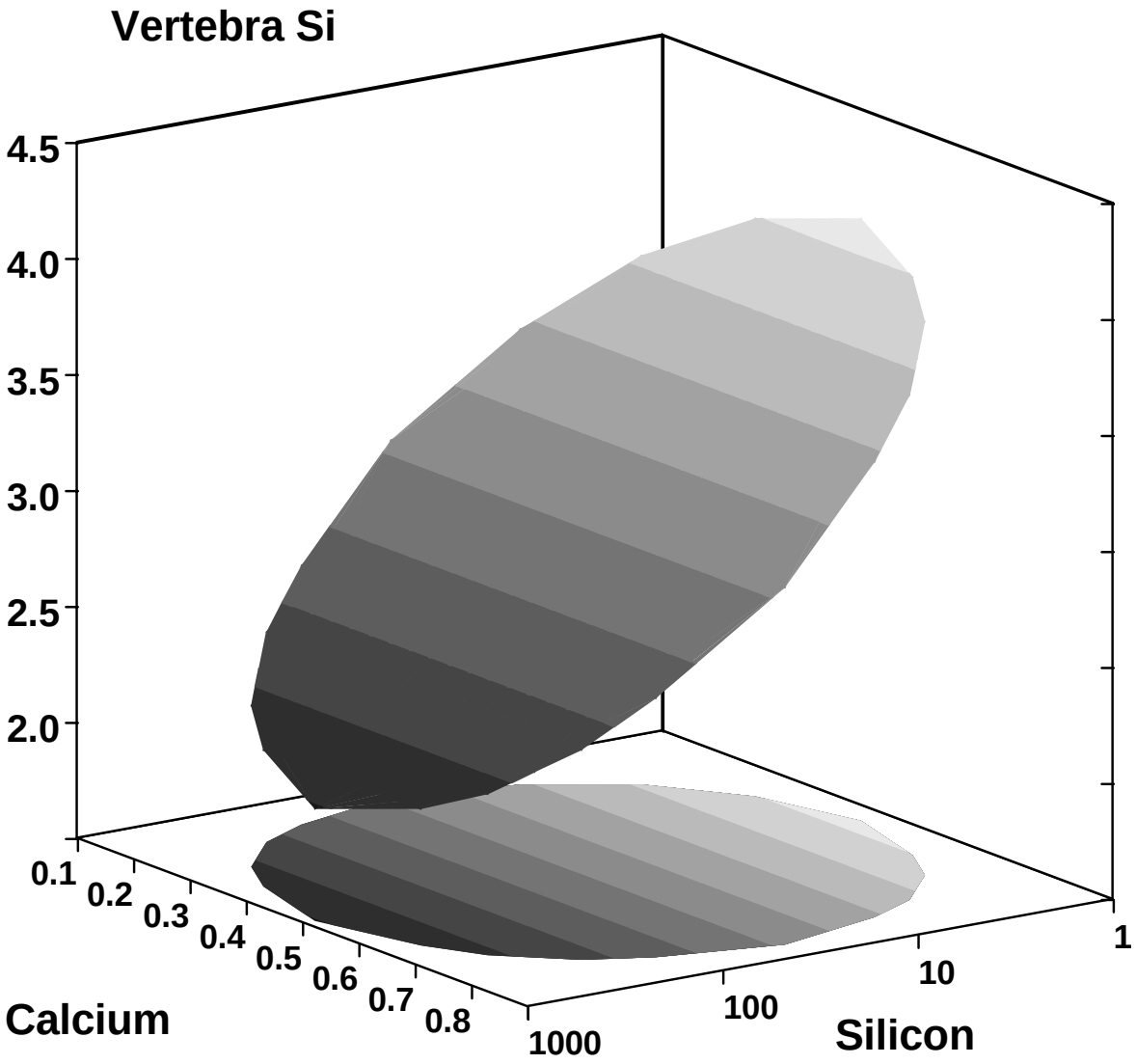

Appendix Figure 20. Response surface plot of vertebra Si. Vertebra silicon is expressed in μg/g dry weight. Dietary calcium is expressed as percent of diet. Dietary silicon is expressed as μg/g diet.

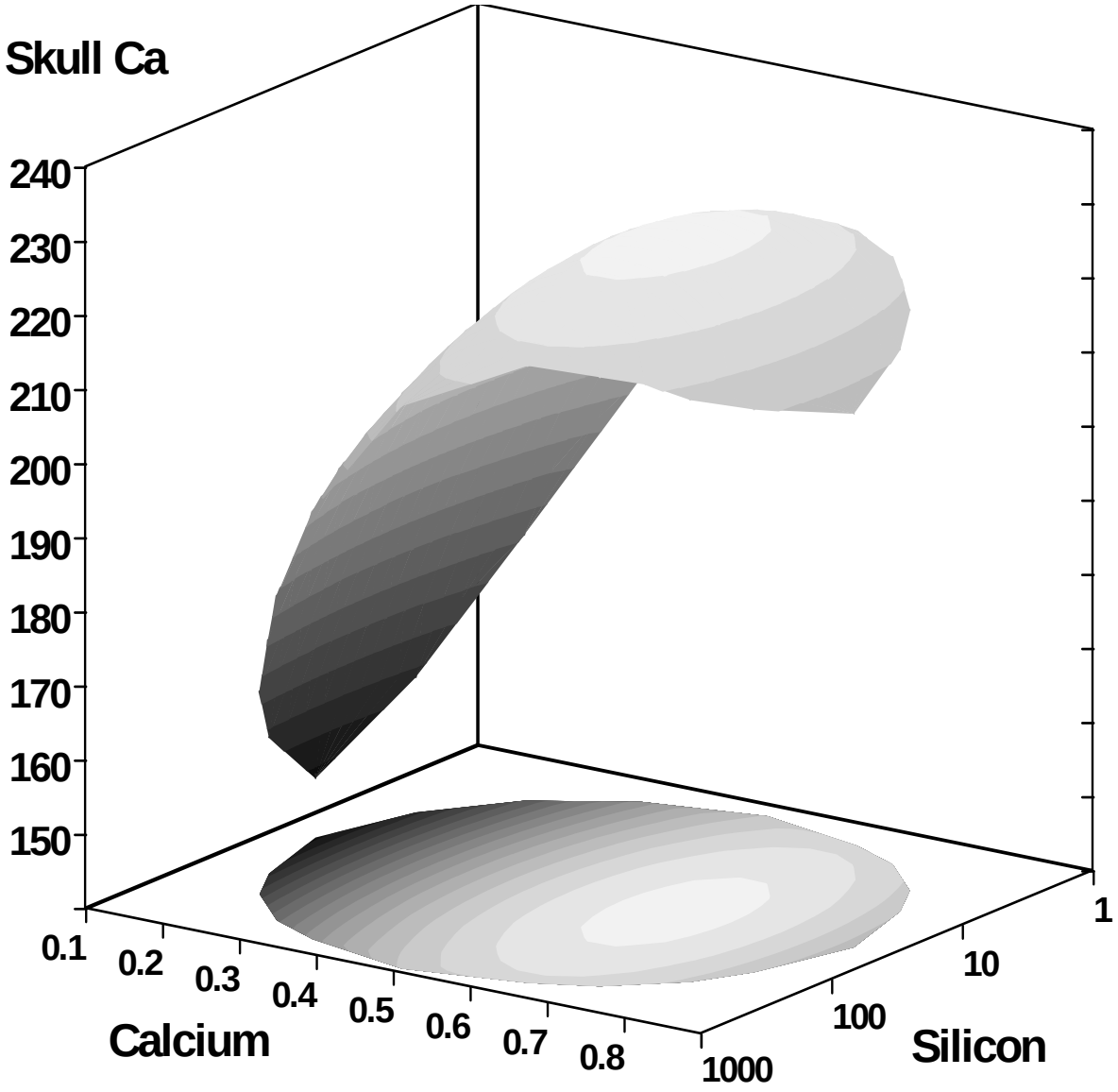

Appendix Figure 21. Response surface plot of skull Ca. Skull calcium is expressed in mg/g dry weight. Dietary calcium is expressed as percent of diet. Dietary silicon is expressed as μg/g diet.

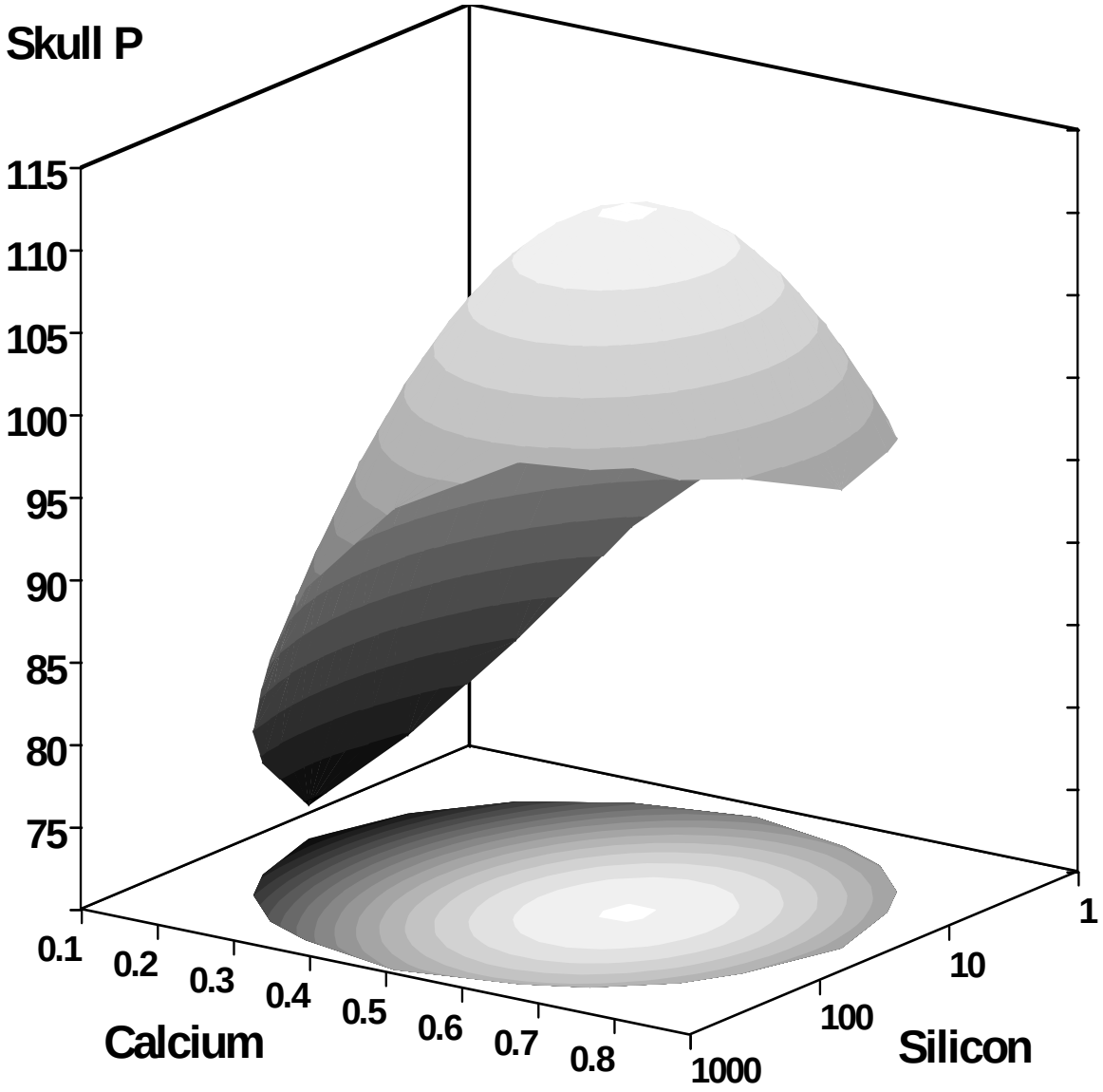

Appendix Figure 22. Response surface plot of skull P. Skull phosphorus is expressed in mg/g dry weight. Dietary calcium is expressed as percent of diet. Dietary silicon is expressed as μg/g diet.

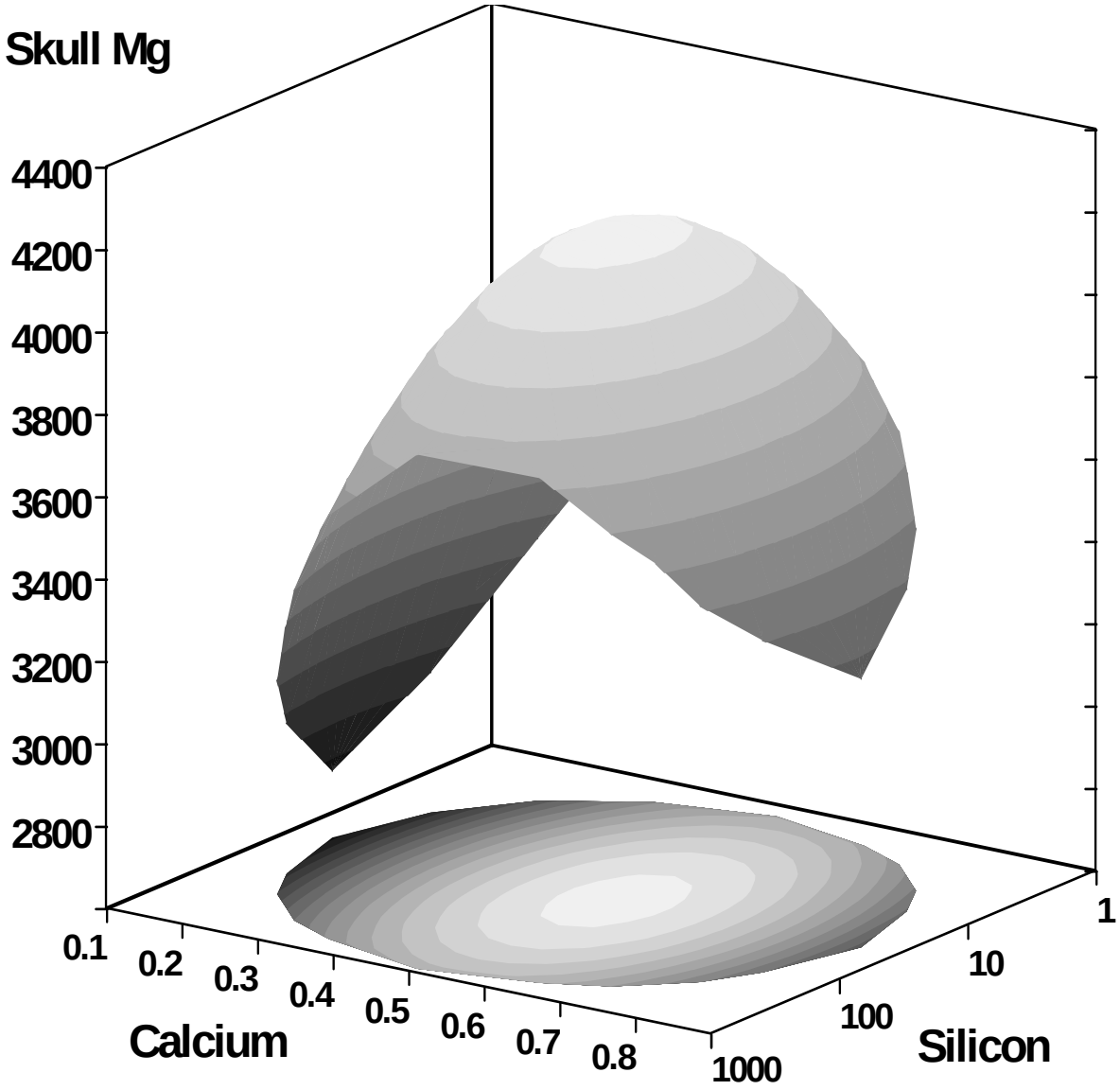

Appendix Figure 23. Response surface plot of skull Mg. Skull magnesium is expressed in μg/g dry weight. Dietary calcium is expressed as percent of diet. Dietary silicon is expressed as μg/g diet.

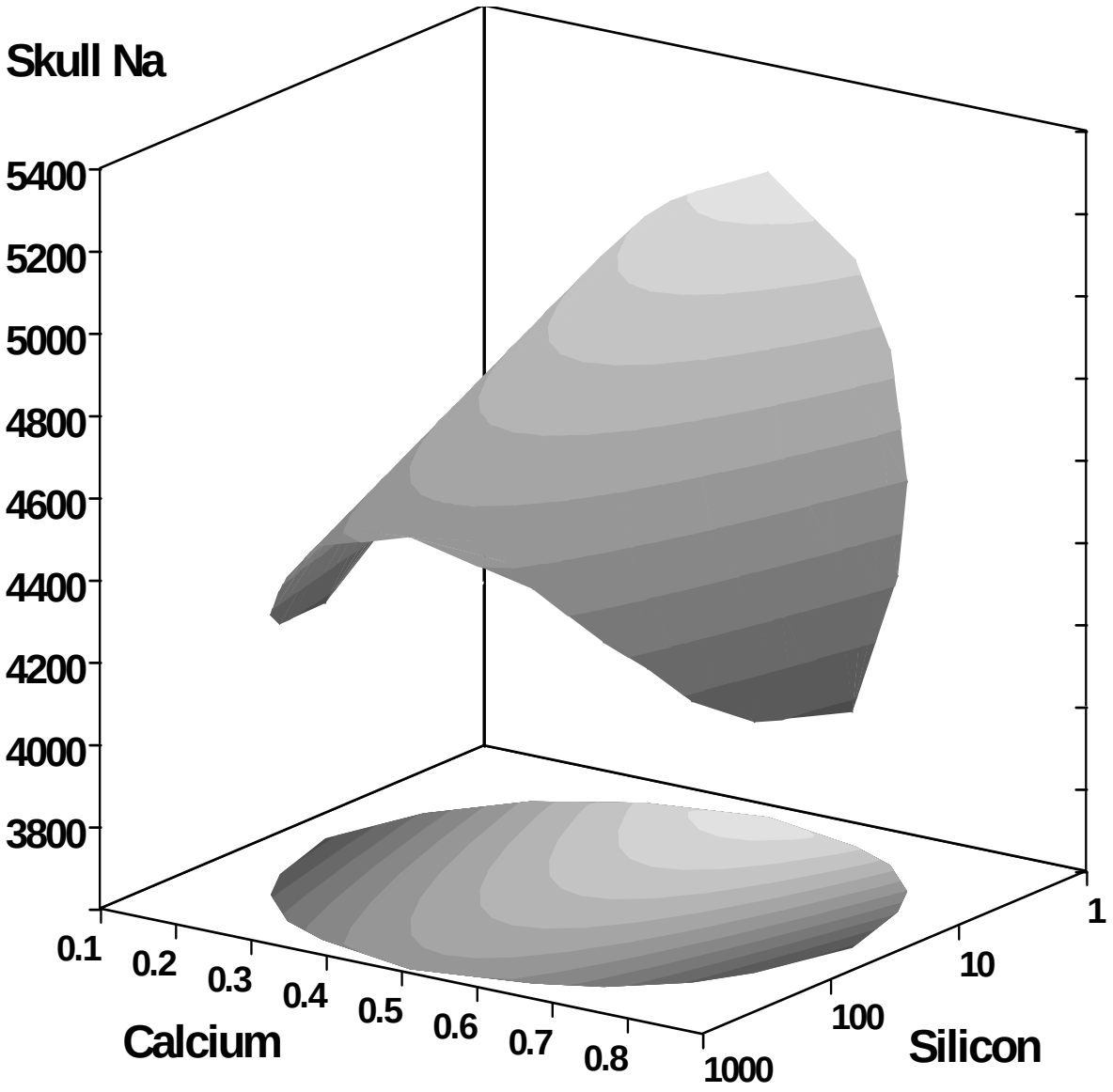

Appendix Figure 24. Response surface plot of skull Na. Skull sodium is expressed in μg/g dry weight. Dietary calcium is expressed as percent of diet. Dietary silicon is expressed as μg/g diet.

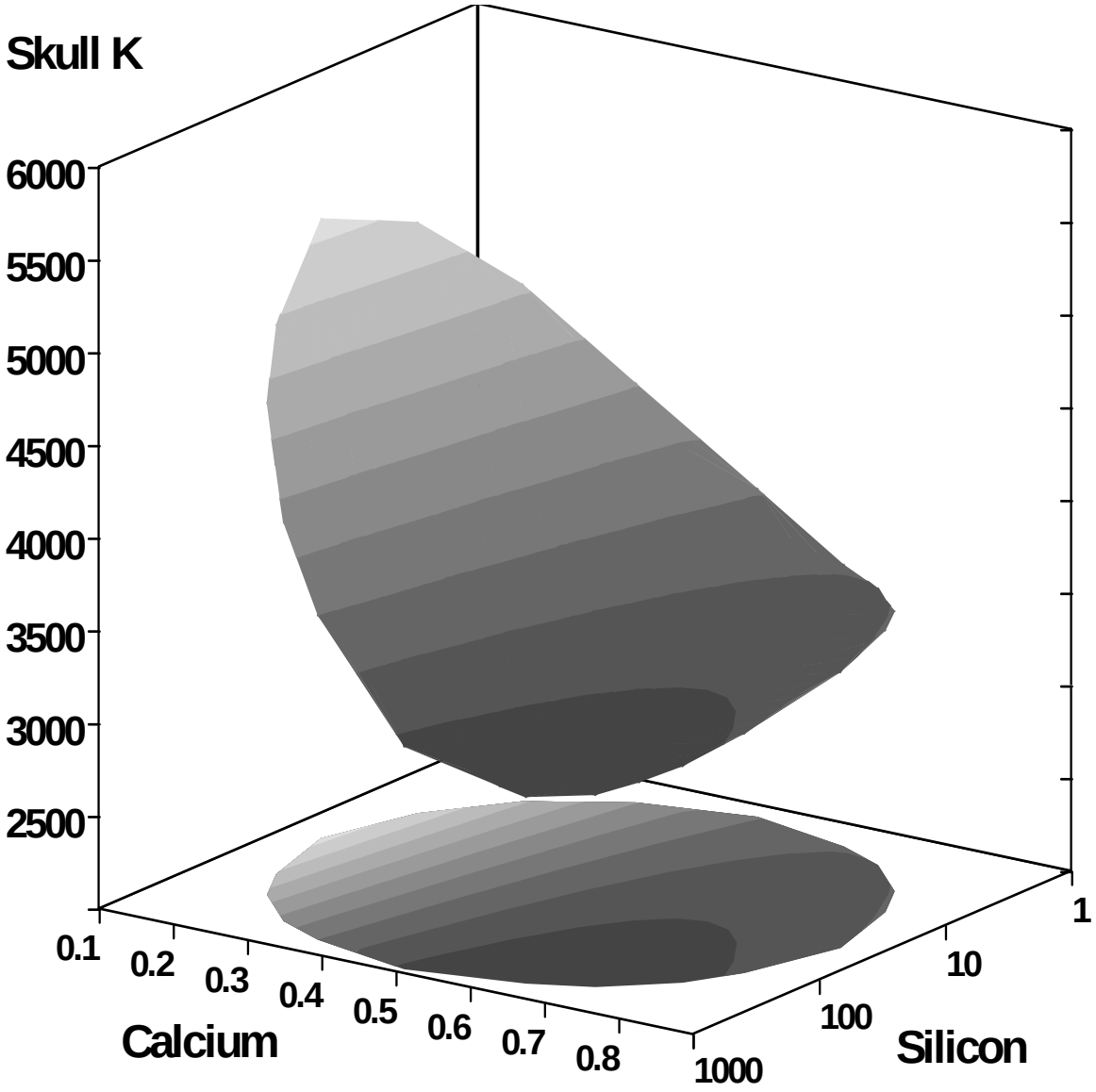

Appendix Figure 25. Response surface plot of skull K. Skull potassium is expressed in μg/g dry weight. Dietary calcium is expressed as percent of diet. Dietary silicon is expressed as μg/g diet.

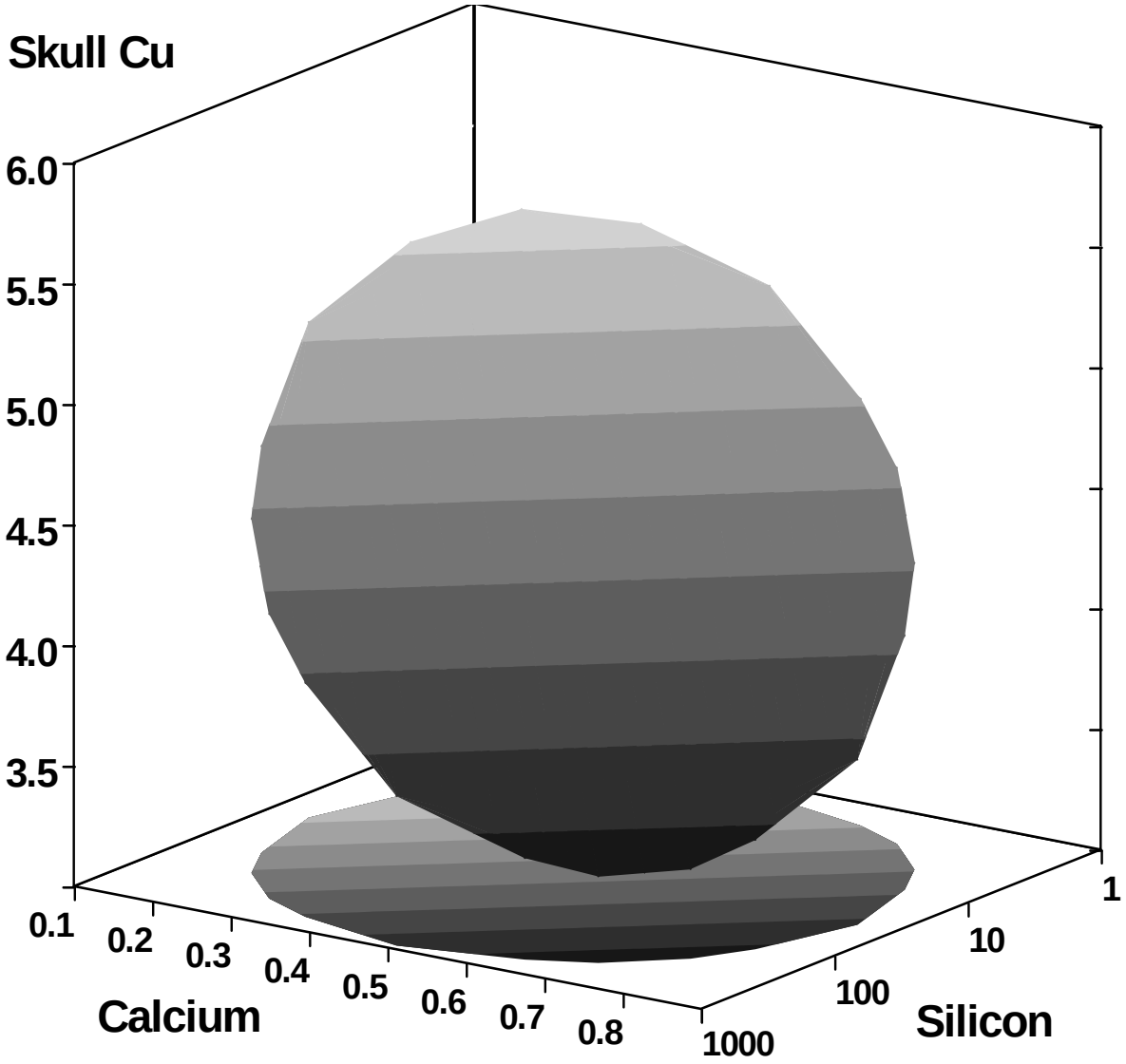

Appendix Figure 26. Response surface plot of skull Cu. Skull copper is expressed in μg/g dry weight. Dietary calcium is expressed as percent of diet. Dietary silicon is expressed as μg/g diet.

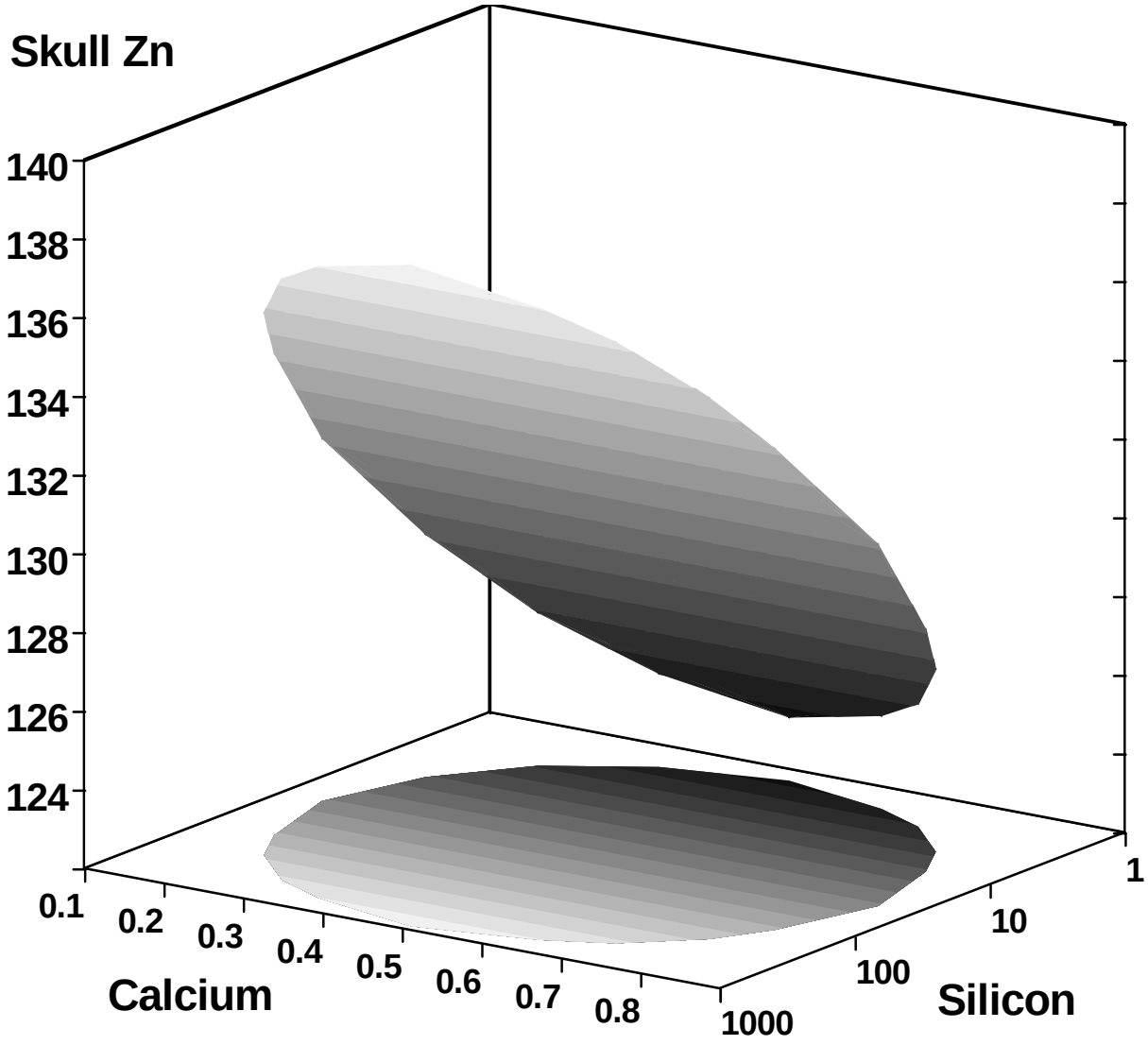

Appendix Figure 27. Response surface plot of skull Zn. Skull zinc is expressed in μg/g dry weight. Dietary calcium is expressed as percent of diet. Dietary silicon is expressed as μg/g diet.

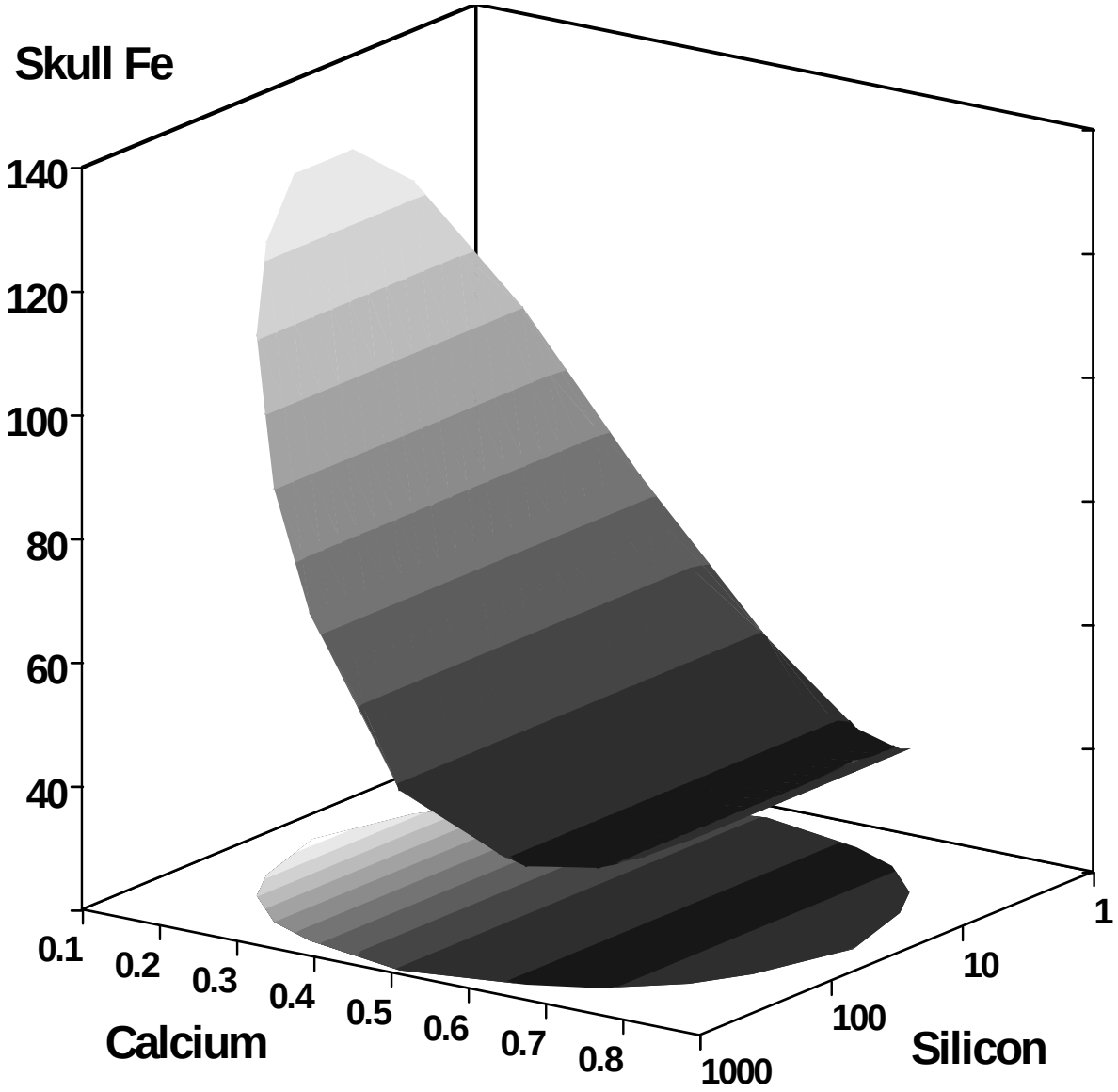

Appendix Figure 28. Response surface plot of skull Fe. Skull iron is expressed in μg/g dry weight. Dietary calcium is expressed as percent of diet. Dietary silicon is expressed as μg/g diet.

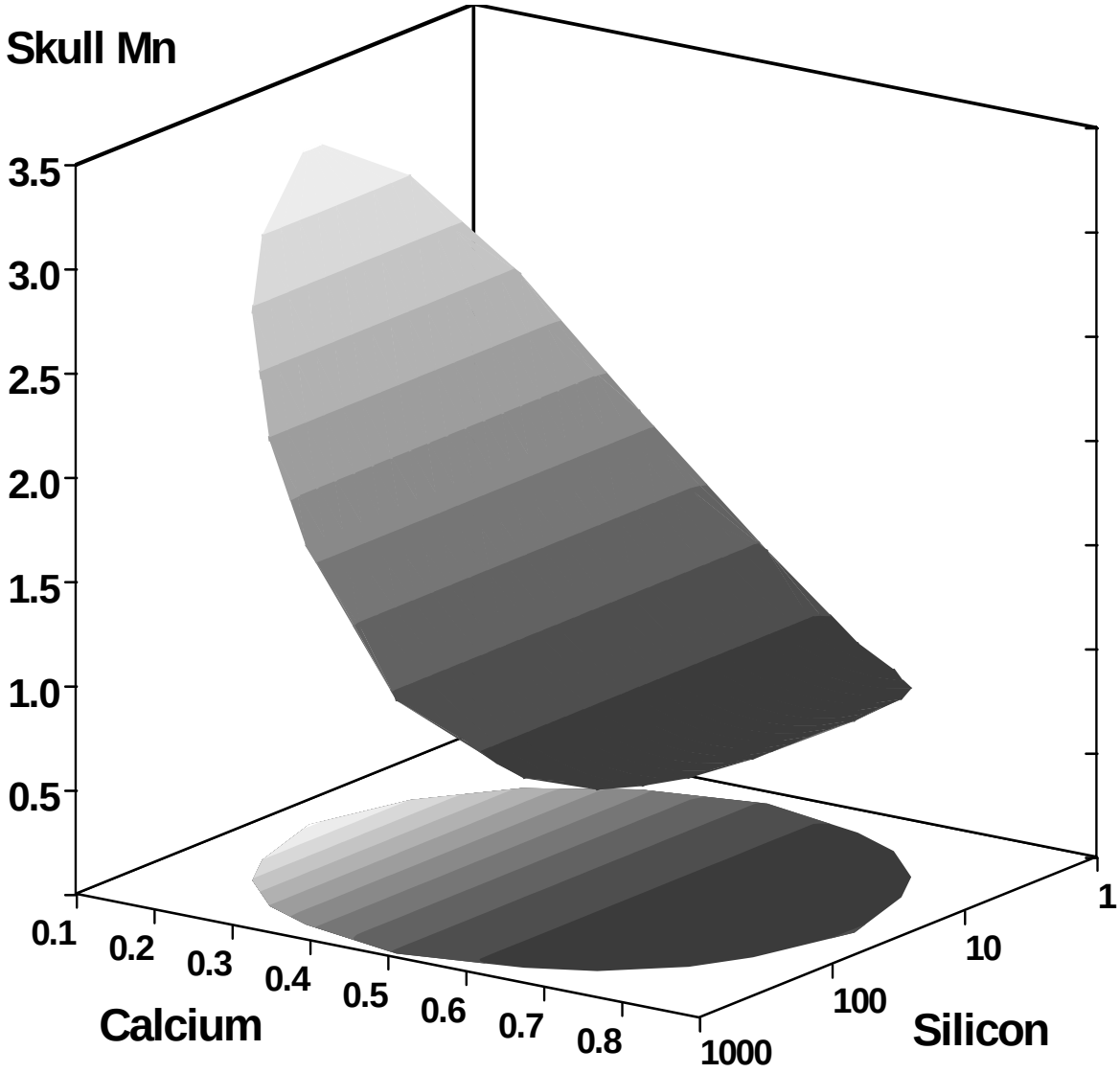

Appendix Figure 29. Response surface plot of skull Mn. Skull manganese is expressed in μg/g dry weight. Dietary calcium is expressed as percent of diet. Dietary silicon is expressed as μg/g diet.

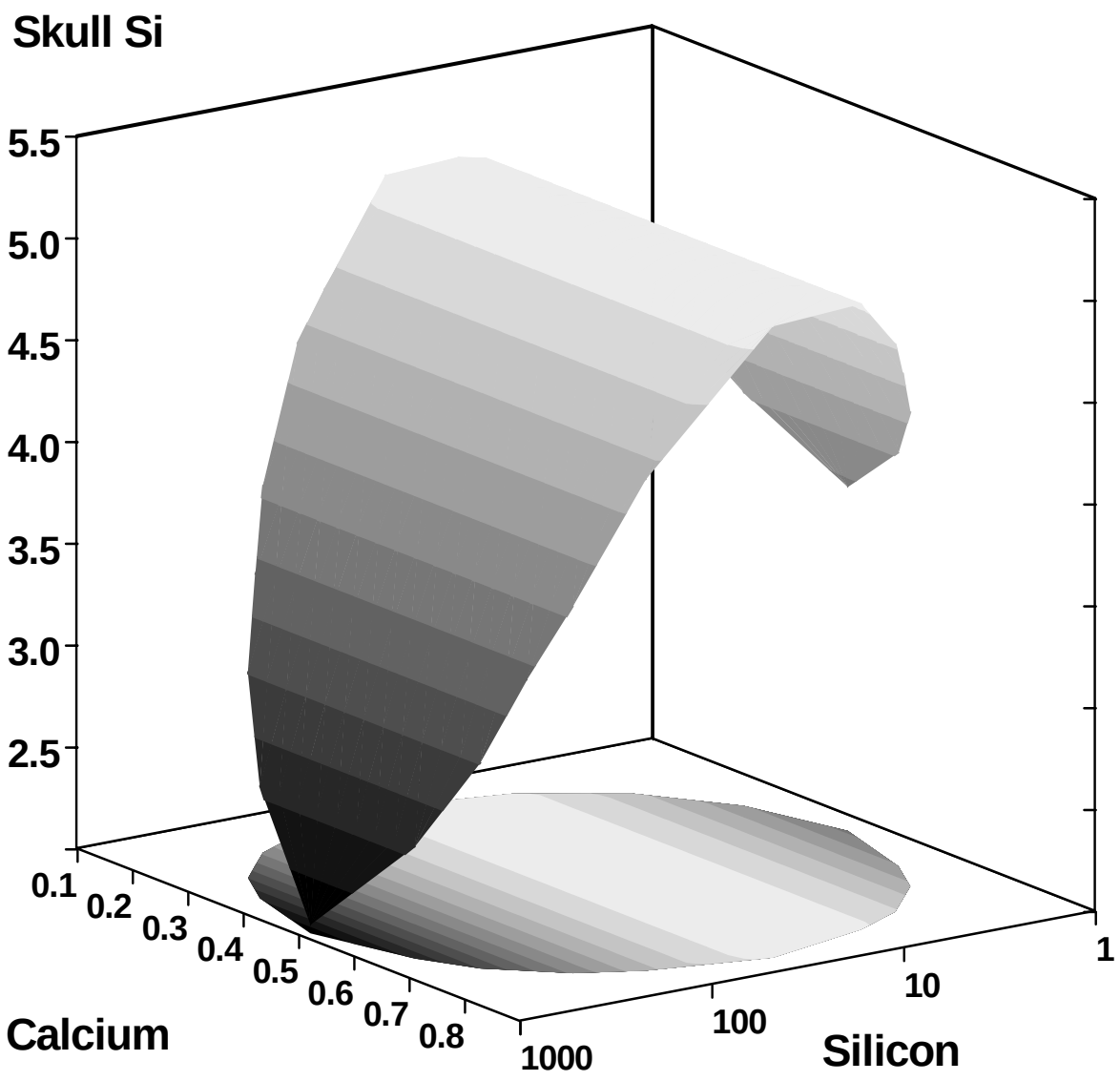

Appendix Figure 30. Response surface plot of skull Si. Skull silicon is expressed in μg/g dry weight. Dietary calcium is expressed as percent of diet. Dietary silicon is expressed as μg/g diet.

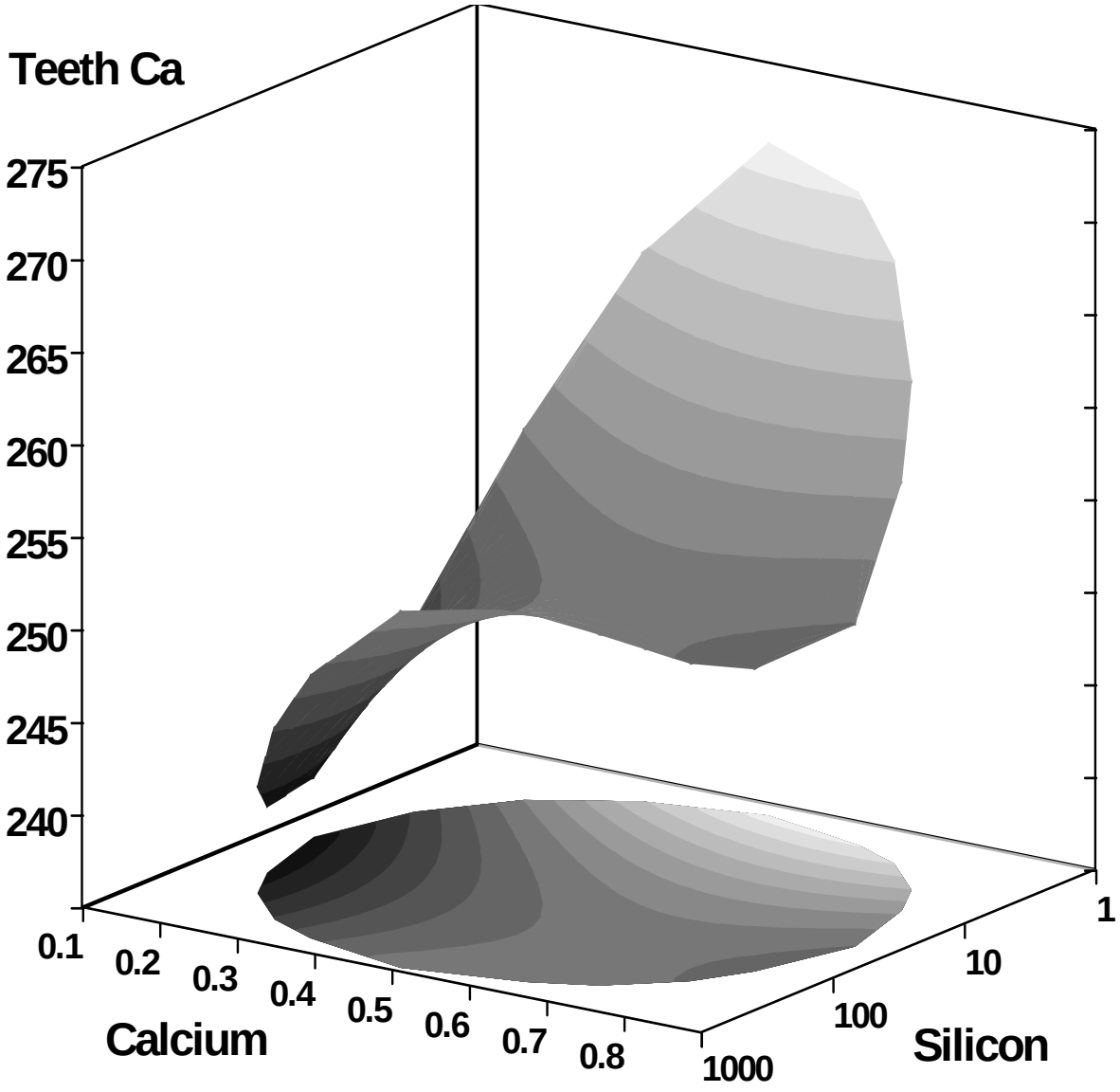

Appendix Figure 31. Response surface plot of teeth Ca. Teeth calcium is expressed in mg/g dry weight. Dietary calcium is expressed as percent of diet. Dietary silicon is expressed as μg/g diet.

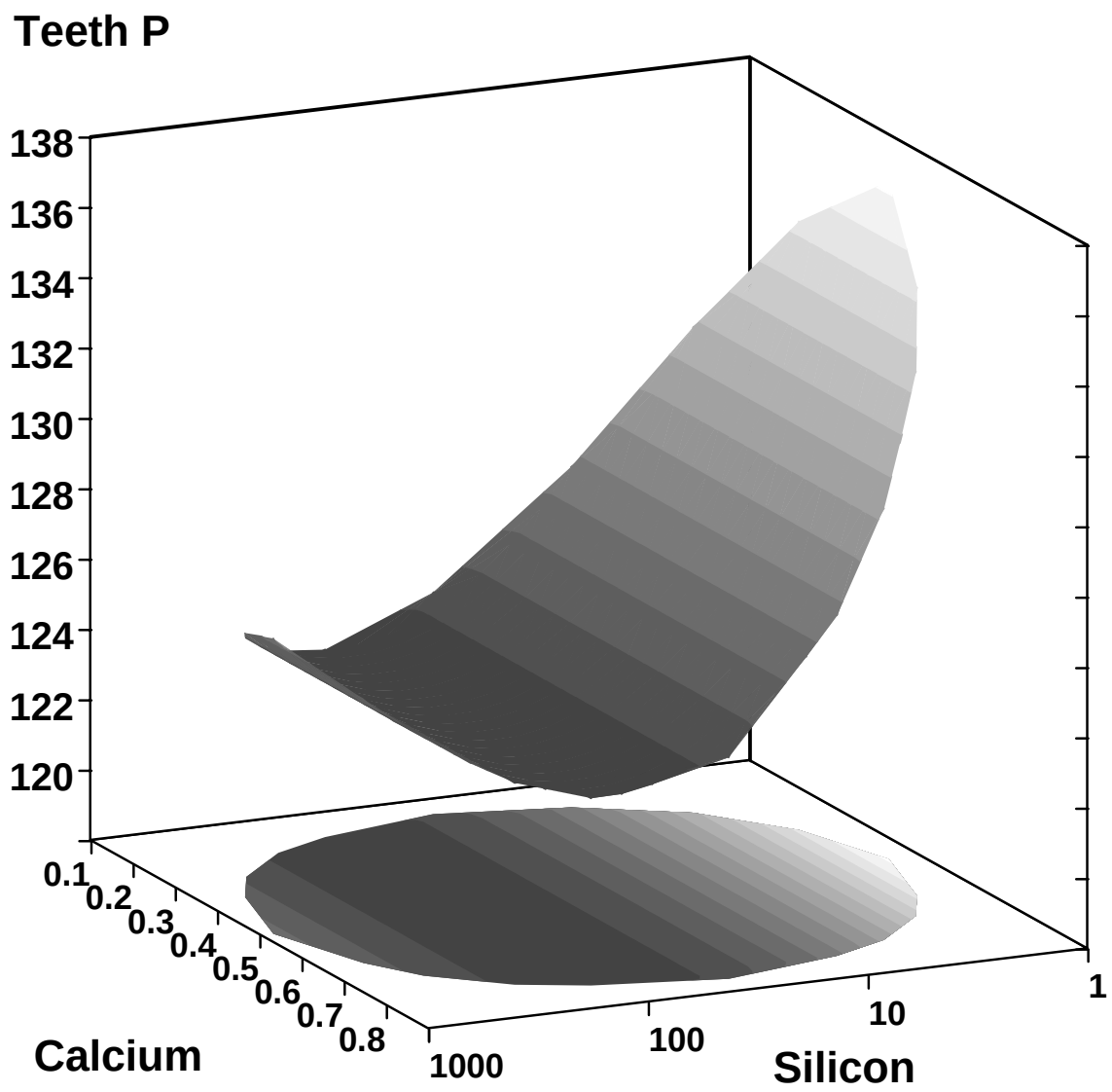

Appendix Figure 32. Response surface plot of teeth P. Teeth phosphorus is expressed in mg/g dry weight. Dietary calcium is expressed as percent of diet. Dietary silicon is expressed as μg/g diet.

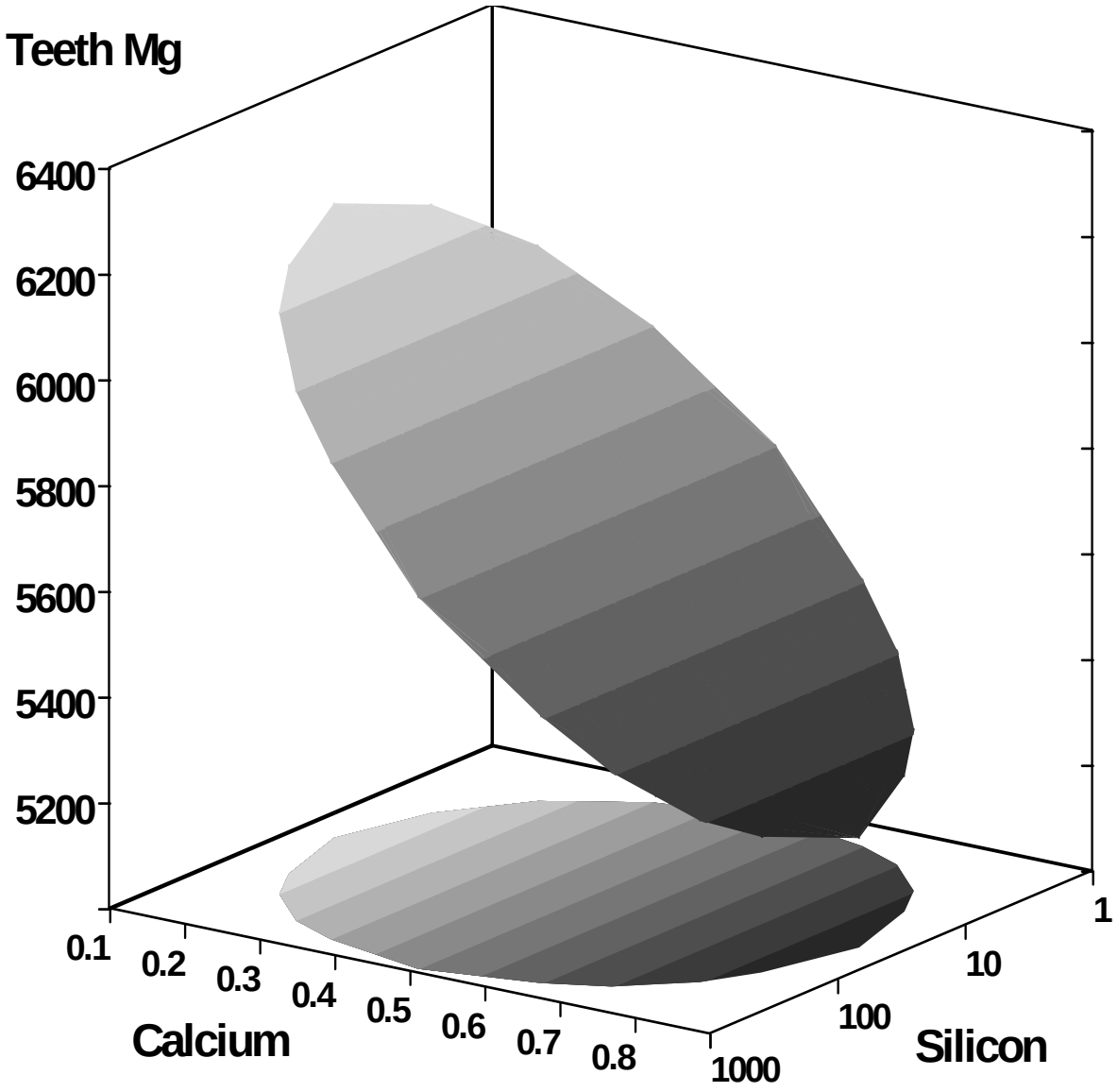

Appendix Figure 33. Response surface plot of teeth Mg. Teeth magnesium is expressed in μg/g dry weight. Dietary calcium is expressed as percent of diet. Dietary silicon is expressed as μg/g diet.

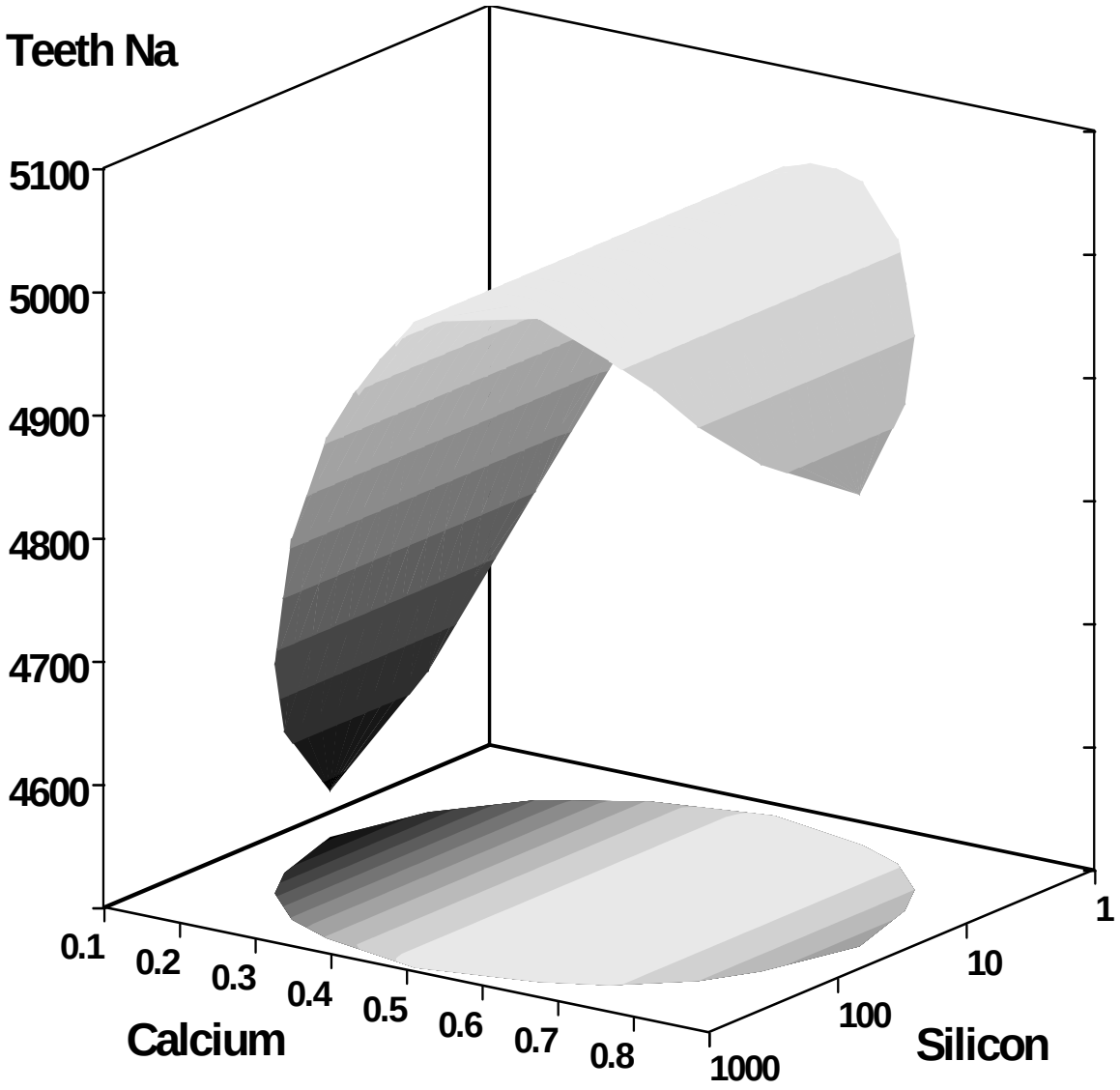

Appendix Figure 34. Response surface plot of teeth Na. Teeth sodium is expressed in μg/g dry weight. Dietary calcium is expressed as percent of diet. Dietary silicon is expressed as μg/g diet.

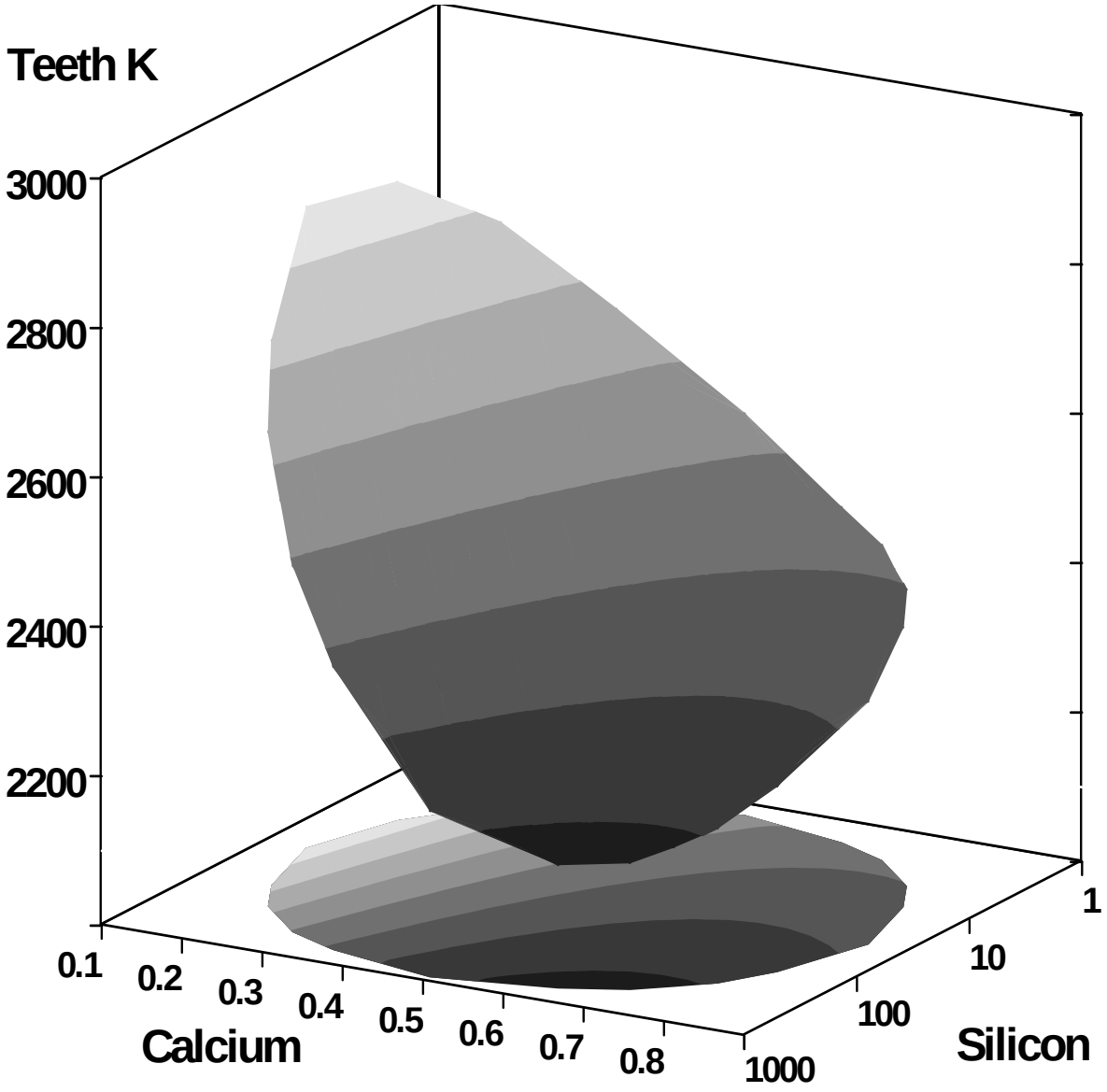

Appendix Figure 35. Response surface plot of teeth K. Teeth potassium is expressed in μg/g dry weight. Dietary calcium is expressed as percent of diet. Dietary silicon is expressed as μg/g diet.

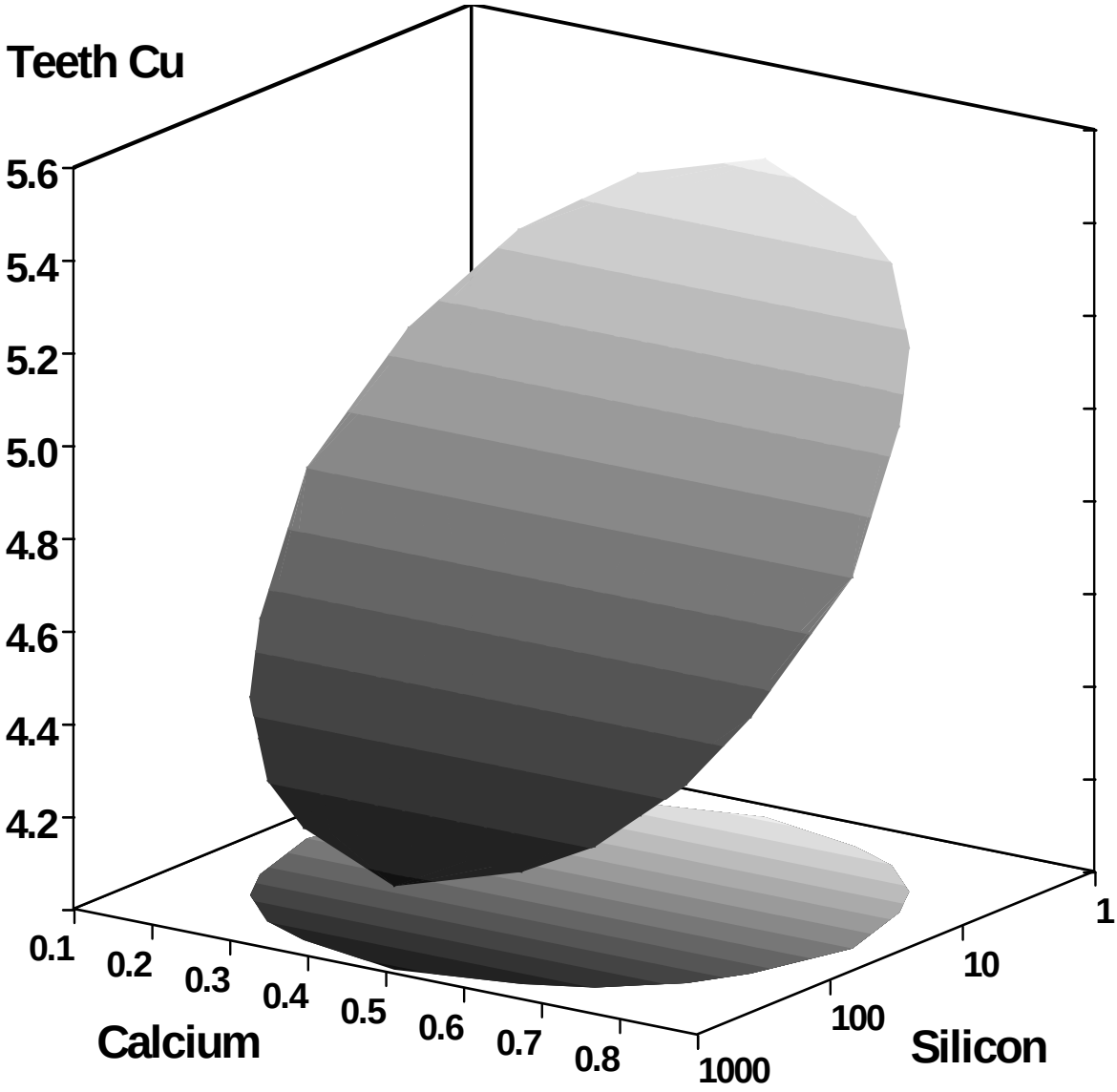

Appendix Figure 36. Response surface plot of teeth Cu. Teeth copper is expressed in μg/g dry weight. Dietary calcium is expressed as percent of diet. Dietary silicon is expressed as μg/g diet.

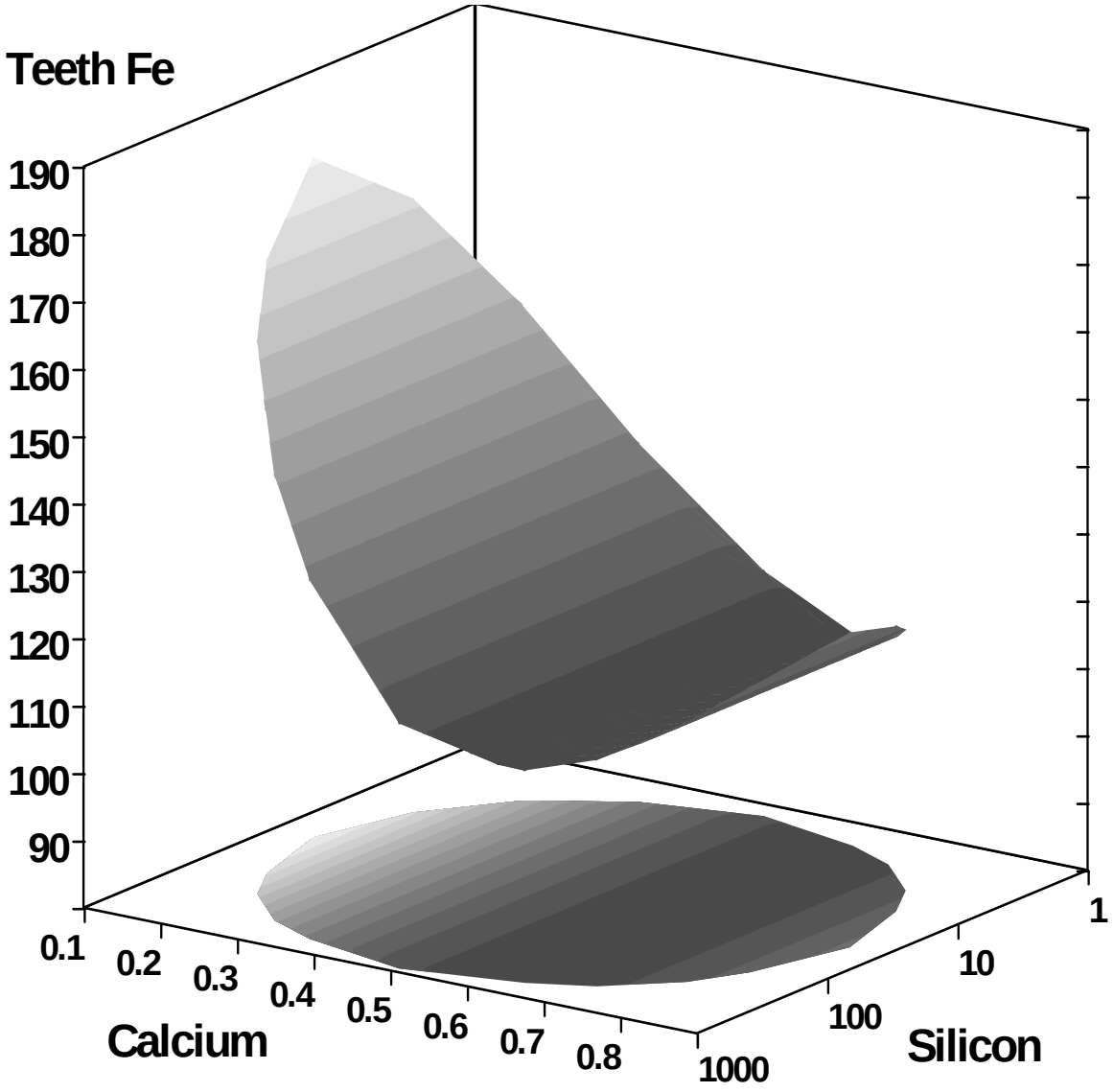

Appendix Figure 37. Response surface plot of teeth Fe. Teeth iron is expressed in μg/g dry weight. Dietary calcium is expressed as percent of diet. Dietary silicon is expressed as μg/g diet.

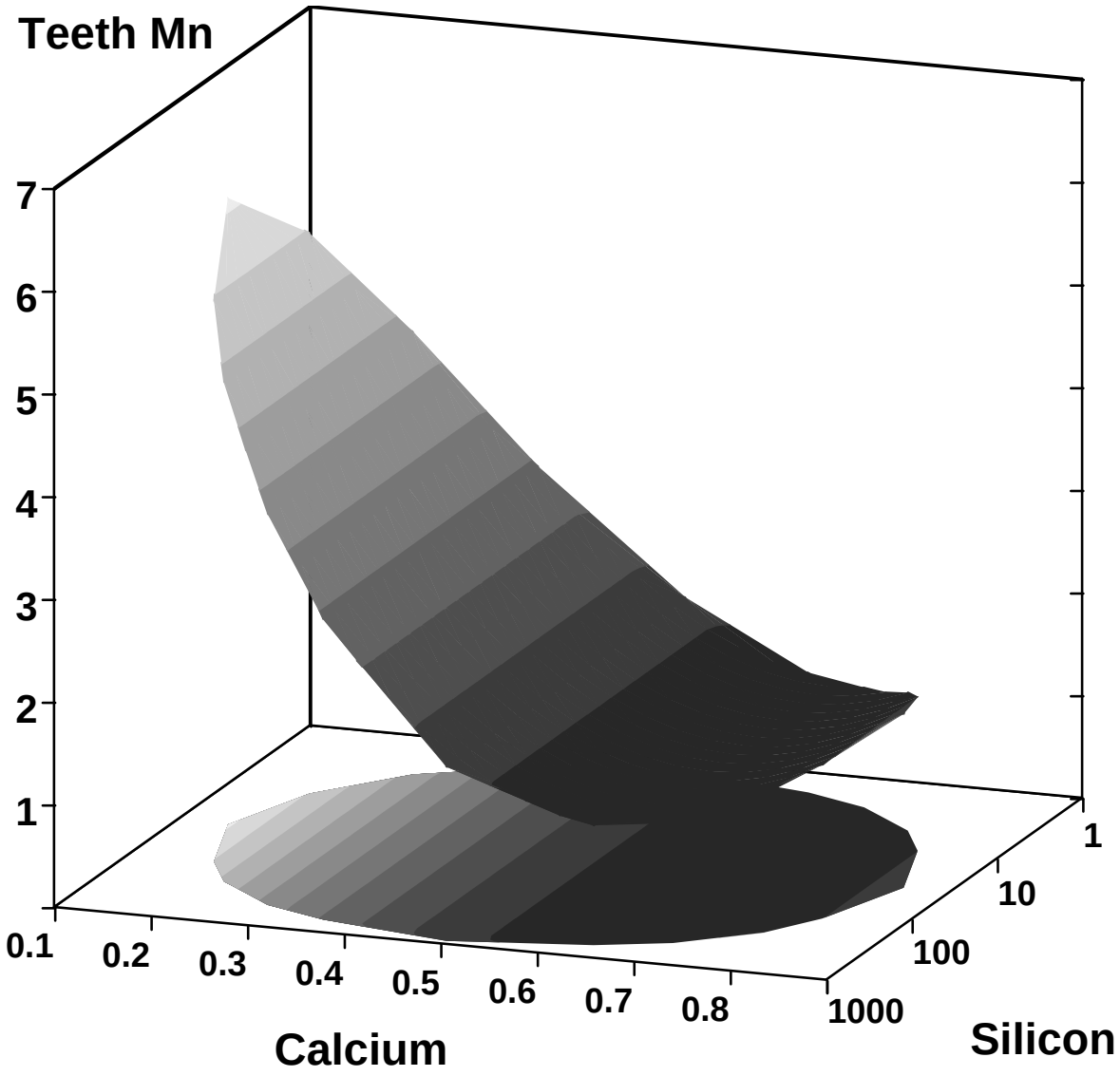

Appendix Figure 38. Response surface plot of teeth Mn. Teeth manganese is expressed in μg/g dry weight. Dietary calcium is expressed as percent of diet. Dietary silicon is expressed as μg/g diet.

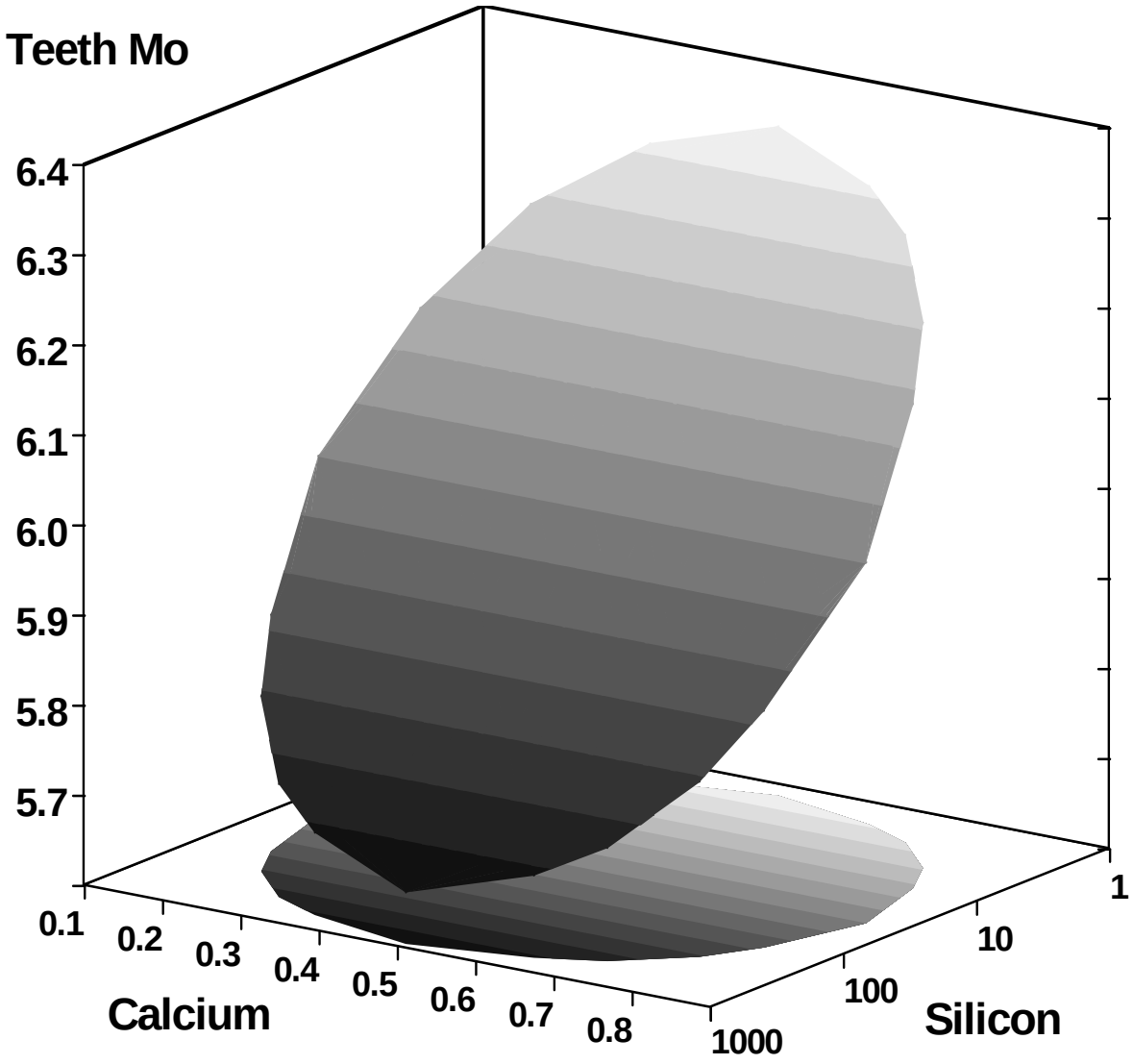

Appendix Figure 39. Response surface plot of teeth Mo. Teeth molybdenum is expressed in μg/g dry weight. Dietary calcium is expressed as percent of diet. Dietary silicon is expressed as μg/g diet.

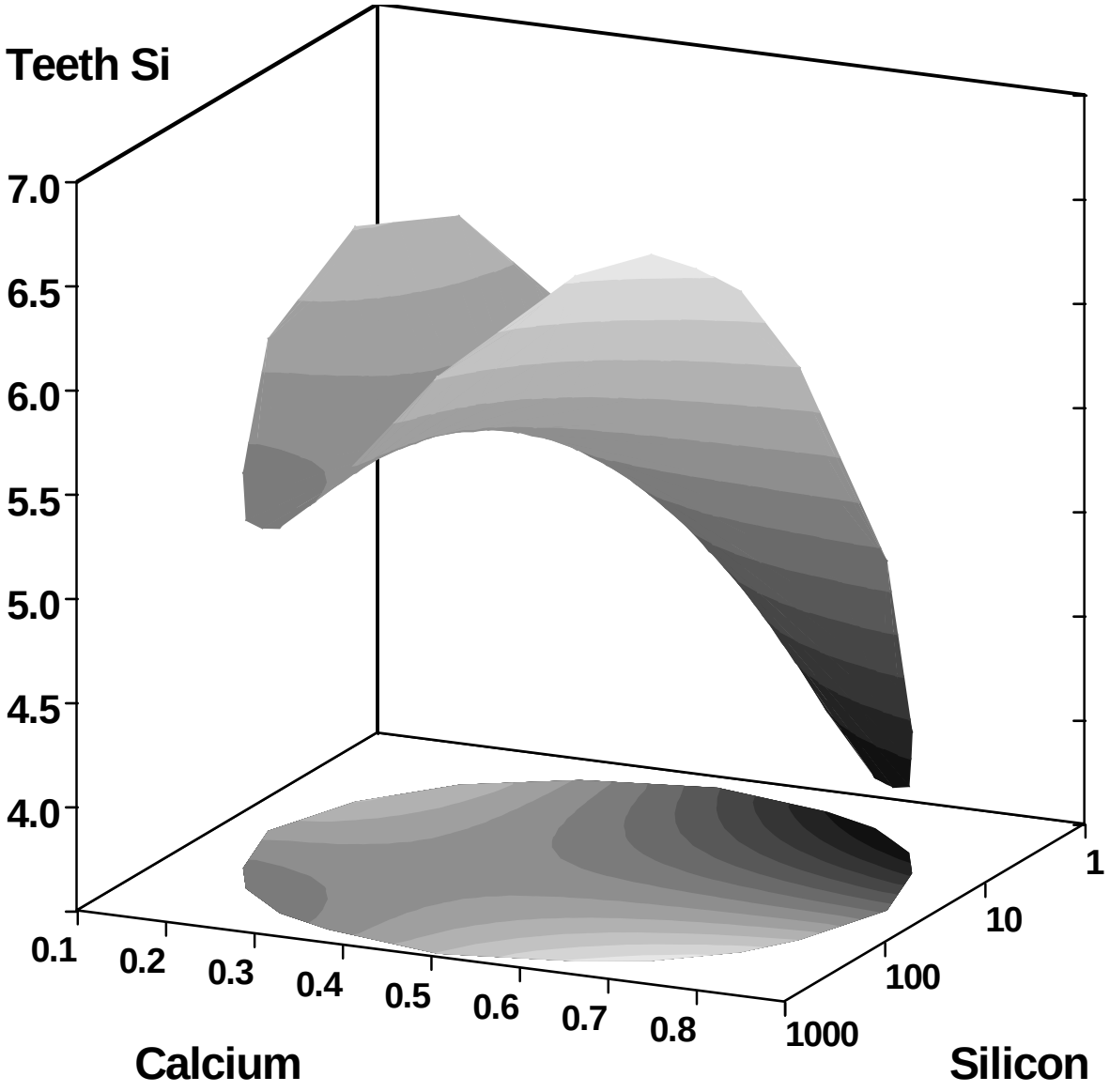

Appendix Figure 40. Response surface plot of teeth Si. Teeth silicon is expressed in μg/g dry weight. Dietary calcium is expressed as percent of diet. Dietary silicon is expressed as μg/g diet.

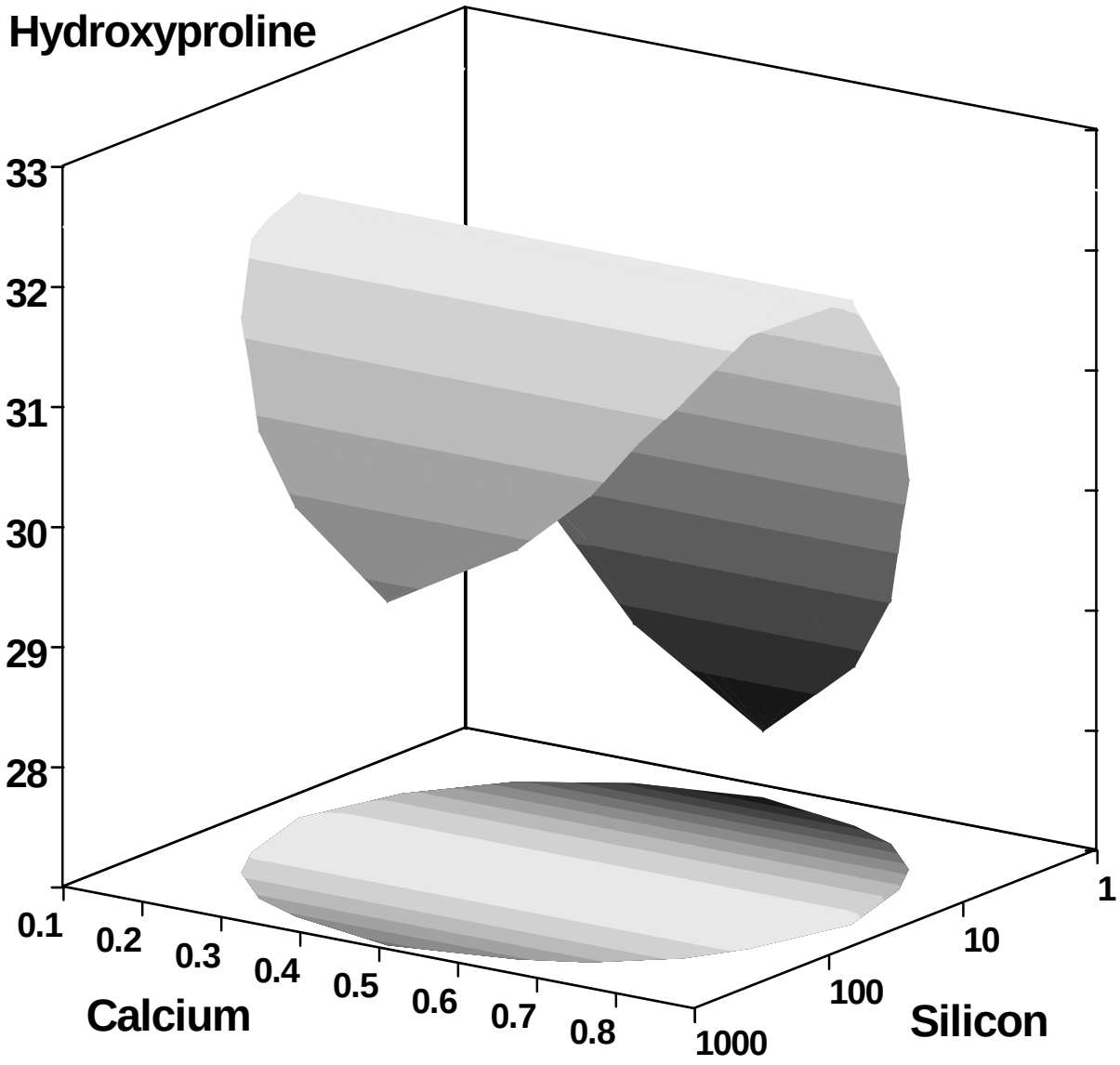

Appendix Figure 41. Response surface plot of humeri hydroxyproline. Hydroxyproline is expressed in mg/g dry weight. Dietary calcium is expressed as percent of diet. Dietary silicon is expressed as μg/g diet.

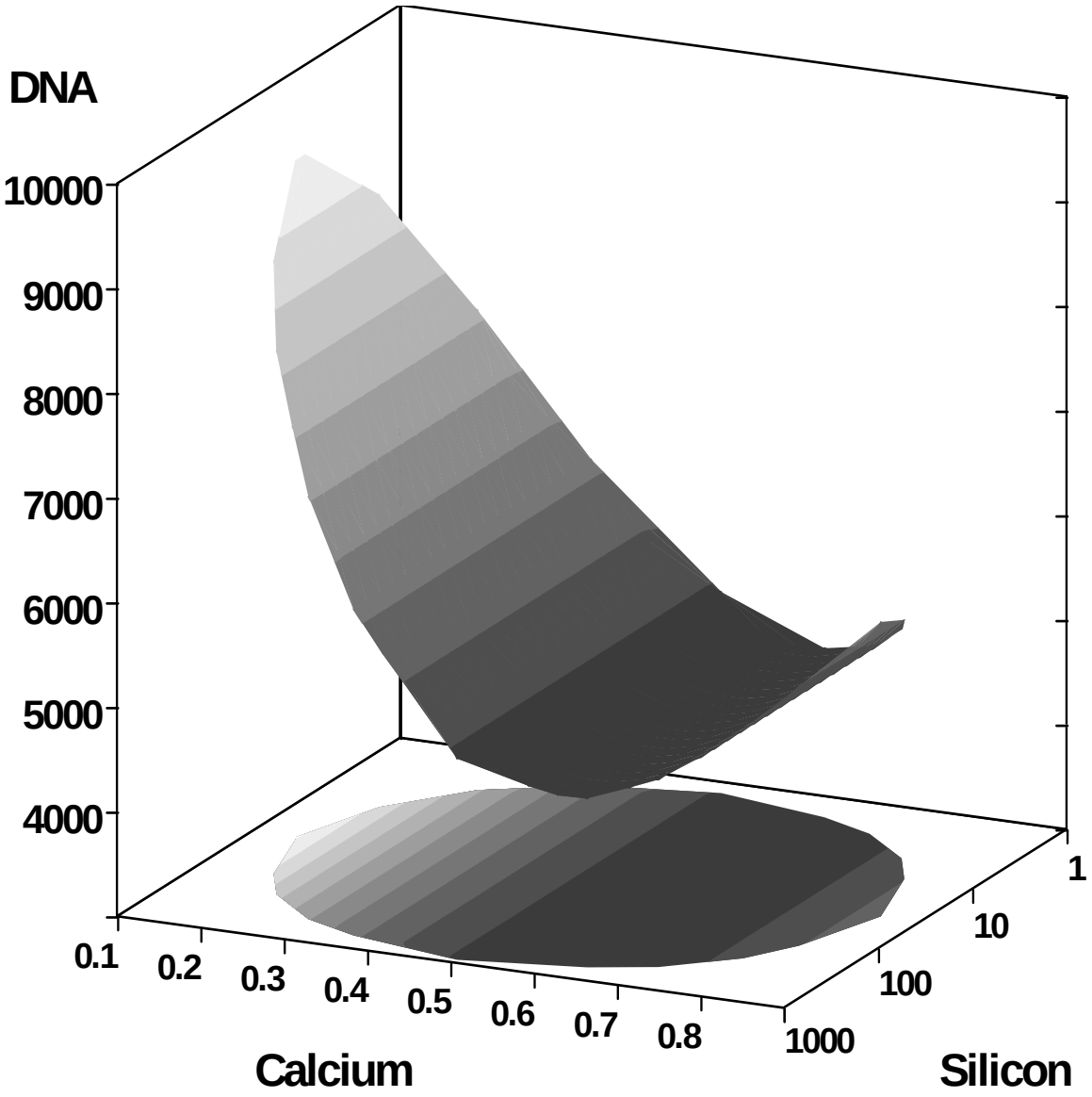

Appendix Figure 42. Response surface plot of humeri DNA. DNA is expressed in μg/g dry weight. Dietary calcium is expressed as percent of diet. Dietary silicon is expressed as μg/g diet.

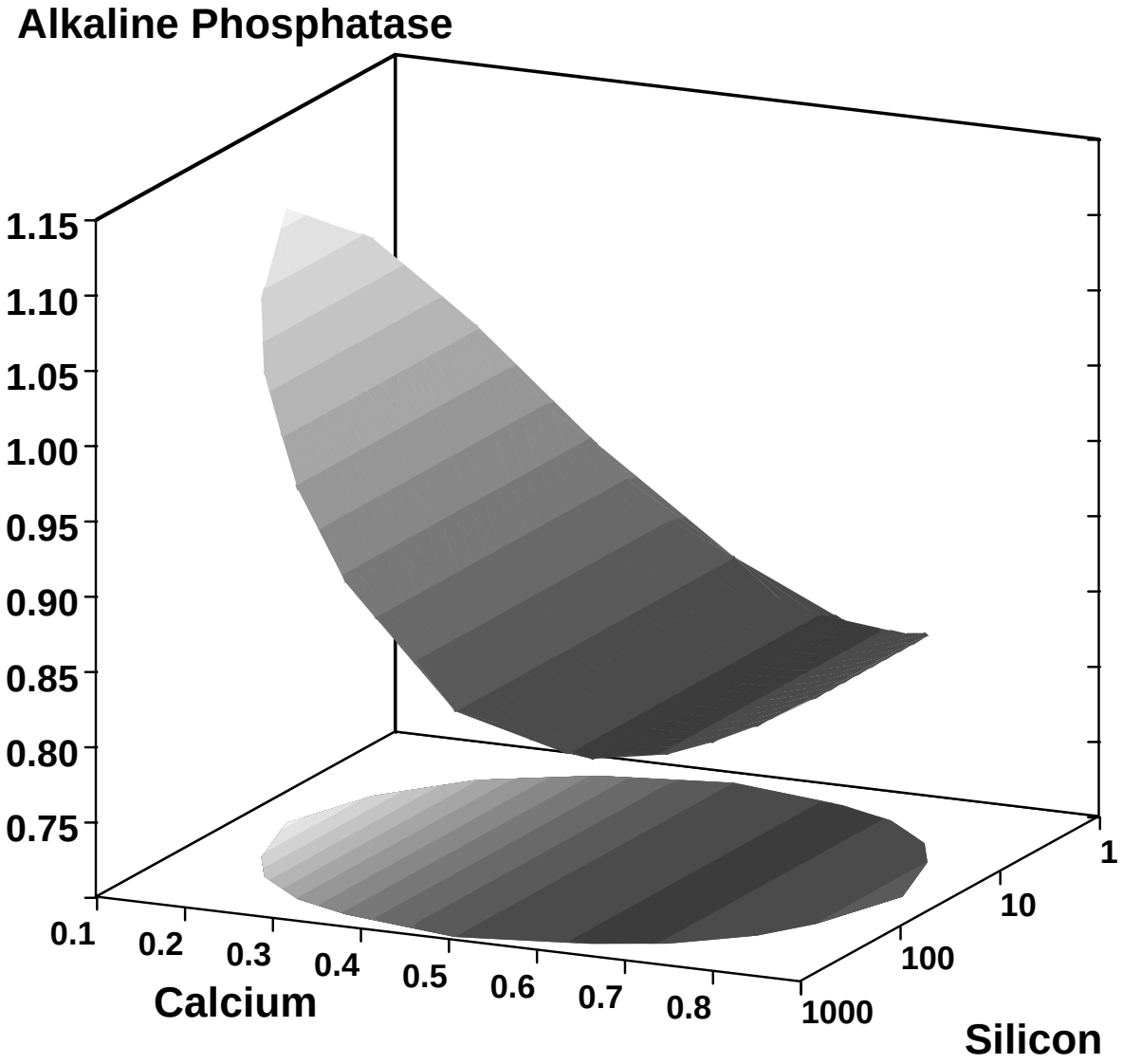

Appendix Figure 43. Response surface plot of plasma alkaline phosphatase. Alkaline phosphatase is expressed in μmoles of ρ-nitrophenol formed/min/mL plasma x 10. Dietary calcium is expressed as percent of diet. Dietary silicon is expressed as μg/g diet.